

NASA TECHNICAL NOTE



NASA TN D-5297

C. I



LOAN COPY: RETURN TO
AFWL (WLIL-2)
KIRTLAND AFB, N MEX

FLOW-FIELD MEASUREMENTS
DOWNSTREAM OF TWO PROTUBERANCES
ON A FLAT PLATE SUBMERGED IN
A TURBULENT BOUNDARY LAYER
AT MACH 2.49 AND 4.44

by *Lana M. Couch*

Langley Research Center
Langley Station, Hampton, Va.

TECH LIBRARY KAFB, NM



0132183

FLOW-FIELD MEASUREMENTS DOWNSTREAM OF TWO PROTUBERANCES
ON A FLAT PLATE SUBMERGED IN A TURBULENT BOUNDARY LAYER
AT MACH 2.49 AND 4.44

By Lana M. Couch

Langley Research Center
Langley Station, Hampton, Va.

NATIONAL AERONAUTICS AND SPACE ADMINISTRATION

For sale by the Clearinghouse for Federal Scientific and Technical Information
Springfield, Virginia 22151 - CFSTI price \$3.00

FLOW-FIELD MEASUREMENTS DOWNSTREAM OF TWO PROTUBERANCES
ON A FLAT PLATE SUBMERGED IN A TURBULENT BOUNDARY LAYER
AT MACH 2.49 AND 4.44

By Lana M. Couch
Langley Research Center

SUMMARY

Pitot pressure, static pressure, and total temperature distributions were obtained on a flat plate and on the portion of a flat plate downstream of a plate-mounted cylinder and of a plate-mounted fairing at free-stream Mach numbers of 2.49 and 4.44. Velocity gradients adjacent to the plate surface downstream of both models were greater than those obtained on the plate surface and indicate higher shearing stress and heat transfer to the plate surface within the model wakes. The extent of mixing downstream of both models, as indicated by velocity profiles, decreased with increasing Mach number. Increasing the unit Reynolds number by a factor of 2 had only a negligible effect on the profiles obtained on the flat plate. Flow patterns on the plate surface (as shown by oil-flow photographs) downstream of both models indicated some regions of similarity.

INTRODUCTION

Numerous experimental investigations have been conducted to define the interference heating associated with a protuberance mounted on a flat-plate surface within a turbulent boundary layer. (See refs. 1 to 5.) Heating rates measured in the wakes of a series of protuberances and reported in reference 1 were substantially higher than those obtained for the undisturbed plate surface at the same free-stream conditions. This increase in heating was assumed to be associated with the protuberances promoting forced mixing within the boundary layer; however, because of the lack of flow measurements within such a wake region, no firm conclusions could be made.

In order to present a picture of the flow above the plate surface and to verify the phenomena causing the heating increase, tests were conducted in the Langley Unitary Plan wind tunnel with a fairing and a right circular cylinder mounted on the tunnel sidewall.

Pitot and static pressures and total temperatures were obtained through the 5.0-inch-thick (0.127-meter-thick) boundary layer downstream of the two models at Mach numbers

of 2.49 and 4.44 and at Reynolds numbers per foot of 1.5×10^6 and 3.0×10^6 (Reynolds numbers per meter of 4.92×10^6 and 9.83×10^6).

SYMBOLS

Factors for converting the units used in this report from the U.S. Customary System to the International System (SI) are given in reference 6.

M free-stream Mach number

p static pressure

p_t stagnation pressure

R Reynolds number

r radius

T_{aw} adiabatic wall temperature

T_t stagnation temperature

T_w wall temperature

u velocity

x surface distance along flat-plate longitudinal midline, measured from aft shoulder of protuberance

y surface distance perpendicular to flat-plate longitudinal midline (in plane of plate surface)

z perpendicular distance from flat-plate surface to adjacent probe surface

δ undisturbed boundary-layer thickness

θ meridian angle (see fig. 2)

Subscripts:

<i>l</i>	local conditions
<i>2</i>	conditions downstream of normal shock wave
∞	free-stream conditions

APPARATUS AND MODELS

Wind Tunnel

The test was conducted in the high Mach number test section of the Langley Unitary Plan wind tunnel (fig. 1) described in reference 7. This variable pressure, continuous-flow tunnel has an asymmetrical sliding-block nozzle that permits a continuous variation in the test-section Mach number from 2.30 to 4.65. The maximum deviation in Mach number over the 4.0- by 4.0-foot (1.219- by 1.219-meter) test section through the range of tests is ± 0.05 .

Models

Flat plate.- In order to utilize the thick, turbulent boundary layer on the tunnel sidewall, a flat plate was mounted in the access door of the test section flush with the sidewall. The flat-plate surface was constructed of 0.05-inch-thick (0.00127-meter-thick) 310 stainless steel and was insulated from the support structure by a 0.375-inch-thick (0.00952-meter-thick) hexagonal fiber-glass honeycomb. The dimensions of the flat plate were 60.00 inches (1.524 meters) by 40.75 inches (1.035 meters). The flat plate is further described in reference 1.

Fairing and cylinder.- Two models were tested; one was a right circular cylinder and the second represented a fairing (fig. 2) such as found on the Saturn vehicle. The cylinder was 12.50 inches (0.318 meter) in height and 2.50 inches (0.0635 meter) in diameter and was mounted with the longitudinal axis perpendicular to the plate surface. The models were attached to the sidewall 4.420 inches (0.112 meter) upstream of the flat-plate leading edge (fig. 1) so that the afterbody shoulder of the fairing and the aft face of the cylinder were coincident. The models were machined from solid aluminum and attached to the door with two steel bolts for the fairing and a steel stud for the cylinder. The fairing consisted of half-cones attached to wedge-shaped bases for the forebody and afterbody and a half-cylinder attached to a rectangular-shaped base for the

centerbody. The front and rear faces of the model formed 30° angles with the base. The overall length of the model was 11.167 inches (0.284 meter) with a width and height of 2.50 inches (0.0635 meter).

INSTRUMENTATION

Pressure and temperature profiles perpendicular to the flat-plate surface were obtained at five longitudinal stations along the midline of the plate. At each of these stations five profiles were obtained by means of probes mounted in a rake assembly so that a plane passing through all five probes would be parallel to the plate surface. The rake assembly was supported and positioned by a traversing mechanism, shown in figure 3, which allowed adjustment of the assembly to the proper location with respect to the plate. The entire assembly was mounted on the tunnel sting support. The available length of traverse was approximately 8.5 inches (0.216 meter) which was over one and one-half times the 5-inch (0.127-meter) height of the undisturbed boundary-layer thickness on the test-section sidewall.

For all measurements the probes were mounted in the rake 1.25 inches (0.032 meter) apart with one end probe alined with the plate midline. The five probes extended away from the midline in the positive y-direction to a distance of 5 inches (0.127 meter) (that is, twice the diameter of the cylinder). The pitot pressure distributions were obtained with pitot probes, 0.070 inch (0.00178 meter) in outside diameter, mounted in the rake. The end of the probe was flattened to a height of 0.003 inch (0.00007 meter). (See fig. 4.) When the stagnation-pressure data had been taken, the pitot probes were cut off 0.50 inch (0.0127 meter) from the leading edge of the rake, and static-pressure heads were soldered to the remaining shafts of the original probes. Static-pressure probes were 0.100 inch (0.0025 meter) in outside diameter with 0.010-inch-thick (0.00025-meter) walls. The pressure probes were connected with 0.100-inch (0.0025-meter) inside diameter tubing to electrical pressure transducers outside the tunnel. Transducers of 10 and 1 psi (68.95 kN/m^2 and 6.895 kN/m^2) were used for the pitot- and static-pressure measurements, respectively. The output of each transducer was recorded on a digital, self-balancing potentiometer. The tunnel stagnation pressure was measured on a precision mercury manometer and the free-stream static pressure was calculated.

In order to measure the total temperatures, a separate assembly, geometrically similar to the pressure rake, was used with the traversing mechanism. The single-shield total temperature probes were 0.068-inch (0.0017 meter) outside diameter and 0.062-inch (0.0016 meter) inside diameter with an outside base diameter of 0.090 inch (0.0023 meter). The probes were constructed mainly of stainless steel and used number 36 gage iron-constantan wire. (See fig. 3.) Prior to the present test, the temperature probes were calibrated for variation in Mach number and Reynolds number; the recovery

factor was found to be 1.0 for the lower Mach number and 0.999 for the higher Mach number over the range of Reynolds numbers involved in this test.

The stagnation temperature inside the test section was measured by a total temperature probe attached to a support which was mounted on the supporting structure for the traversing mechanism. Also, the flat-plate temperatures, measured by thermocouples in the plate surface, were recorded periodically for each set of test conditions on a self-balancing potentiometer.

In order to determine the vertical position of the probes, a servo-type digitizer was calibrated for counts relative to perpendicular distance from the plate. Based on repeatability, the z values are accurate to ± 0.005 inch (± 0.000127 meter).

TEST CONDITIONS

The tests were conducted at a Mach number of 2.49 for Reynolds numbers per foot of 1.5×10^6 and 3.0×10^6 (Reynolds numbers per meter of 4.92×10^6 and 9.83×10^6) and at $M = 4.44$ for Reynolds number per foot of 3.0×10^6 (Reynolds number per meter of 9.83×10^6). The tunnel stagnation temperature was approximately $610^\circ R$ ($330^\circ K$) at $M = 2.49$ and $635^\circ R$ ($353^\circ K$) at $M = 4.44$.

The data for both Reynolds numbers are presented for the flat plate. However, only the data for the higher Reynolds number are presented for the flat plate with attached protuberances. Data were taken at five stations on the flat plate: $x = 6.88, 10.00, 15.00, 22.50$, and 30.00 inches ($x = 0.175, 0.254, 0.381, 0.572$, and 0.762 meter). In interpreting the data downstream of the protuberances, it should be pointed out that the first station was measured 6.88 inches (0.175 meter) downstream from the rear surface of the cylinder and from the afterbody shoulder of the fairing. Therefore, the first station is 6.88 inches (0.175 meter) from the cylinder, but only 2.575 inches (0.9654 meter) from the afterbody vertex of the fairing. Also, note definition of z in symbols.

RESULTS AND DISCUSSION

A complete listing of the data obtained in this investigation is presented in tables I to IV for the various configurations. See index preceding tables.

Flat-Plate Pitot-Pressure Profiles

Ratios of the local measured pitot pressure to the free-stream measured pitot pressure (measurements were taken only at two stations on the flat plate) along the flat-plate midline are presented in figure 5 as a function of z/δ for all test conditions. The pressure ratios decreased in magnitude by approximately 4 percent from the first to the fifth

station; however, as will be shown later in the report, the velocity levels remained approximately the same. For a factor-of-two increase in unit Reynolds number at the lower Mach number, the pressure ratios remained essentially constant. However, for an increase in Mach number from 2.49 to 4.44, the pitot-pressure profile through the boundary layer was somewhat fuller for the lower Mach number, as would be expected.

The spanwise distributions of the pitot-pressure ratios across the flat plate through the boundary layer at the first and fifth stations were essentially constant, and, therefore, are not presented in figure form.

Flat-Plate Static Pressure Profiles

Ratios of the local static to the free-stream static pressures through the boundary layer are presented in figure 6 for the first and fifth stations along the plate midline at all test conditions. Although the static pressures are essentially constant through the boundary layer, as would be expected, some measured values were less than free-stream static pressures by approximately 2 to 3 percent at $M = 2.49$ and 5 percent at $M = 4.44$. No particular significance is attached to this indicative pressure gradient, since the associated variations in pressure are within the accuracy of the instrumentation. Little variation was found in the static-pressure distributions through the boundary layer across the span of the flat plate for the range of test conditions.

Flat-Plate Total-Temperature Profiles

Presented in figure 7 are the ratios of the measured local total temperature to free-stream total temperature through the boundary layer on the flat plate for $M = 2.49$, $R/\text{ft} = 1.5 \times 10^6$ and 3.0×10^6 ($R/\text{m} = 4.92 \times 10^6$ and 9.83×10^6) and $M = 4.44$, $R/\text{ft} = 3.0 \times 10^6$ ($R/\text{m} = 9.8 \times 10^6$). With the exception of the negligible Reynolds number effect, the effects of the Mach number on the profiles cannot be determined from the data in this form, since the value of T_w/T_{aw} varied slightly for the different test conditions. In an attempt to correlate the temperature profiles from all test conditions, the parameter $\frac{T_{t,l} - T_w}{T_{t,\infty} - T_w}$ was evaluated for each measurement, as suggested by Bertram (ref. 8), and is presented in figure 8 as a function of u_l/u_∞ . In general, the data of this investigation tend to fall within a relatively narrow band. Also presented in figure 8 is the theory of Walz (ref. 9) which is insensitive to Mach number and valid for arbitrary heat transfer. The crosshatched areas represent the data of references 10 and 11. For adiabatic-wall conditions which were approximated in this test, energy considerations dictate that at some point within the boundary layer, $T_{t,l}$ should be greater than $T_{t,\infty}$; however, this condition was not indicated either by the data or by the theory of Walz. A possible explanation for this condition not occurring in the data is that the temperature of

the tunnel sidewall, upstream of the thin-skin plate surface, was less than the adiabatic value since the tunnel sidewall reacts more slowly to variations in temperature than the thin-skin plate does.

Flat-Plate Velocity Profiles

Ratios of local velocity to free-stream velocity through the boundary layer along the flat-plate midline are presented in figure 9. The values of the local velocity were computed by using measured pitot and static pressures and measured total temperature. There were no significant effects of Mach number, Reynolds number, or longitudinal station, on the velocity distributions as shown in figure 9.

Flat Plate With Attached Cylinder

Flow model. - In order to facilitate the discussion of the measurements obtained downstream of the cylinder, a flow model, based primarily on the data obtained in this report and on flow visualization studies reported in reference 4, has been defined in figure 10. The sketch presented in figure 10(a) was made from full-size oil-flow photographs. The flow directly adjacent to the plate surface has been divided into three main regions (fig. 10(a)): (1) the reversed-flow region upstream of the cylinder, (2) the flow impingement or vortex region downstream of the reversed-flow region, and (3) the wake core. The wake consists of all the flow affected by and downstream of the cylinder; whereas the wake core is the bounded region downstream of the cylinder with the flow generally aligned along the plate midline. The reversed-flow region (region 1, fig. 10(b)) is created by the high-pressure air between the bow shock and the forward surface of the cylinder feeding upstream in the subsonic portion of the boundary layer. At the upstream boundary of the reversed-flow region, the boundary layer separates from the sidewall, forms an oblique shock which intersects the bow shock, and thus forms a λ -type shock system. (See ref. 4.) Such a λ -type shock formation was partially observed in high-speed schlieren motion pictures in a previous test conducted in the Langley Unitary Plan wind tunnel upstream of a cylindrical-leading-edge fin model (ref. 12) and completely shown in a schlieren photograph in reference 13. The flow upstream of the cylinder, bordering the reversed-flow region, contains a dividing or stagnating streamline; the flow below this boundary has a velocity component directed toward the plate surface and continues through the reversed-flow region. The flow above this boundary has a velocity component directed away from the plate and continues to flow around the cylinder. With increasing θ , for $0^\circ < \theta < 90^\circ$ the extent of reversed flow decreases such that at $\theta = 90^\circ$ it is negligible. Flow lines emanate from the forward section of the cylinder in approximately radial directions. (See fig. 10(c).) With increasing distance from the

cylinder, these lines are deflected away from the radial direction and eventually approach the curvature of or merge with the forward separation line and the impingement region boundaries.

The flow lines forming region 2 (fig. 10(d)) are first apparent in the vicinity of $\theta \approx 60^\circ$ and are bounded by the model wake core and the flow lines emanating from region 1. On the plate surface within region 2 is a "herringbone" flow pattern (as defined in ref. 4), which is indicative of a flow-impingement region on the plate surface. The impinging flow within this region is visualized as having passed over the reversed-flow region (region 1) upstream of the cylinder and offset from the plane of symmetry containing the plate midline and the model axis. Although the herringbone pattern does not appear on the oil-flow photographs of reference 4 for $\theta < 60^\circ$ (the oil was completely removed from the plate surface in this region near the model base), it is believed that this impingement pattern actually extends upstream of this location near the base of the cylinder. This belief is substantiated by an oil-flow photograph in reference 13 which shows the herringbone pattern extending to the forward section of the cylinder near the plate midline.

As a result of the forced mixing within the impingement region, low momentum air in the initially undisturbed region of the boundary layer adjacent to the plate surface is mixed with the higher momentum air from the outer regions of the boundary layer. Voitenko, Zubkov, and Panov (ref. 13) suggest that the flow influencing the impingement region on the flat plate consists of two vortices of opposite rotations, which originate near the plate surface directly in front of the cylinder. Whether such a cyclic vortex flow exists or not, and there is no direct indication of it in the measurements, the velocity profiles perpendicular to the plate surface would be expected to have higher velocities than those obtained for the flat plate. The experimental profiles obtained in region 2 indicated higher velocities than those obtained on the flat plate, as will be shown subsequently.

At the rear of the cylinder a region of reversed flow is fed by part of the upstream flow that passes around the cylinder into the wake region. The wake-core boundary of region 3, as shown in figure 10(e), is well defined in the oil-flow photographs from reference 4 for approximately 5 cylinder diameters downstream. Within this region the streamlines at the plate surface have velocity components directed away from the vertical plane of symmetry and toward the wake-core boundary. The magnitude of this velocity component decreases with increasing distance downstream; thus, for distances greater than approximately 5 diameters, the flow on each side of the boundary is aligned and the wake boundary is indistinct. The slight deflection of the flow in region 2 outboard of the wake core results from the shock wave originating from the compression region at the neck of the wake core.

Isometrics.- In an attempt to obtain a qualitative, quasi-three-dimensional representation of the flow field behind the models, pitot pressure, static pressure, and velocity distributions downstream of the cylinder are presented in isometric form in figures 11, 12, and 13, respectively, for both Mach numbers at a Reynolds number per foot of 3.0×10^6 ($R/m = 9.83 \times 10^6$). The vertical curves represent the profiles obtained perpendicular to the plate surface for constant values of x and y , whereas, the horizontal curves represent fairings through constant values of x and z/δ .

When the distributions for the two Mach numbers are compared, the trends of the variables, in general, are essentially the same, the maximum and minimum values of the gradients occurring at different locations throughout the profiles, as would be expected.

Examining the distributions at each station along the plate midline, both the movement of the gradients outward from the midline and upward from the plate and the diffusing of the gradients toward the rear of the plate can be seen. The path of the trailing-edge shock wave has the most prominent effect on the parameters due to its extension through the entire height of the survey. For the lower Mach number (figs. 11(a), 12(a), and 13(a)), the shock wave passes mainly through the first three stations (no data were taken at station 4) - passing approximately through the second probe location at the first station. In figures 11(b), 12(b), and 13(b), $M = 4.44$, the path of the shock wave can be identified at all five stations since it is located somewhat closer to the plate midline plane of symmetry because of the decreased shock angle. The effects of the shock wave in the lower regions of the profiles are not distinct because of the proximity to the plate surface and the mixing of the air in this region. The effects of the shock wave are not well defined in the velocity distributions (fig. 13); however, slight variations are apparent at both Mach numbers. Gradients in the static-pressure distribution have almost completely dispersed and the ratios have returned to a constant value at the fifth station for the lower Mach numbers. (See fig. 12(a).)

Longitudinal distributions.- Distributions of pitot pressure, static pressure, total temperature, and velocity plotted for five stations along the midline of the flat plate are presented in figures 14, 15, 16, and 17, respectively. Also, shown in figures 14, 16, and 17 for the purpose of comparison are the corresponding flat-plate profiles (solid lines).

Pitot-pressure profiles along the midline for $M = 2.49$ are shown in figure 14(a). For the first station, $x = 6.875$ inches (0.175 meter), the measured pitot pressures decrease with decreasing z/δ for $0.6 < z/\delta < 1.4$, as would be expected, however, for $0.25 < z/\delta < 0.5$ the measured pitot pressures increase with decreasing z/δ . The maximum measured pressures at $z/\delta \approx 0.2$ are approximately of the same magnitude as those measured for $z/\delta > 1.0$. The increase in pitot pressure for $z/\delta < 0.5$ is believed to result from (1) the forced mixing occurring in region 2 discussed previously as well as

the wake core mixing, and (2) the fact that the flow within the lower portion of the boundary layer, after passing through the separation shock wave and the deflected leg of the normal shock wave upstream of the cylinder, has a lower Mach number and, therefore, a higher total pressure after passing through the trailing-edge shock wave than the flow which passes only through the normal and trailing-edge shock waves. With increasing distance downstream of the cylinder, the gradients in the pitot-pressure profiles associated with these flow phenomena tend to decrease. At a Mach number of 4.44 (fig. 14(b)) similar results are shown, the major difference being that the gradients occur at smaller values of z/δ .

In the wake-core region adjacent to the plate, the magnitudes of the pitot pressure, total temperature, and velocity ratios (figs. 14, 16, and 17(a)) are greater than the corresponding values obtained for the flat plate. This increase remains fairly constant at the lower Mach number. However, at $M = 4.44$ (figs. 14(b) and 17(b)) the wake core has dissipated to the extent that all the velocity and the pitot-pressure distributions at stations 4 and 5 are nearly identical to those for flat-plate boundary-layer flow through $z/\delta \approx 0.10$. Also, the static-pressure profiles in figure 15 return to almost flat-plate flow with some effect remaining because of the cylinder. In figure 16(b), $M = 4.44$, the increasing height of the maximum value of the temperature ratios with increasing downstream distance seems to indicate a vertical growth in the height of the core region of the wake (slightly indicated in fig. 14(b)).

Increased magnitudes in the velocity ratios over the flat-plate values across the wake-core region up to $z/\delta \approx 0.3$ (fig. 17(a)) are due to the increased degree of mixing of the higher momentum air into the lower regions of the boundary layer. The resultant increase in velocity gradient at the plate surface increases the shearing stress and, similarly, the heat transfer to the plate surface, as was found in the wake of several protuberance models mounted on a flat plate. (See ref. 1.) At the higher Mach number (fig. 17(b)) the similarity of the velocity distribution to those obtained for the flat plate suggests that possibly the mixing action is less thorough and decreases with increasing Mach number.

Spanwise distributions. - The distributions at the several spanwise stations of pitot pressure, static pressure, total temperature, and velocity are presented for both Mach numbers in figures 18, 19, 20, and 21, respectively, for stations 1, 3, and 5. (Hereafter, these profiles are referred to as spanwise distributions.) The core region of the wake can be determined in the pitot pressure and velocity distributions at $M = 2.49$ (figs. 18(a) and 21(a)) by the generally constant range of pressure extending from $0.05 \leq z/\delta \leq 0.24$. (See figs. 11(a) and 13(a).) Only the midline probe is affected at station 1; at station 5, both the first and second probes appear to be within the wake-core region. However, at $M = 4.44$, the region of the wake core is indiscernible, as it was in the longitudinal distributions.

By examining the overall trends of increasing or decreasing ratios above $z/\delta \approx 0.60$ for the outward progression of the probes from the midline in the pitot-pressure distributions (fig. 18), the reversal of the general trend of increasing ratios at each z/δ indicates the path of the trailing-edge shock wave. Comparable effects in the static-pressure and velocity distributions indicate that at $M = 4.44$ (fig. 18(b)), the shock passes between probes 2 and 3, 3 and 4, and possibly 4 and 5, at stations 1, 3, and 5, respectively, and lies somewhat closer to the midline plane of symmetry than at the lower Mach number. The decrease in the pitot- and static-pressure distributions (for example, probe 3 at station 1), figures 18 and 19, respectively, is due to the expansion of the flow around the cylinder since the flow is not within the envelope of the shock wave. Probes 4 and 5, located further from the midline plane of symmetry, tend to recover somewhat toward the flat-plate pitot-pressure distribution. Comparable situations exist for the static-pressure and velocity ratios.

In figure 20, $M = 2.49$, station 1, the spanwise total-temperature distributions show a symmetrical decrease around $z/\delta \approx 0.55$ – the same general location as the effects shown in the pitot-pressure distribution. The temperature gradients in the wake of the cylinder disperse with increasing distance downstream; this behavior is somewhat similar to the behavior of the flow downstream of a cylinder in free-stream flow.

It should be noted that the unusual variation in the velocity distribution obtained at $M = 4.44$, station 3, probe 5 (fig. 21(b)) was also obtained at the same position for $M = 2.49$ (fig. 21(a)) with the variation spread over a larger vertical distance. Therefore, it appears that the variation in figure 21(b) should not be attributed to data inaccuracy.

Flat Plate With Attached Fairing

Flow model. - The flow model for the fairing is shown in figure 22 and is based on flow-visualization studies stemming mainly from the data of this report and from reference 1. From a comparison of the oil-flow photograph of figure 22(a) with the illustration in figure 22(b), regions 1, 2, and 3 are the reversed-flow, impingement, and wake-core regions, respectively. The trailing-edge shock wave is roughly conical in shape; whereas for the cylinder it consists of two vertical planar shock waves. The shock wave, aft of the fairing, extends downstream from the compression region at the wake neck and appears to lie on the plate approximately tangential to the outboard boundary of region 2. Shown in figure 22(c) is an illustration of the flow expansion over the fairing, indicating the localized separation regions at the forward and aft vertices and the two shoulders of the model. These small separation regions are due to the inability of the flow to negotiate the required turning angle. The flow-impingement region (fig. 22(d)) indicates the direction of the flow as it rolls from the afterbody of the fairing. When the flows in the impingement regions

for both models are compared, the impinging flow downstream of the cylinder is characterized by a herringbone pattern; however, only the outboard half of that pattern appears downstream of the fairing. Apparently, only the "half-herringbone" develops since the flow over the top of the fairing is included in this region, whereas downstream of the cylinder all the flow affecting the similar region must have passed around the cylinder. The impinging flow in region 2 is vortical in the sense that it does roll to some extent as it flows down the conical region of the fairing and along the plate surface. However, there is no direct indication that an extensive cyclic vortex exists downstream of the fairing.

The impingement region (region 2) is actually part of the wake; however, upon closer examination of the oil-flow photograph, a narrower core region (symmetric about the plate midline) bounded by the impingement regions can be seen. (See fig. 22(e).)

Isometrics. - Isometric plots of pitot pressure, static pressure, and velocity distributions downstream of the fairing are presented for both Mach numbers in figures 23, 24, and 25, respectively. The effects of two shock waves, one originating from the forebody and the other from the trailing edge of the fairing, and the expansion fan from the afterbody shoulder are most evident in these distributions, especially at the higher Mach number. The effects of the expansion fan and the trailing-edge shock wave are adjacent in the vertical plane, and the effects of the trailing-edge shock wave extend through the distributions at $x = 30.00$ inches (0.762 meter) at the higher Mach number. An expansion fan is indicated by the decrease in pressure with decreasing z/δ and the increase in the velocity ratios for the same region. The path of the trailing-edge shock wave can be identified by the increasing pressure gradient with decreasing z/δ , by the overall decrease in velocity ratios in the enclosed area, and its projected origin from the compression region of the afterbody vertex. The effects of the shock wave and the expansion fan in the distributions occur at higher values of z/δ for increasing x and at lower values for increasing y ; thus, a conical distribution for both the shock wave and the expansion fan was indicated as expected. With increasing distance downstream the expansion fan diverges and the gradients across the expansion region decrease; also, at some point downstream the trailing-edge shock wave crossing the expansion region would cancel some of the predominant effects of each. The sharply decreasing gradients in the upper part of the pressure distributions are attributed to the presence of the oblique shock wave which originates at the fairing forebody. The original path of the shock wave is altered to the extent that it is within the range of instrumentation at the higher Mach number because of the intersection of the expansion fans of the forebody and afterbody shoulders with the oblique shock wave. These effects are most evident in the pitot- and static-pressure ratios at $M = 4.44$ (figs. 23(b) and 24(b)).

For the lower Mach number the major effects generally have dissipated at the last station; however, at $M = 4.44$ the path of the trailing-edge shock wave is still very evident at station 5.

Longitudinal distributions.- In order to examine in greater detail the local flow properties downstream of the fairing, pitot pressure, static pressure, total temperature, and velocity ratios are presented in figures 26, 27, 28, and 29, respectively. In figure 27, the decreasing spread of the effect of the trailing-edge shock wave with increasing longitudinal distance along the plate suggests that this wave may not be one discrete shock wave, but a series of compression waves which, with increasing distance from their origin, converge into a single wave. The effects of the shock wave from the model forebody are present only in the upper regions of the first station profile and only at the high Mach number, where the shock angle is less. The pitot-pressure distributions at $M = 2.49$ (fig. 26(a)) downstream of the fairing are slightly fuller than the distribution obtained on the flat plate. The increase over the flat-plate values for the fairing is somewhat less than that obtained for the cylinder. Although the region of the wake core is not readily apparent in the pitot-pressure distributions, wake-core effects seem to be indicated in the static-pressure distributions (fig. 27) by the generally decreasing pressure gradient with increasing z/δ , the maximum height being approximately 1 inch (0.0254 meter), present at both Mach numbers and continuing through station 5. A similar type of effect is also present in the static-pressure distributions downstream of the cylinder. (See fig. 15(b).) At $M = 2.49$ and 4.44, station 5, the static-pressure ratios have nearly recovered to the free-stream pressure, except for the influence of both the wake-core and the trailing-edge shock wave.

Total-temperature distributions downstream of the fairing are presented for comparison with flat-plate temperature ratios in figure 28. The trends of the distributions are similar at both Mach numbers, the magnitudes of the ratios differing somewhat in the regions of the profiles above $z/\delta \approx 0.40$. However, below $z/\delta \approx 0.40$ the effects of the wake and the heating at the surface show a definite influence on the total temperature ratios. Velocity distributions (fig. 29) show mainly the presence of the expansion region and the trailing-edge shock wave at $M = 2.49$ and the increased heating over the flat-plate value, which would result from the higher velocity gradient at both Mach numbers adjacent to the plate surface in the wake-core region.

Spanwise distributions.- Presented in figures 30, 31, 32, and 33 are the spanwise distributions of pitot pressure, static pressure, total temperature, and velocity, respectively. The paths of the shock waves from the trailing-edge compression region and the forebody and the effect of the expansion region can be seen at station 1 in figures 30(a), 30(b), 31(a), and 31(b). However, because of the inclination of the forward shock wave, only the effects of the aft shock wave and the expansion region are apparent in the velocity profiles at $M = 2.49$. (See fig. 33(a).) In figure 33(b), $M = 4.44$, even the path of the trailing-edge shock wave is nearly unnoticeable. The conical shape of both waves is apparent from the distributions. The pitot-pressure ratios in figure 30(a) at stations 3 and 5, probes 3 and 4, respectively, and in figure 30(b) at station 5, probe 3, and the

corresponding velocity distributions show the effects of an undetermined phenomenon at $z/\delta \approx 0.05$, since the location of these probes is not at the border of two regions, but within the impingement region adjacent to the wake core. Also, this effect is localized, since none of the ratios from the other probes show comparable effects in this region.

The total temperature distributions below $z/\delta \approx 0.20$ (fig. 32(a)) show an increase for probe 1 at stations 3 and 5 over the main grouping of the data, but not at station 1 because of its proximity to the rear of the fairing. Apparently, the fairly constant variation between the ratios at probe 1 and the remainder of the probes at stations 3 and 5 is not due to flow angularity, since the difference would be expected to decrease with an increasing distance downstream of the fairing. Although the variations are small, they are fairly consistent and no explanation is offered other than the possibility that the variations might be due to the mixing in these regions. In figure 32(b), $M = 4.44$, the variation obtained for the midline location (probe 1) does appear to be due to flow angularity, since it tends to diminish with increasing x .

CONCLUDING REMARKS

Pitot-pressure, static-pressure, and total-temperature distributions were obtained on a flat plate and on the portion of a flat plate downstream of a plate-mounted cylinder and of a plate-mounted fairing at free-stream Mach numbers of 2.49 and 4.44.

Velocity gradients adjacent to the plate surface downstream of both models were greater than those obtained on the plate surface; thus, higher shearing stress and heat transfer to the plate surface within the model wakes are indicated. The extent of mixing downstream of both models, as indicated by velocity profiles, decreased with increasing Mach number.

Increasing the unit Reynolds number by a factor of 2 had only a negligible effect on the profiles obtained on the flat plate. Flow patterns on the plate surface (as shown by oil-flow photographs) downstream of both the cylinder and the fairing indicated some regions of similarity.

Langley Research Center,

National Aeronautics and Space Administration,

Langley Station, Hampton, Va., April 3, 1969,

126-13-02-10-23.

REFERENCES

1. Couch, Lana Murphy; Stallings, Robert L., Jr.; and Collins, Ida K.: Heat-Transfer Measurements on a Flat Plate With Attached Protuberances in a Turbulent Boundary Layer at Mach Numbers of 2.49, 3.51, and 4.44. NASA TN D-3736, 1966.
2. Stallings, Robert L., Jr.; and Collins, Ida K.: Heat-Transfer Measurements on a Flat Plate and Attached Protuberances in a Turbulent Boundary Layer at Mach Numbers of 2.65, 3.51, and 4.44. NASA TN D-2428, 1964.
3. Price, Earl A.; Howard, Paul W.; and Stallings, Robert L., Jr.: Heat-Transfer Measurements on a Flat Plate and Attached Fins at Mach Numbers of 3.51 and 4.44. NASA TN D-2340, 1964.
4. Burbank, Paige B.; Newlander, Robert A.; and Collins, Ida K.: Heat-Transfer and Pressure Measurements on a Flat-Plate Surface and Heat-Transfer Measurements on Attached Protuberances in a Supersonic Turbulent Boundary Layer at Mach Numbers of 2.65, 3.51, and 4.44. NASA TN D-1372, 1962.
5. Truitt, Robert W.: Hypersonic Turbulent Boundary-Layer Interference Heat Transfer in Vicinity of Protuberances. AIAA J. (Tech. Notes), vol. 3, no. 9, Sept. 1965, pp. 1754-1755.
6. Mechtly, E. A.: The International System of Units - Physical Constants and Conversion Factors. NASA SP-7012, 1964.
7. Anon.: Manual for Users of the Unitary Plan Wind Tunnel Facilities of the National Advisory Committee for Aeronautics. NACA 1956.
8. Bertram, Mitchel H.; and Neal, Luther, Jr.: Recent Experiments in Hypersonic Turbulent Boundary Layers. Presented to the AGARD Specialists Meeting on Recent Developments in Boundary-Layer Research (Naples, Italy), May 10-14, 1965.
9. Walz, A.: Compressible Turbulent Boundary Layers. The Mechanics of Turbulence. Gordon and Breach Science Publ., c.1964, pp. 299-350.
10. Adcock, Jerry B.; Peterson, John B., Jr.; and McRee, Donald I.: Experimental Investigation of a Turbulent Boundary Layer at Mach 6, High Reynolds Numbers, and Zero Heat Transfer. NASA TN D-2907, 1965.
11. Lobb, R. Kenneth; Winkler, Eva M.; and Persh, Jerome: NOL Hypersonic Tunnel No. 4 Results VII: Experimental Investigation of Turbulent Boundary Layers in Hypersonic Flow. NAVORD Rept. 3880, U.S. Nav. Ord. Lab., Mar. 1, 1955.
12. Price, Earl A., Jr.; and Stallings, Robert L., Jr.: Investigation of Turbulent Separated Flows in the Vicinity of Fin-Type Protuberances at Supersonic Mach Numbers. NASA TN D-3804, 1967.

13. Voitenko, D. M.; Zubkov, A. I.; and Panov, Yu. A.: Supersonic Gas Flow Past a Cylindrical Obstacle on a Plate. Fluid Dyn., vol. 1, no. 1, Jan.-Feb. 1966, pp. 84-88.

INDEX TO TABULAR DATA

	Page
TABLE I.- INSTRUMENTATION LOCATIONS	18
TABLE II.- MEASUREMENTS OBTAINED FOR PLATE	19
(a) Total-pressure ratio	19
(b) Static-pressure ratio	21
(c) Total-temperature ratio	23
(d) Velocity ratio	25
TABLE III.- MEASUREMENTS OBTAINED FOR PLATE WITH CYLINDER	27
(a) Total-pressure ratio	27
(b) Static-pressure ratio	32
(c) Total-temperature ratio	37
(d) Velocity ratio	42
TABLE IV.- MEASUREMENTS OBTAINED FOR PLATE WITH FAIRING	47
(a) Total-pressure ratio	47
(b) Static-pressure ratio	52
(c) Total-temperature ratio	57
(d) Velocity ratio	62

TABLE I.- INSTRUMENTATION LOCATIONS

(a) Flat-plate longitudinal stations

Station	x	
	in.	m
1	6.875	0.175
2	10.000	.254
3	15.000	.381
4	22.500	.572
5	30.000	.762

(b) Spanwise instrumentation locations

Probe	y	
	in.	m
1	0	0
2	1.25	.032
3	2.50	.063
4	3.75	.094
5	5.00	.127

TABLE II.- MEASUREMENTS OBTAINED FOR PLATE - Continued

(a) Total-pressure ratio - Concluded

 $x = 6.875$ in. (0.175 m); $M = 4.44; R = 3.00 \times 10^6$ per ft (9.83×10^6 per m)

$\frac{z}{\delta}$	$\frac{(\bar{p}_{t,2})_L}{(\bar{p}_{t,2})_\infty}$ for probe -				
	1	2	3	4	5
.000	.0768	.0916	.0715	.0843	.1087
.004	.1257	.1112	.1237	.1261	.0856
.010	.1469	.1416	.1487	.1476	.1359
.020	.1756	.1731	.1800	.1776	.1789
.030	.1936	.1927	.2008	.1991	.2009
.040	.2117	.2112	.2206	.2184	.2219
.060	.2425	.2427	.2519	.2495	.2554
.080	.2669	.2688	.2791	.2763	.2837
.100	.2924	.2927	.3041	.3010	.3099
.120	.3073	.3101	.3229	.3225	.3340
.140	.3275	.3307	.3437	.3450	.3571
.160	.3444	.3492	.3625	.3622	.3749
.180	.3667	.3731	.3854	.3858	.4011
.200	.3837	.3916	.4052	.4051	.4189
.240	.4145	.4231	.4417	.4427	.4619
.280	.4528	.4589	.4803	.4813	.5017
.320	.4814	.4894	.5127	.5156	.5384
.360	.5154	.5241	.5481	.5521	.5783
.400	.5483	.5567	.5815	.5864	.6129
.460	.5940	.6024	.6295	.6347	.6642
.520	.6439	.6524	.6795	.6873	.7208
.580	.6916	.6979	.7233	.7302	.7649
.660	.7565	.7621	.7891	.7947	.8279
.740	.8213	.8273	.8547	.8590	.8938
.820	.8892	.8871	.9111	.9094	.9420
.900	.9500	.9438	.9625	.9569	.9811
.980	.9901	.9773	.9872	.9770	.9944
1.100	1.0170	.9982	1.0022	.9913	1.0021
1.200	1.0202	1.0048	1.0074	.9956	1.0042
1.400	1.0199	1.0066	1.0101	.9985	1.0060

 $x = 30.000$ in. (0.762 m); $M = 4.44; R = 3.00 \times 10^6$ per ft (9.83×10^6 per m)

$\frac{z}{\delta}$	$\frac{(\bar{p}_{t,2})_L}{(\bar{p}_{t,2})_\infty}$ for probe -				
	1	2	3	4	5
.000	.0641	.0895	.0632	.0692	.0866
.004	.0981	.0873	.0955	.1057	.0762
.010	.1363	.1286	.1372	.1390	.1275
.020	.1629	.1590	.1664	.1669	.1674
.030	.1830	.1808	.1883	.1883	.1904
.040	.1990	.1981	.2060	.2066	.2103
.060	.2287	.2286	.2373	.2388	.2449
.080	.2552	.2568	.2655	.2656	.2732
.100	.2775	.2786	.2895	.2892	.3005
.120	.2977	.2992	.3103	.3107	.3214
.140	.3136	.3166	.3281	.3300	.3424
.160	.3317	.3340	.3468	.3482	.3613
.180	.3481	.3529	.3661	.3681	.3817
.200	.3657	.3687	.3833	.3869	.4011
.240	.3944	.4003	.4157	.4212	.4399
.280	.4294	.4329	.4501	.4534	.4734
.320	.4581	.4655	.4856	.4909	.5154
.360	.4868	.4915	.5127	.5210	.5479
.400	.5204	.5292	.5520	.5604	.5875
.460	.5664	.5752	.5992	.6090	.6380
.520	.6131	.6230	.6514	.6626	.6957
.580	.6577	.6654	.6931	.7056	.7428
.660	.7257	.7360	.7682	.7807	.8194
.740	.7863	.7947	.8246	.8355	.8762
.820	.8542	.8599	.8881	.8966	.9326
.900	.9062	.9056	.9298	.9363	.9693
.980	.9551	.9512	.9674	.9674	.9944
1.100	.9958	.9874	.9959	.9902	1.0074
1.200	1.0043	.9982	1.0063	1.0021	1.0179
1.400	1.0145	1.0056	1.0143	1.0103	1.0259
1.500	1.0177	1.0077	1.0164	1.0114	1.0248

$\frac{z}{\delta}$					
	1	2	3	4	5

$\frac{z}{\delta}$					
	1	2	3	4	5

TABLE II.- MEASUREMENTS OBTAINED FOR PLATE - Continued

(b) Static-pressure ratio

$x = 6.875$ in. (0.175 m);
 $M = 2.49; R = 1.50 \times 10^6$ per ft (4.92×10^6 per m)

$\frac{z}{\delta}$	$\frac{p_l}{p_\infty}$ for probe -				
	1	2	3	4	5
.000	.9959	1.0009	1.0123	1.0144	.9979
.100	.9971	1.0168	1.0266	1.0221	.9956
.200	.9905	.9936	1.0066	1.0073	.9828
.400	.9798	.9786	.9866	.9911	.9744
.580	.9802	.9790	.9887	.9944	.9815
.820	.9885	.9876	.9955	1.0005	.9879
.980	.9904	.9902	.9967	1.0090	.9927
1.200	.9898	.9919	1.0024	1.0138	.9966
1.400	.9954	.9959	1.0036	1.0145	.9951

$x = 30.000$ in. (0.762 m);
 $M = 2.49; R = 1.50 \times 10^6$ per ft (4.92×10^6 per m)

$\frac{z}{\delta}$	$\frac{p_l}{p_\infty}$ for probe -				
	1	2	3	4	5
.200	1.0032	1.0090	1.0200	1.0257	1.0082
.100	1.0043	1.0161	1.0300	1.0314	1.0086
.200	.9990	.9954	1.0101	1.0144	.9923
.400	1.0005	1.0002	1.0117	1.0159	.9993
.580	.9949	.9961	1.0053	1.0109	.9942
.820	.9961	.9984	1.0088	1.0145	.9986
.980	.9834	.9850	.9941	.9998	.9831
1.200	.9951	.9945	1.0036	1.0093	.9937
1.400	.9986	.9988	1.0064	1.0120	.9969

$x = 6.875$ in. (0.175 m);
 $M = 2.49; R = 3.00 \times 10^6$ per ft (9.83×10^6 per m)

$\frac{z}{\delta}$	$\frac{p_l}{p_\infty}$ for probe -				
	1	2	3	4	5
.000	.9979	1.0030	1.0056	1.0077	1.0058
.010	.9953	.9987	1.0028	1.0042	.9986
.020	.9943	.9994	1.0023	1.0039	.9977
.030	.9921	1.0003	1.0050	1.0040	.9963
.040	.9896	.9990	1.0020	1.0028	.9939
.060	.9900	1.0029	1.0063	1.0056	.9944
.080	.9928	1.0071	1.0125	1.0090	.9964
.100	.9981	1.0036	1.0172	1.0111	1.0001
.120	.9993	1.0028	1.0151	1.0092	.9972
.140	.9948	.9912	1.0040	.9994	.9900
.160	.9905	.9836	.9954	.9928	.9847
.180	.9884	.9792	.9901	.9883	.9808
.200	.9888	.9782	.9881	.9874	.9804
.240	.9950	.9841	.9899	.9902	.9841
.280	1.0024	.9965	.9967	.9956	.9908
.320	1.00052	1.0051	1.0026	.9986	.9950
.360	.9992	1.0005	1.0023	.9976	.9938
.400	.9900	.9883	.9973	.9959	.9933
.460	.9867	.9847	.9935	.9950	.9942
.520	.9863	.9838	.9905	.9912	.9888
.580	.9857	.9927	.9800	.9891	.9861
.660	.9862	.9842	.9880	.9893	.9876
.740	.9871	.9857	.9907	.9900	.9884
.820	.9872	.9856	.9906	.9902	.9878
.900	.9844	.9834	.9867	.9877	.9856
.980	.9736	.9708	.9730	.9741	.9713
1.100	.9815	.9823	.9815	.9822	.9797
1.200	.9855	.9838	.9801	.9868	.9838
1.400	.9892	.9858	.9850	.9893	.9863
1.500	.9897	.9865	.9891	.9898	.9848

$x = 30.000$ in. (0.762 m);
 $M = 2.49; R = 3.00 \times 10^6$ per ft (9.83×10^6 per m)

$\frac{z}{\delta}$	$\frac{p_l}{p_\infty}$ for probe -				
	1	2	3	4	5
.000	.9886	.9938	.9982	.9960	.9904
.100	.9885	1.0003	1.0082	1.0025	.9824
.200	.9769	.9757	.9853	.9795	.9667
.400	.9640	.9677	.9677	.9677	.9623
.580	.9702	.9676	.9717	.9728	.9698
.820	.9804	.9785	.9800	.9810	.9779
.980	.9800	.9799	.9856	.9895	.9938
1.200	.9798	.9813	.9868	.9900	.9846
1.400	.9856	.9849	.9867	.9874	.9809

TABLE II.- MEASUREMENTS OBTAINED FOR PLATE - Continued

(b) Static-pressure ratio - Concluded

 $x = 6.875$ in. (0.175 m); $M = 4.44; R = 3.00 \times 10^6$ per ft (9.83×10^6 per m)

$\frac{z}{\delta}$	$\frac{p_l}{p_\infty}$ for probe -				
	1	2	3	4	5
.000	1.0070	1.0336	1.0554	1.1517	1.0208
.100	1.0033	1.0236	1.0468	1.1432	1.0108
.200	.9941	1.0069	1.0276	1.1261	.9975
.400	.9849	1.0003	1.0190	1.1196	.9908
.580	.9739	.9869	1.0062	1.1068	.9775
.820	.9739	.9836	1.0083	1.1068	.9809
.980	.9794	.9869	1.0083	1.1089	.9809
1.200	.9831	.9869	1.0083	1.1089	.9809
1.400	.9831	.9903	1.0105	1.1132	.9842

 $x = 30.000$ in. (0.762 m); $M = 4.44; R = 3.00 \times 10^6$ per ft (9.83×10^6 per m)

$\frac{z}{\delta}$	$\frac{p_l}{p_\infty}$ for probe -				
	1	2	3	4	5
.000	.9886	1.0169	1.0447	1.1432	1.0275
.010	.9886	1.0169	1.0447	1.1453	1.0275
.020	.9905	1.0169	1.0447	1.1453	1.0275
.030	.9905	1.0169	1.0447	1.1475	1.0242
.040	.9886	1.0169	1.0426	1.1475	1.0208
.060	.9868	1.0136	1.0404	1.1432	1.0175
.080	.9854	1.0089	1.0368	1.1394	1.0127
.100	.9831	1.0036	1.0319	1.1346	1.0108
.120	.9794	.9969	1.0254	1.1303	1.0042
.140	.9721	.9903	1.0169	1.1218	.9975
.160	.9666	.9836	1.0083	1.1154	.9908
.180	.9629	.9803	1.0040	1.1132	.9875
.200	.9597	.9722	.9984	1.1074	.9828
.240	.9556	.9669	.9912	1.1025	.9775
.280	.9537	.9669	.9891	1.1004	.9775
.320	.9505	.9622	.9855	1.0967	.9728
.360	.9519	.9636	.9848	1.0982	.9775
.400	.9500	.9636	.9869	1.1004	.9775
.460	.9487	.9622	.9855	1.0988	.9795
.520	.9500	.9636	.9891	1.1025	.9809
.580	.9524	.9656	.9941	1.1074	.9861
.660	.9574	.9702	.9998	1.1132	.9942
.740	.9592	.9736	1.0040	1.1154	.9975
.820	.9611	.9769	1.0040	1.1175	1.0008
.900	.9647	.9769	1.0062	1.1175	1.0008
.980	.9684	.9803	1.0062	1.1175	1.0008
1.100	.9703	.9836	1.0083	1.1196	1.0008
1.200	.9707	.9855	1.0112	1.1223	1.0028
1.400	.9776	.9936	1.0212	1.1303	1.0142
1.500	.9817	.9989	1.0283	1.1373	1.0194

$\frac{z}{\delta}$					
	1	2	3	4	5

$\frac{z}{\delta}$					
	1	2	3	4	5

TABLE II.- MEASUREMENTS OBTAINED FOR PLATE - Continued

(c) Total-temperature ratio - Concluded

x = 6.875 in. (0.175 m);

M = 4.44; R = 3.00×10^6 per ft (9.83×10^6 per m)

$\frac{z}{\delta}$	$\frac{T_{t,L}}{T_{t,\infty}}$ for probe -				
	1	2	3	4	5
.000	.9036	.9055	.9019	.9019	.9044
.010	.9069	.9060	.9093	.9098	.9084
.020	.9132	.9081	.9138	.9152	.9144
.030	.9197	.9135	.9206	.9214	.9213
.040	.9268	.9181	.9251	.9272	.9269
.060	.9331	.9227	.9311	.9327	.9338
.080	.9398	.9296	.9368	.9393	.9390
.100	.9410	.9302	.9393	.9414	.9430
.120	.9460	.9339	.9420	.9464	.9457
.140	.9459	.9354	.9433	.9434	.9451
.160	.9475	.9367	.9452	.9487	.9520
.180	.9532	.9407	.9498	.9530	.9544
.200	.9535	.9426	.9506	.9526	.9534
.240	.9536	.9436	.9512	.9540	.9574
.280	.9630	.9510	.9569	.9599	.9620
.320	.9625	.9518	.9597	.9645	.9663
.360	.9716	.9622	.9679	.9738	.9762
.400	.9680	.9583	.9665	.9693	.9720
.460	.9722	.9616	.9691	.9740	.9754
.520	.9736	.9655	.9716	.9772	.9787
.580	.9768	.9681	.9729	.9786	.9807
.660	.9853	.9766	.9826	.9870	.9874
.740	.9843	.9764	.9831	.9864	.9867
.820	.9892	.9818	.9853	.9918	.9925
.900	.9935	.9864	.9909	.9944	.9952
.980	.9952	.9892	.9922	.9956	.9952
1.100	.9920	.9877	.9907	.9924	.9933
1.200	.9932	.9895	.9919	.9949	.9960
1.400	.9979	.9932	.9960	.9972	.9969
1.500	.9953	.9915	.9947	.9947	.9948

x = 30.000 in. (0.762 m);

M = 4.44; R = 3.00×10^6 per ft (9.83×10^6 per m)

$\frac{z}{\delta}$	$\frac{T_{t,L}}{T_{t,\infty}}$ for probe -				
	1	2	3	4	5
.000	.9059	.9084	.9047	.9052	.9073
.010	.9060	.9049	.9082	.9072	.9081
.020	.9136	.9091	.9153	.9169	.9186
.030	.9199	.9132	.9205	.9232	.9236
.040	.9257	.9179	.9257	.9278	.9291
.060	.9323	.9232	.9307	.9338	.9361
.080	.9370	.9260	.9347	.9367	.9376
.100	.9413	.9313	.9394	.9412	.9439
.120	.9429	.9315	.9411	.9419	.9445
.140	.9491	.9388	.9456	.9485	.9510
.160	.9443	.9346	.9443	.9463	.9483
.180	.9500	.9379	.9455	.9489	.9491
.200	.9515	.9410	.9487	.9527	.9546
.240	.9571	.9462	.9520	.9562	.9586
.280	.9594	.9477	.9553	.9572	.9588
.320	.9653	.9532	.9600	.9640	.9667
.360	.9645	.9533	.9593	.9644	.9656
.400	.9661	.9555	.9628	.9648	.9667
.460	.9732	.9636	.9702	.9735	.9764
.520	.9731	.9623	.9697	.9725	.9754
.580	.9769	.9678	.9717	.9785	.9801
.660	.9818	.9722	.9784	.9825	.9838
.740	.9805	.9717	.9760	.9813	.9828
.820	.9890	.9811	.9875	.9898	.9910
.900	.9924	.9850	.9903	.9928	.9932
.980	.9916	.9859	.9892	.9928	.9931
1.100	.9964	.9920	.9942	.9987	.9991
1.200	.9943	.9897	.9936	.9979	.9936
1.400	.9941	.9908	.9925	.9960	.9965
1.500	.9979	.9933	.9964	.9969	.9972

$\frac{z}{\delta}$					
	1	2	3	4	5

$\frac{z}{\delta}$					
	1	2	3	4	5

TABLE II.- MEASUREMENTS OBTAINED FOR PLATE - Continued

(d) Velocity ratio

$x = 6.875$ in. (0.175 m);
 $M = 2.49$; $R = 1.50 \times 10^6$ per ft (4.92×10^6 per m)

$\frac{z}{\delta}$	$\frac{u_L}{u_\infty}$ for probe -				
	1	2	3	4	5
.000	.5058	.4751	.4599	.5005	.5509
.100	.7741	.7619	.7641	.7597	.7689
.200	.8327	.8220	.8230	.8192	.8293
.400	.9087	.9002	.9027	.8983	.9062
.580	.9551	.9481	.9491	.9447	.9494
.820	.9881	.9819	.9841	.9801	.9847
.980	.9905	.9855	.9865	.9819	.9874
1.200	.9946	.9897	.9895	.9854	.9906
1.400	.9926	.9882	.9866	.9848	.9909

$x = 30.000$ in. (0.762 m);
 $M = 2.49$; $R = 1.50 \times 10^6$ per ft (4.92×10^6 per m)

$\frac{z}{\delta}$	$\frac{u_L}{u_\infty}$ for probe -				
	1	2	3	4	5
.000	.4636	.4613	.4435	.4662	.5160
.100	.7666	.7544	.7568	.7519	.7602
.200	.8238	.8155	.8170	.8113	.8186
.400	.8939	.8854	.8877	.8821	.8892
.580	.9411	.9327	.9357	.9289	.9364
.820	.9794	.9728	.9729	.9691	.9757
.980	.9919	.9868	.9871	.9842	.9900
1.200	.9924	.9882	.9889	.9866	.9916
1.400	.9925	.9880	.9890	.9865	.9914

$x = 6.875$ in. (0.175 m);
 $M = 2.49$; $R = 3.00 \times 10^6$ per ft (9.83×10^6 per m)

$\frac{z}{\delta}$	$\frac{u_L}{u_\infty}$ for probe -				
	1	2	3	4	5
.000	.5021	.5007	.4919	.5138	.5651
.100	.6328	.6172	.6243	.6258	.5988
.200	.6801	.6680	.6721	.6715	.6616
.300	.7071	.6965	.7007	.7006	.6983
.400	.7281	.7183	.7208	.7176	.7177
.600	.7572	.7449	.7481	.7473	.7492
.800	.7784	.7640	.7642	.7642	.7683
.100	.7912	.7806	.7832	.7810	.7855
.120	.8063	.7978	.7974	.7942	.7983
.140	.8172	.8100	.8093	.8073	.8109
.160	.8286	.8236	.8245	.8221	.8244
.180	.8382	.8323	.8344	.8336	.8362
.200	.8477	.8439	.8459	.8464	.8442
.240	.8632	.8565	.8588	.8573	.8608
.280	.8790	.8738	.8766	.8722	.8727
.320	.8938	.8867	.8911	.8881	.8889
.360	.9075	.9007	.9040	.9031	.9040
.400	.9228	.9151	.9175	.9143	.9145
.460	.9364	.9301	.9315	.9292	.9305
.520	.9517	.9447	.9441	.9412	.9429
.580	.9592	.9549	.9573	.9560	.9600
.660	.9789	.9743	.9758	.9730	.9738
.740	.9877	.9823	.9826	.9803	.9819
.820	.9938	.9898	.9900	.9887	.9900
.900	.9953	.9917	.9926	.9923	.9939
.980	.9970	.9931	.9945	.9926	.9937
1.100	.9981	.9948	.9960	.9948	.9959
1.200	.9981	.9954	.9958	.9952	.9965
1.400	.9975	.9950	.9953	.9944	.9954

$x = 30.000$ in. (0.762 m);
 $M = 2.49$; $R = 3.00 \times 10^6$ per ft (9.83×10^6 per m)

$\frac{z}{\delta}$	$\frac{u_L}{u_\infty}$ for probe -				
	1	2	3	4	5
.000	.4959	.4957	.4887	.5064	.5393
.100	.7826	.7723	.7768	.7751	.7793
.200	.8408	.8342	.8366	.8359	.8401
.400	.9121	.9057	.9098	.9074	.9104
.580	.9575	.9518	.9544	.9519	.9529
.820	.9911	.9855	.9872	.9850	.9864
.980	.9965	.9922	.9934	.9920	.9938
1.200	.9991	.9950	.9944	.9938	.9956
1.400	.9983	.9960	.9962	.9954	.9971

TABLE II.- MEASUREMENTS OBTAINED FOR PLATE - Concluded

(d) Velocity ratio - Concluded

$x = 6.875$ in. (0.175 m);
 $M = 4.44$; $R = 3.00 \times 10^6$ per ft (9.83×10^6 per m)

$\frac{z}{\delta}$	$\frac{u_l}{u_\infty}$ for probe -				
	1	2	3	4	5
.000	.4452	.4885	.4073	.4321	.5374
.100	.7816	.7732	.7802	.7610	.7902
.200	.8411	.8376	.8436	.8279	.8524
.400	.9073	.9026	.9102	.8987	.9193
.580	.9461	.9412	.9457	.9372	.9556
.820	.9802	.9751	.9771	.9695	.9815
.980	.9953	.9901	.9904	.9808	.9858
1.200	.9973	.9934	.9927	.9828	.9944
1.400	.9988	.9945	.9942	.9831	.9941

$x = 30.000$ in. (0.762 m);
 $M = 4.44$; $R = 3.00 \times 10^6$ per ft (9.83×10^6 per m)

$\frac{z}{\delta}$	$\frac{u_l}{u_\infty}$ for probe -				
	1	2	3	4	5
.000	.3920	.4859	.3661	.3669	.4750
.010	.6005	.5789	.5893	.5694	.5753
.020	.6453	.6318	.6384	.6176	.6447
.030	.6745	.6632	.6691	.6483	.6771
.040	.6961	.6859	.6919	.6716	.7016
.060	.7298	.7204	.7257	.7076	.7387
.080	.7557	.7476	.7524	.7332	.7632
.100	.7750	.7676	.7730	.7539	.7850
.120	.7909	.7836	.7893	.7704	.8001
.140	.8039	.7977	.8024	.7855	.8150
.160	.8154	.8091	.8158	.7981	.8251
.180	.8285	.8224	.8280	.8112	.8394
.200	.8378	.8323	.8380	.8224	.8465
.240	.8544	.8501	.8550	.8404	.8692
.280	.8712	.8649	.8710	.8551	.8791
.320	.8838	.8788	.8849	.8712	.8947
.360	.8940	.8884	.8943	.8819	.9046
.400	.9057	.9012	.9074	.8940	.9162
.460	.9202	.9159	.9213	.9095	.9304
.520	.9329	.9280	.9340	.9227	.9375
.580	.9440	.9392	.9427	.9339	.9548
.660	.9577	.9531	.9577	.9481	.9671
.740	.9680	.9631	.9660	.9574	.9707
.820	.9798	.9749	.9785	.9683	.9751
.900	.9870	.9818	.9841	.9743	.9842
.980	.9909	.9864	.9871	.9774	.9917
1.100	.9947	.9904	.9898	.9801	.9924
1.200	.9951	.9909	.9909	.9791	.9837
1.400	.9956	.9917	.9904	.9809	.9853
1.500	.9976	.9927	.9920	.9810	.9924

$\frac{z}{\delta}$					
	1	2	3	4	5

$\frac{z}{\delta}$					
	1	2	3	4	5

TABLE III.- MEASUREMENTS OBTAINED FOR PLATE WITH CYLINDER - Continued

(a) Total-pressure ratio - Continued

 $x = 30.000 \text{ in. (0.762 m)}$ $M = 2.49; R = 3.00 \times 10^6 \text{ per ft (9.83} \times 10^6 \text{ per m)}$

$\frac{z}{\delta}$	$\frac{(p_{t,2})_L}{(p_{t,2})_\infty}$ for probe -				
	1	2	3	4	5
.000	.2262	.2181	.1981	.2033	.2201
.004	.2801	.2387	.2265	.2308	.2072
.010	.3573	.3193	.2791	.2718	.2521
.020	.4168	.3808	.3280	.3127	.3028
.030	.4546	.4182	.3596	.3414	.3373
.040	.4795	.4421	.3821	.3612	.3594
.060	.5083	.4688	.4125	.3946	.3974
.080	.5281	.4896	.4383	.4223	.4309
.100	.5438	.5056	.4612	.4503	.4599
.120	.5508	.5139	.4756	.4695	.4803
.140	.5527	.5170	.4861	.4869	.4994
.160	.5542	.5225	.4972	.4995	.5143
.180	.5614	.5304	.5102	.5161	.5285
.200	.5626	.5355	.5215	.5300	.5415
.240	.5701	.5505	.5476	.5580	.5683
.280	.5761	.5661	.5734	.5861	.5979
.320	.5781	.5793	.5978	.6124	.6262
.360	.5856	.5987	.6304	.6442	.6563
.400	.5867	.6099	.6577	.6712	.6826
.460	.5824	.6194	.6888	.7076	.7187
.520	.5713	.6148	.7111	.7432	.7578
.580	.5571	.5963	.7180	.7713	.7836
.660	.5378	.5659	.6867	.8007	.8296
.740	.5245	.5440	.6378	.7907	.8473
.820	.5202	.5368	.5988	.7435	.8431
.900	.5247	.5453	.5973	.6828	.8086
.980	.5386	.5623	.6195	.6435	.7809
1.100	.5549	.5818	.6581	.6386	.7418
1.200	.5589	.5853	.6797	.6795	.7020
1.400	.5478	.5717	.6746	.7211	.7620

$\frac{z}{\delta}$					
	1	2	3	4	5

$\frac{z}{\delta}$					
	1	2	3	4	5

$\frac{z}{\delta}$					
	1	2	3	4	5

TABLE III.- MEASUREMENTS OBTAINED FOR PLATE WITH CYLINDER - Continued

(a) Total-pressure ratio - Concluded

 $x = 30.000 \text{ in. (} 0.762 \text{ m)}$ $M = 4.44; R = 3.00 \times 10^6 \text{ per ft (} 9.83 \times 10^6 \text{ per m)}$

$\frac{z}{\delta}$	$\frac{(p_{t,2})_L}{(p_{t,2})_\infty}$ for probe -				
	1	2	3	4	5
.000	.0631	.0732	.0574	.0726	.0794
.004	.0897	.0745	.0778	.0673	.0867
.010	.1322	.1343	.1394	.1328	.1528
.020	.1620	.1702	.1780	.1746	.1947
.030	.1800	.1903	.2020	.2015	.2220
.040	.1973	.2115	.2260	.2262	.2472
.060	.2204	.2419	.2614	.2637	.2870
.080	.2476	.2659	.2896	.2949	.3185
.100	.2544	.2333	.3126	.3196	.3447
.120	.2668	.2991	.3350	.3438	.3714
.140	.2745	.3134	.3491	.3625	.3908
.160	.2820	.3202	.3627	.3786	.4076
.180	.2873	.3289	.3773	.3936	.4223
.200	.2916	.3344	.3867	.4054	.4380
.240	.2958	.3423	.4044	.4269	.4653
.280	.2969	.3420	.4148	.4473	.4936
.320	.2958	.3387	.4200	.4688	.5128
.360	.2926	.3311	.4200	.4892	.5471
.400	.2895	.3224	.4117	.5042	.5712
.450	.2923	.3033	.3898	.5139	.5975
.520	.2767	.2945	.3700	.5042	.5121
.580	.2725	.2931	.3564	.4774	.6121
.660	.2703	.2920	.3564	.4301	.5943
.740	.2767	.2775	.3710	.4912	.5545
.820	.2984	.3115	.3008	.4076	.5146
.900	.3022	.3235	.4065	.4366	.5094
.980	.3171	.3344	.4180	.4677	.5198
1.100	.3330	.3441	.4274	.4967	.5471
1.200	.3426	.3474	.4305	.5031	.5817
1.400	.3490	.3445	.4274	.4978	.5912
1.500	.3511	.3474	.4242	.4881	.5912

$\frac{z}{\delta}$					
	1	2	3	4	5

$\frac{z}{\delta}$					
	1	2	3	4	5

$\frac{z}{\delta}$					
	1	2	3	4	5

TABLE III.- MEASUREMENTS OBTAINED FOR PLATE WITH CYLINDER - Continued

(b) Static-pressure ratio - Continued

 $x = 30.000 \text{ in. (} 0.762 \text{ m)}$; $M = 2.49; R = 3.00 \times 10^6 \text{ per ft (} 9.83 \times 10^6 \text{ per m)}$

$\frac{z}{\delta}$	$\frac{p_l}{p_\infty}$ for probe -				
	1	2	3	4	5
.000	.9636	.9624	.9622	.9633	.9607
.010	.9572	.9574	.9592	.9606	.9535
.020	.9559	.9554	.9591	.9594	.9532
.030	.9546	.9557	.9590	.9590	.9523
.040	.9512	.9553	.9583	.9579	.9509
.060	.9455	.9529	.9604	.9597	.9490
.080	.9464	.9510	.9684	.9680	.9516
.100	.9503	.9486	.9721	.9710	.9519
.120	.9440	.9447	.9715	.9700	.9531
.140	.9355	.9335	.9619	.9612	.9469
.160	.9318	.9276	.9521	.9510	.9405
.180	.9291	.9240	.9459	.9448	.9375
.200	.9288	.9232	.9440	.9430	.9361
.280	.9235	.9168	.9354	.9390	.9336
.320	.9210	.9139	.9328	.9364	.9324
.360	.9197	.9113	.9296	.9332	.9299
.400	.9183	.9084	.9264	.9304	.9286
.460	.9176	.9088	.9259	.9310	.9313
.520	.9180	.9111	.9274	.9332	.9347
.580	.9184	.9144	.9308	.9365	.9380
.660	.9191	.9181	.9325	.9361	.9383
.740	.9235	.9229	.9361	.9368	.9392
.820	.9288	.9283	.9405	.9416	.9429
.900	.9340	.9330	.9437	.9480	.9454
.980	.9384	.9364	.9453	.9507	.9449
1.100	.9436	.9406	.9477	.9517	.9479
1.200	.9463	.9438	.9488	.9502	.9494
1.400	.9455	.9451	.9446	.9503	.9590
1.500	.9260	.9389	.9487	.9566	.9646

$\frac{z}{\delta}$					
	1	2	3	4	5

$\frac{z}{\delta}$					
	1	2	3	4	5

$\frac{z}{\delta}$					
	1	2	3	4	5

TABLE III.- MEASUREMENTS OBTAINED FOR PLATE WITH CYLINDER - Continued
 (b) Static-pressure ratio - Concluded

$x = 30.000$ in. (0.762 m);

$M = 4.44; R = 3.00 \times 10^6$ per ft (9.83×10^6 per m)

$\frac{z}{\delta}$	$\frac{p_l}{p_\infty}$ for probe -				
	1	2	3	4	5
.000	1.0157	1.0407	1.0566	1.1510	1.0212
.010	1.0199	1.0422	1.0581	1.1526	1.0226
.020	1.0190	1.0422	1.0581	1.1548	1.0226
.030	1.0176	1.0407	1.0566	1.1531	1.0179
.040	1.0190	1.0422	1.0581	1.1548	1.0160
.060	1.0190	1.0422	1.0581	1.1548	1.0126
.080	1.0157	1.0374	1.0544	1.1510	1.0112
.100	1.0098	1.0255	1.0452	1.1419	1.0026
.120	.9987	1.0154	1.0323	1.1311	.9959
.140	.9936	1.0073	1.0265	1.1274	.9945
.160	.9913	1.0054	1.0237	1.1268	.9926
.180	.9877	1.0054	1.0215	1.1247	.9959
.200	.9844	1.0006	1.0180	1.1209	.9945
.240	.9821	.9987	1.0172	1.1204	.9992
.280	.9752	.9939	1.0115	1.1124	1.0012
.320	.9711	.9920	1.0087	1.1096	1.0059
.360	.9674	.9886	1.0065	1.1096	1.0093
.400	.9619	.9853	1.0044	1.1096	1.0126
.460	.9582	.9853	1.0044	1.1139	1.0126
.520	.9545	.9819	1.0044	1.1139	1.0126
.580	.9490	.9819	1.0065	1.1182	1.0160
.660	.9471	.9786	1.0108	1.1247	1.0260
.740	.9458	.9806	1.0115	1.1252	1.0312
.820	.9490	.9853	1.0172	1.1311	1.0360
.900	.9545	.9886	1.0215	1.1354	1.0360
.980	.9605	.9939	1.0265	1.1381	1.0379
1.100	.9734	1.0040	1.0330	1.1445	1.0446
1.200	.9858	1.0154	1.0409	1.1505	1.0494
1.400	.9973	1.0207	1.0459	1.1531	1.0512
1.500	1.0047	1.0274	1.0459	1.1531	1.0546

$\frac{z}{\delta}$					
	1	2	3	4	5

$\frac{z}{\delta}$					
	1	2	3	4	5

$\frac{z}{\delta}$					
	1	2	3	4	5

TABLE III.- MEASUREMENTS OBTAINED FOR PLATE WITH CYLINDER - Continued

(c) Total-temperature ratio - Continued

 $x = 30.000$ in. (0.762 m); $M = 2.49; R = 3.00 \times 10^6$ per ft (9.83×10^6 per m)

$\frac{z}{\delta}$	$\frac{T_{t,L}}{T_{t,\infty}}$ for probe -				
	1	2	3	4	5
.000	.9471	.9513	.9487	.9473	.9384
.010	.9470	.9506	.9491	.9479	.9386
.020	.9549	.9538	.9561	.9527	.9438
.030	.9689	.9626	.9640	.9590	.9496
.040	.9776	.9693	.9709	.9611	.9535
.060	.9873	.9769	.9785	.9667	.9603
.080	.9928	.9812	.9823	.9718	.9653
.100	.9939	.9802	.9814	.9713	.9672
.120	.9971	.9837	.9841	.9757	.9714
.140	.9974	.9818	.9834	.9762	.9737
.160	.9974	.9840	.9847	.9788	.9762
.180	.9969	.9819	.9844	.9790	.9777
.200	1.0002	.9850	.9880	.9833	.9813
.240	.9981	.9840	.9883	.9854	.9830
.280	.9986	.9855	.9889	.9863	.9842
.320	1.0037	.9918	.9952	.9906	.9886
.360	1.0009	.9922	.9965	.9911	.9892
.400	1.0012	.9955	1.0003	.9935	.9908
.460	1.0014	.9983	1.0022	.9990	.9967
.520	.9979	.9974	1.0016	1.0015	.9985
.580	.9924	.9925	.9971	1.0008	.9980
.660	.9890	.9883	.9932	1.0024	1.0009
.740	.9843	.9847	.9882	.9988	.9998
.820	.9848	.9857	.9886	.9957	.9962
.900	.9860	.9856	.9912	.9947	.9955
.980	.9921	.9904	.9959	.9945	.9963
1.100	.9958	.9935	.9976	.9959	.9969
1.200	.9978	.9951	.9984	.9978	.9972
1.400	.9964	.9955	.9970	.9976	.9975
1.500	1.0007	.9962	.9974	.9976	.9975

$\frac{z}{\delta}$					
	1	2	3	4	5

$\frac{z}{\delta}$					
	1	2	3	4	5

$\frac{z}{\delta}$					
	1	2	3	4	5

TABLE III.- MEASUREMENTS OBTAINED FOR PLATE WITH CYLINDER - Continued

(c) Total-temperature ratio - Concluded

 $x = 30.000$ in. (0.762 m); $M = 4.44; R = 3.00 \times 10^6$ per ft (9.83×10^6 per m)

$\frac{z}{\delta}$	$\frac{T_{t,l}}{T_{t,\infty}}$ for probe -				
	1	2	3	4	5
.000	.9151	.9207	.9163	.9187	.9173
.010	.9175	.9191	.9238	.9238	.9204
.020	.9240	.9226	.9325	.9304	.9276
.030	.9340	.9317	.9417	.9409	.9385
.040	.9385	.9366	.9467	.9442	.9421
.060	.9519	.9489	.9638	.9566	.9566
.080	.9583	.9545	.9689	.9611	.9615
.100	.9676	.9634	.9786	.9674	.9686
.120	.9717	.9670	.9827	.9693	.9701
.140	.9748	.9711	.9868	.9715	.9727
.160	.9794	.9764	.9900	.9766	.9764
.180	.9847	.9797	.9921	.9795	.9784
.200	.9861	.9826	.9948	.9815	.9805
.240	.9887	.9859	.9948	.9842	.9820
.280	.9902	.9875	.9964	.9886	.9847
.320	.9893	.9851	.9912	.9919	.9870
.360	.9885	.9822	.9879	.9957	.9911
.400	.9852	.9783	.9846	.9967	.9935
.460	.9814	.9744	.9804	.9958	.9963
.520	.9788	.9739	.9795	.9941	.9995
.580	.9731	.9693	.9732	.9822	.9943
.660	.9704	.9700	.9715	.9763	.9897
.740	.9745	.9717	.9740	.9797	.9895
.820	.9778	.9744	.9776	.9851	.9897
.900	.9861	.9797	.9847	.9928	.9955
.980	.9903	.9810	.9884	.9942	.9957
1.100	.9949	.9840	.9936	.9951	.9960
1.200	.9971	.9863	.9961	.9968	.9977
1.400	.9956	.9859	.9956	.9949	.9959
1.500	.9945	.9855	.9940	.9945	.9961

$\frac{z}{\delta}$	1	2	3	4	5

$\frac{z}{\delta}$					
	1	2	3	4	5

$\frac{z}{\delta}$	1	2	3	4	5

TABLE III.- MEASUREMENTS OBTAINED FOR PLATE WITH CYLINDER - Continued

(d) Velocity ratio - Continued

$x = 30.000$ in. (0.762 m);
 $M = 2.49$; $R = 3.00 \times 10^6$ per ft (9.83×10^6 per m)

$\frac{z}{\delta}$	$\frac{u_l}{u_\infty}$ for probe -				
	1	2	3	4	5
.000	.5494	.5376	.4990	.5089	.5383
.010	.7020	.6683	.6240	.6144	.5887
.020	.7520	.7245	.6781	.6617	.6505
.030	.7835	.7561	.7097	.6917	.6867
.040	.8037	.7752	.7310	.7102	.7081
.060	.8261	.7961	.7563	.7387	.7417
.080	.8391	.8111	.7736	.7585	.7670
.100	.8472	.8211	.7877	.7769	.7872
.120	.8532	.8277	.7973	.7905	.8006
.140	.8572	.8324	.8066	.8044	.8149
.160	.8593	.8382	.8168	.8161	.8265
.180	.8637	.8429	.8261	.8276	.8357
.200	.8649	.8462	.8337	.8366	.8439
.280	.8740	.8654	.8654	.8687	.8749
.320	.8774	.8749	.8794	.8830	.8892
.360	.8801	.8849	.8954	.8978	.9029
.400	.8810	.8921	.9093	.9104	.9141
.460	.8793	.8976	.9227	.9268	.9295
.520	.8722	.8942	.9301	.9400	.9433
.580	.8624	.8826	.9295	.9480	.9505
.660	.8507	.8651	.9155	.9583	.9657
.740	.8406	.8512	.8927	.9536	.9703
.820	.8365	.8460	.8740	.9347	.9648
.900	.8383	.8493	.8739	.9106	.9530
.980	.8475	.8594	.8862	.8942	.9440
1.100	.8553	.8636	.9021	.8920	.9314
1.200	.8575	.8701	.9109	.9102	.9187
1.400	.8519	.8637	.9098	.9261	.9380

$\frac{z}{\delta}$					
	1	2	3	4	5

$\frac{z}{\delta}$					
	1	2	3	4	5

$\frac{z}{\delta}$					
	1	2	3	4	5

TABLE III.- MEASUREMENTS OBTAINED FOR PLATE WITH CYLINDER - Concluded

(d) Velocity ratio - Concluded

$x = 30.000$ in. (0.762 m);
 $M = 4.44; R = 3.00 \times 10^6$ per ft (9.83×10^6 per m)

$\frac{z}{\delta}$	$\frac{u_l}{u_\infty}$ for probe -				
	1	2	3	4	5
.000	.3802	.4103	.3897	.3865	.4552
.010	.5912	.5900	.5969	.5631	.6260
.020	.6430	.6489	.6594	.6332	.6851
.030	.6712	.6787	.6919	.6708	.7186
.040	.6935	.7038	.7191	.6986	.7434
.060	.7225	.7369	.7562	.7363	.7798
.080	.7462	.7617	.7820	.7642	.8035
.100	.7623	.7800	.8023	.7842	.8218
.120	.7769	.7952	.8197	.8023	.8376
.140	.7860	.8067	.8324	.8152	.8496
.160	.7936	.8151	.8415	.8256	.8600
.180	.8003	.8217	.8501	.8345	.8617
.200	.8045	.8268	.8552	.8416	.8738
.240	.8092	.8334	.8650	.8526	.8813
.280	.8112	.8342	.874	.8635	.8917
.320	.8115	.8323	.8715	.8742	.8979
.360	.8093	.8268	.8699	.8827	.9080
.400	.8065	.8204	.8649	.8879	.9119
.460	.8009	.8102	.8516	.8904	.9223
.520	.7965	.8041	.8436	.8863	.9179
.580	.7928	.7992	.8341	.8717	.9073
.660	.7902	.7991	.8322	.8493	.9051
.740	.7969	.8044	.8406	.8377	.8859
.820	.8061	.8126	.8509	.8423	.8905
.900	.8169	.8208	.8595	.8569	.8914
.980	.8275	.8273	.8558	.8700	.8985
1.100	.8367	.8325	.8712	.8803	.9076
1.200	.8401	.8326	.8717	.8818	.9073
1.400	.8409	.8321	.8695	.8789	.9132
1.500	.8405	.8304	.8678	.8755	.9135

$\frac{z}{\delta}$					
	1	2	3	4	5

$\frac{z}{\delta}$					
	1	2	3	4	5

$\frac{z}{\delta}$					
	1	2	3	4	5

TABLE IV.- MEASUREMENTS OBTAINED FOR PLATE WITH FAIRING - Continued

(a) Total-pressure ratio - Continued

$x = 30.000$ in. (0.762 m);
 $M = 2.49$; $R = 3.00 \times 10^6$ per ft (9.83×10^6 per m)

$\frac{z}{\delta}$	$\frac{(p_{t,2})_L}{(p_{t,2})_\infty}$ for probe -				
	1	2	3	4	5
.000	.2772	.2451	.2206	.2002	.1910
.004	.2650	.2369	.2128	.1955	.2107
.010	.2839	.2591	.2614	.2389	.2497
.020	.4604	.3527	.3362	.2734	.2772
.030	.5294	.4923	.3756	.3239	.3000
.040	.5712	.4230	.3974	.3425	.3144
.060	.6035	.4535	.4234	.3538	.3416
.080	.6205	.4084	.4436	.3597	.3662
.100	.6356	.4800	.4596	.3651	.3876
.120	.6357	.4812	.4676	.3663	.4041
.140	.6510	.4935	.4848	.3757	.4281
.160	.6566	.5103	.4956	.3840	.4481
.180	.6666	.5133	.5076	.3954	.4687
.200	.6722	.5248	.5213	.4188	.4858
.240	.5967	.5553	.5522	.4670	.5292
.280	.7159	.5834	.5844	.5184	.5670
.320	.7432	.6237	.6151	.5671	.6075
.360	.7551	.6437	.6423	.6110	.6353
.400	.7752	.6312	.6721	.6537	.6739
.450	.8138	.7212	.7061	.5947	.7135
.520	.8272	.7512	.7515	.7450	.7598
.580	.8555	.8137	.7307	.7834	.8054
.640	.9356	.9484	.8397	.8334	.8554
.740	.9114	.9850	.9733	.9775	.9772
.810	.9341	.9144	.9187	.9164	.9353
.900	.9444	.9343	.9011	.9410	.9562
.940	.9541	.9455	.9566	.9570	.9525
1.100	.9684	.9520	.9754	.9785	.9846
1.200	.9775	.9725	.9849	.9956	.9974
1.400	.9953	.9875	.9922	.9919	.9951
1.500	.9971	.9837	.9940	.9932	.9958

$\frac{z}{\delta}$					
	1	2	3	4	5

$\frac{z}{\delta}$					
	1	2	3	4	5

$\frac{z}{\delta}$					
	1	2	3	4	5

TABLE IV.- MEASUREMENTS OBTAINED FOR PLATE WITH FAIRING - Continued

(a) Total-pressure ratio - Concluded

 $x = 30.000$ in. (0.762 m); $M = 4.44; R = 3.00 \times 10^6$ per ft (9.83×10^6 per m)

$\frac{z}{\delta}$	$\frac{(p_t, 2)}{(p_t, 2)_\infty} L$ for probe -				
	1	2	3	4	5
.000	.7589	.0742	.7592	.0570	.0639
.014	.0795	.6733	.7582	.0549	.0618
.019	.1582	.1470	.1115	.0914	.1122
.020	.1354	.1850	.1449	.1193	.1426
.030	.2177	.2046	.1616	.1333	.1584
.040	.2411	.2242	.1762	.1473	.1741
.050	.2698	.2503	.1940	.1688	.2014
.080	.2879	.2597	.2023	.1870	.2235
.100	.3057	.2745	.2086	.2042	.2455
.120	.3113	.2375	.2169	.2236	.2655
.140	.3220	.3015	.2274	.2429	.2864
.150	.3305	.3071	.2378	.2580	.3222
.180	.3443	.3212	.2556	.2805	.3253
.200	.3571	.3352	.2754	.2984	.3431
.240	.3825	.3513	.3203	.3407	.3430
.280	.4134	.3927	.3705	.3837	.4240
.320	.4400	.4113	.4143	.4245	.4628
.350	.4587	.4492	.4561	.4675	.5048
.400	.4932	.4712	.4927	.5073	.5468
.450	.5272	.5071	.5178	.5594	.6114
.500	.5612	.5452	.5783	.5750	.6117
.530	.5931	.5359	.6211	.5923	.7332
.660	.6340	.6342	.5765	.7114	.7593
.740	.6399	.6354	.7444	.7802	.8375
.820	.7569	.7622	.4185	.4522	.9100
.900	.8356	.8353	.8781	.9738	.4572
.980	.9026	.9011	.9313	.7439	.9950
1.100	.9717	.9774	.9887	.9983	.9824
1.200	1.0111	1.0055	1.0211	1.0144	.9241
1.400	.9579	.9163	.8302	.8253	.8659
1.500	.3080	.8335	.8248	.8414	.8306

$\frac{z}{\delta}$	1	2	3	4	5

$\frac{z}{\delta}$	1	2	3	4	5

$\frac{z}{\delta}$	1	2	3	4	5

TABLE IV.- MEASUREMENTS OBTAINED FOR PLATE WITH FAIRING - Continued

(b) Static-pressure ratio

 $x = 6.875$ in. (0.175 m); $M = 2.49; R = 1.50 \times 10^6$ per ft (4.92×10^6 per m) $x = 10.000$ in. (0.254 m); $M = 2.49; R = 1.50 \times 10^6$ per ft (4.92×10^6 per m)

$\frac{z}{\delta}$	$\frac{p_l}{p_\infty}$ for probe -				
	1	2	3	4	5
.000	1.1692	1.0647	.9463	.6825	.8335
.010	1.1539	1.0492	.9457	.6811	.8225
.020	1.1375	1.0537	.9543	.6754	.8181
.030	1.1252	1.0554	.9548	.6708	.8174
.040	1.1169	1.0590	.9479	.6681	.8165
.060	1.0987	1.0649	.9345	.6611	.8122
.080	1.0831	1.0668	.9322	.6573	.8087
.100	1.0712	1.0711	.9298	.6565	.8085
.120	1.0655	1.0765	.9261	.6535	.8062
.140	1.0670	1.0805	.9150	.6483	.8048
.160	1.0736	1.0849	.8963	.6439	.8013
.180	1.0814	1.0832	.8743	.6438	.8010
.200	1.0887	1.0926	.8356	.6445	.8021
.240	1.1008	1.0958	.7374	.6487	.8098
.280	1.1102	1.1009	.6306	.6542	.8217
.320	1.1122	1.1138	.5459	.6582	.8235
.360	1.1019	1.0915	.5139	.6618	.8394
.400	1.0789	1.0462	.5020	.6699	.8508
.460	1.0215	.8994	.5005	.6873	.8709
.520	.9442	.6951	.5210	.7181	.8859
.580	.8110	.5652	.5584	.7599	.8852
.660	.5394	.5190	.6162	.8136	.8595
.740	.5034	.5359	.6722	.8468	.8341
.820	.5558	.5835	.7218	.8134	.8458
.900	.6345	.6566	.7628	.7971	.8853
.980	.7213	.7416	.7982	.8251	.9380
1.100	.8430	.8398	.8342	.9093	1.0362
1.200	.8576	.8501	.8865	.9884	1.1170
1.400	.9618	.9805	1.0514	1.1557	1.2754
1.500	1.0516	1.0732	1.1432	1.2411	1.3570

$\frac{z}{\delta}$	$\frac{p_l}{p_\infty}$ for probe -				
	1	2	3	4	5
.000	1.0930	1.0706	1.0192	1.0114	.8441
.010	1.0841	1.0631	1.0084	1.0041	.8489
.020	1.0744	1.0582	1.0091	1.0062	.8450
.030	1.0687	1.0575	1.0137	1.0080	.8443
.040	1.0633	1.0572	1.0166	1.0059	.8382
.060	1.0531	1.0574	1.0168	1.0025	.8328
.080	1.0463	1.0578	1.0168	1.0011	.8267
.100	1.0434	1.0635	1.0220	1.0056	.8179
.120	1.0416	1.0718	1.0336	1.0114	.7952
.140	1.0428	1.0774	1.0422	1.0157	.7808
.160	1.0448	1.0794	1.0501	1.0187	.7580
.180	1.0434	1.0747	1.0521	1.0171	.7412
.200	1.0413	1.0676	1.0513	1.0127	.7245
.240	1.0433	1.0595	1.0521	1.0078	.7051
.280	1.0485	1.0570	1.0560	.9975	.6949
.320	1.0584	1.0587	1.0646	.9645	.6920
.360	1.0669	1.0621	1.0739	.8952	.6931
.400	1.0738	1.0571	1.0834	.7904	.6950
.460	1.0814	1.0735	1.0921	.6938	.7000
.520	1.0875	1.0817	1.0852	.6291	.7154
.580	1.0960	1.0850	.9796	.6313	.7376
.660	1.0942	1.0634	.6902	.6523	.7703
.740	.9989	.8700	.5946	.6846	.8082
.820	.7237	.6329	.6196	.7318	.8482
.900	.5791	.6008	.6646	.7849	.8599
.980	.5976	.6204	.7019	.8237	.8298
1.100	.6773	.6884	.7554	.8221	.8274
1.200	.7586	.7667	.8093	.8287	.8743
1.400	.8738	.8634	.8692	.9214	.9955
1.500	.8866	.8851	.9184	.9843	1.0607

 $x = 15.000$ in. (0.381 m); $M = 2.49; R = 1.50 \times 10^6$ per ft (4.92×10^6 per m) $x = 30.000$ in. (0.762 m); $M = 2.49; R = 1.50 \times 10^6$ per ft (4.92×10^6 per m)

$\frac{z}{\delta}$	$\frac{p_l}{p_\infty}$ for probe -				
	1	2	3	4	5
.000	1.0449	1.0417	1.0128	1.0314	1.0130
.010	1.0420	1.0374	1.0101	1.0287	1.0098
.020	1.0400	1.0356	1.0099	1.0271	1.0114
.030	1.0348	1.0342	1.0088	1.0253	1.0111
.040	1.0338	1.0350	1.0118	1.0261	1.0107
.060	1.0283	1.0333	1.0134	1.0248	1.0079
.080	1.0270	1.0355	1.0169	1.0240	1.0079
.100	1.0287	1.0404	1.0238	1.0259	1.0106
.120	1.0286	1.0426	1.0309	1.0287	1.0127
.140	1.0230	1.0413	1.0360	1.0324	1.0137
.160	1.0151	1.0358	1.0404	1.0368	1.0149
.180	1.0107	1.0330	1.0388	1.0367	1.0125
.200	1.0074	1.0238	1.0356	1.0342	1.0095
.240	1.0072	1.0198	1.0311	1.0275	1.0056
.280	1.0078	1.0181	1.0274	1.0231	1.0039
.320	1.0081	1.0161	1.0265	1.0208	1.0030
.360	1.0107	1.0155	1.0253	1.0210	1.0037
.400	1.0141	1.0147	1.0250	1.0222	1.0060
.460	1.0191	1.0170	1.0273	1.0251	1.0106
.520	1.0280	1.0223	1.0326	1.0312	1.0198
.580	1.0334	1.0283	1.0391	1.0391	1.0307
.660	1.0392	1.0369	1.0501	1.0543	1.0272
.740	1.0478	1.0487	1.0635	1.0721	.9175
.820	1.0562	1.0579	1.0741	1.0798	.7589
.900	1.0679	1.0636	1.0870	1.0900	.7048
.980	1.0767	1.0771	1.0823	.7991	.7202
1.100	1.0577	1.0097	.7822	.7215	.7676
1.200	.7504	.7195	.7034	.7563	.8137
1.400	.7687	.7155	.7592	.8271	.8375
1.500	.7576	.7617	.7961	.8455	.8313

$\frac{z}{\delta}$	$\frac{p_l}{p_\infty}$ for probe -				
	1	2	3	4	5
.000	1.0279	1.0266	1.0254	1.0268	1.0191
.010	1.0281	1.0246	1.0235	1.0257	1.0171
.020	1.0266	1.0233	1.0233	1.0240	1.0168
.030	1.0261	1.0233	1.0234	1.0234	1.0169
.040	1.0251	1.0229	1.0222	1.0215	1.0154
.060	1.0250	1.0262	1.0214	1.0193	1.0131
.080	1.0245	1.0330	1.0237	1.0180	1.0122
.100	1.0246	1.0353	1.0295	1.0188	1.0122
.120	1.0178	1.0341	1.0366	1.0223	1.0133
.140	1.0092	1.0287	1.0407	1.0278	1.0167
.160	.9998	1.0194	1.0364	1.0306	1.0164
.180	.9990	1.0150	1.0332	1.0325	1.0175
.200	.9969	1.0091	1.0272	1.0307	1.0149
.240	.9944	1.0023	1.0214	1.0235	1.0093
.280	.9932	.9995	1.0172	1.0172	1.0043
.320	.9955	1.0300	1.0170	1.0163	1.0037
.360	.9972	1.0010	1.0168	1.0154	1.0035
.400	.9974	1.0006	1.0157	1.0143	1.0042
.460	.9973	1.0015	1.0148	1.0148	1.0063
.520	.9973	1.0010	1.0136	1.0157	1.0068
.580	1.0033	1.0021	1.0140	1.0168	1.0091
.660	1.0087	1.0058	1.0154	1.0190	1.0106
.740	1.0114	1.0083	1.0185	1.0214	1.0141
.820	1.0108	1.0100	1.0199	1.0234	1.0159
.900	1.0097	1.0101	1.0214	1.0257	1.0204
.980	1.0103	1.0112	1.0235	1.0300	1.0260
1.100	1.0129	1.0152	1.0273	1.0352	1.0333
1.200	1.0185	1.0186	1.0295	1.0388	1.0378
1.400	1.0336	1.0318	1.0465	1.0572	1.0453
1.500	1.0409	1.0407	1.0557	1.0636	.9342

TABLE IV.- MEASUREMENTS OBTAINED FOR PLATE WITH FAIRING - Continued

(b) Static-pressure ratio - Continued

$x = 30.000$ in. (0.762 m);
 $M = 2.49$; $R = 1.50 \times 10^6$ per ft (4.92×10^6 per m)

$\frac{z}{\delta}$	$\frac{p_l}{p_\infty}$ for probe -				
	1	2	3	4	5
.000	1.0179	1.0165	1.0200	1.0186	1.0090
.010	1.0145	1.0150	1.0178	1.0164	1.0052
.020	1.0154	1.0147	1.0180	1.0165	1.0031
.030	1.0139	1.0134	1.0170	1.0156	1.0039
.040	1.0114	1.0128	1.0149	1.0128	1.0030
.060	1.0106	1.0165	1.0153	1.0118	1.0012
.080	1.0107	1.0221	1.0190	1.0111	1.0002
.100	1.0159	1.0287	1.0307	1.0149	1.0011
.120	1.0107	1.0233	1.0347	1.0183	1.0013
.140	1.0022	1.0172	1.0364	1.0228	1.0030
.160	.9973	1.0100	1.0320	1.0249	1.0048
.180	.9930	1.0027	1.0235	1.0235	1.0041
.200	.9919	.9990	1.0185	1.0221	1.0037
.240	.9884	.9924	1.0110	1.0132	.9971
.280	.9858	.9899	1.0065	1.0072	.9936
.320	.9845	.9871	1.0023	1.0030	.9907
.360	.9841	.9850	.9989	1.0003	.9987
.400	.9841	.9835	.9968	.9982	.9871
.460	.9851	.9839	.9943	.9971	.9975
.520	.9858	.9833	.9937	.9965	.9880
.580	.9868	.9870	.9962	.9991	.9917
.660	.9897	.9885	.9991	1.0026	.9955
.740	.9971	.9930	1.0019	1.0069	.9999
.820	1.0014	.9975	1.0041	1.0084	1.0011
.900	1.0023	1.0000	1.0065	1.0115	1.0047
.980	1.0035	1.0022	1.0106	1.0177	1.0092
1.100	1.0038	1.0036	1.0154	1.0240	1.0128
1.200	1.0024	1.0051	1.0187	1.0272	1.0176
1.400	1.0086	1.0073	1.0175	1.0275	1.0198
1.500	1.0091	1.0073	1.0193	1.0293	1.0209

$x = 10.000$ in. (0.254 m);
 $M = 2.49$; $R = 3.00 \times 10^6$ per ft (9.83×10^6 per m)

$\frac{z}{\delta}$	$\frac{p_l}{p_\infty}$ for probe -				
	1	2	3	4	5
.000	1.1158	1.0656	.9427	.9779	.9147
.004	1.1118	1.0620	.9376	.9789	.8199
.010	1.1009	1.0519	.9231	.9709	.8165
.020	1.0884	1.0469	.9310	.9769	.8105
.030	1.0797	1.0458	.9399	.9808	.8052
.040	1.0696	1.0472	.9444	.9814	.8040
.060	1.0522	1.0460	.9381	.9769	.7949
.080	1.0408	1.0472	.9380	.9786	.7870
.100	1.0404	1.0535	.9469	.9832	.7755
.120	1.0399	1.0640	.9651	.9867	.7514
.140	1.0303	1.0667	.9823	.9877	.7473
.160	1.0231	1.0599	.9913	.9863	.7080
.180	1.0205	1.0511	.9970	.9333	.6931
.200	1.0209	1.0450	.9997	.9792	.6449
.240	1.0294	1.0408	1.0098	.9749	.6731
.280	1.0358	1.0390	1.0206	.9520	.6705
.320	1.0440	1.0406	1.0328	.9948	.6715
.360	1.0529	1.0441	1.0457	.7792	.6752
.400	1.0590	1.0502	1.0543	.6692	.6798
.460	1.0654	1.0624	1.0761	.5416	.6896
.520	1.0763	1.0746	1.0537	.5840	.7057
.580	1.0960	1.0856	.8969	.5988	.7324
.660	1.1076	1.0535	.5948	.6250	.7683
.740	.9365	.7655	.5666	.6633	.8116
.820	.6174	.5854	.6046	.7116	.8456
.900	.5575	.5830	.6436	.7645	.8195
.980	.5927	.6086	.6881	.8028	.8037
1.100	.6781	.6826	.7405	.7948	.8208
1.200	.7580	.7630	.7937	.8092	.8691
1.400	.8743	.8628	.8590	.9076	.9329
1.500	.8800	.8790	.9087	.9716	.1.0598

$x = 6.875$ in. (0.175 m);
 $M = 2.49$; $R = 3.00 \times 10^6$ per ft (9.83×10^6 per m)

$\frac{z}{\delta}$	$\frac{p_l}{p_\infty}$ for probe -				
	1	2	3	4	5
.000	1.1959	.9811	.9270	.6206	.8240
.010	1.1693	.9469	.9255	.6141	.8083
.020	1.1406	.9763	.9445	.6135	.8052
.030	1.1187	.9942	.9466	.6150	.8041
.040	1.1006	.9979	.9345	.6137	.8016
.060	1.0661	1.0181	.9116	.6120	.7953
.080	1.0302	1.0244	.8975	.6135	.7939
.100	1.0196	1.0350	.8881	.6178	.7972
.120	1.0259	1.0477	.8689	.6115	.7965
.140	1.0406	1.0555	.8506	.6057	.7918
.160	1.0529	1.0650	.8272	.6050	.7884
.180	1.0649	1.0757	.7755	.6075	.7900
.200	1.0760	1.0820	.7109	.6088	.7927
.240	1.1025	1.0948	.5886	.6155	.8031
.280	1.1265	1.1127	.4999	.6210	.8162
.320	1.1417	1.1310	.4672	.6258	.8275
.360	1.1314	1.1208	.4625	.6301	.8353
.400	1.0889	1.0453	.4528	.6416	.8482
.460	.9872	.7932	.4720	.6654	.8701
.520	.9065	.5708	.5000	.6996	.8769
.580	.7324	.4922	.5386	.7419	.8669
.660	.4744	.4875	.5995	.8027	.8274
.740	.4842	.5158	.6557	.8162	.8111
.820	.5484	.5693	.7005	.7735	.8351
.900	.6333	.6498	.7484	.7725	.8821
.940	.7246	.7411	.7893	.8095	.9396
1.100	.8419	.8372	.8211	.9923	1.0316
1.200	.8459	.8411	.8776	.9772	1.1170
1.400	.9568	.9743	1.0428	1.1445	1.2759
1.500	1.0482	1.0686	1.1327	1.2287	1.3439

$x = 15.000$ in. (0.381 m);
 $M = 2.49$; $R = 3.00 \times 10^6$ per ft (9.83×10^6 per m)

$\frac{z}{\delta}$	$\frac{p_l}{p_\infty}$ for probe -				
	1	2	3	4	5
.000	1.0577	1.0421	.9714	1.0019	.9995
.010	1.0497	1.0317	.927	.9953	.9953
.020	1.0458	1.0293	.9617	.9937	.9962
.030	1.0405	1.0270	.9633	.9931	.9950
.040	1.0283	.9674	.9937	.9952	.
.060	1.0259	1.0306	.9730	.9953	.9941
.080	1.0271	1.0289	.9800	.9954	.9930
.100	1.0293	1.0269	.9931	.9981	.9966
.120	1.0144	1.0244	1.0027	1.0023	.9997
.140	1.0032	1.0201	1.0084	1.0069	1.0010
.160	.9971	1.0128	1.0067	1.0093	.9937
.180	.9948	1.0085	1.0041	1.0063	.9939
.200	.9949	1.0061	1.0016	1.0009	.9887
.240	.9943	1.0050	.9991	.9912	.9842
.280	.9954	1.0049	.9994	.9896	.9847
.320	.9992	1.0041	.7994	.9901	.9850
.360	1.0015	1.0028	.9996	.9914	.9865
.400	1.0060	1.0039	1.0020	.9952	.9904
.460	1.0139	1.0066	1.0057	1.0006	.9964
.520	1.0220	1.0125	1.0119	1.0080	1.0069
.580	1.0260	1.0201	1.0198	1.0183	1.0172
.660	1.0289	1.0274	1.0298	1.0341	.9842
.740	1.0362	1.0370	1.0412	1.0517	.8184
.820	1.0462	1.0468	1.0540	1.0519	.6961
.900	1.0580	1.0569	1.0690	.9058	.6837
.980	1.0639	1.0645	1.0607	.7086	.7137
1.100	1.0219	.9362	.7030	.6979	.7661
1.200	.6911	.6787	.6877	.7395	.8124
1.400	.7072	.7067	.7468	.8068	.8234
1.500	.7573	.7541	.7829	.8246	.8236

TABLE IV.- MEASUREMENTS OBTAINED FOR PLATE WITH FAIRING - Continued

(b) Static-pressure ratio - Continued

$x = 30.000$ in. (0.762 m);
 $M = 2.49$; $R = 3.00 \times 10^6$ per ft (9.83×10^6 per m)

$\frac{z}{\delta}$	$\frac{p_l}{p_\infty}$ for probe -					$\frac{z}{\delta}$	1	2	3	4	5
	1	2	3	4	5						
	.000	1.0191	1.0192	1.0193	.9949	1.0001					
.010	1.0155	1.0153	1.0153	.9900	.9752						
.020	1.0139	1.0113	1.0101	.9997	.9961						
.040	1.0048	1.0135	1.0095	.9847	.9912						
.080	1.0171	1.0113	1.0210	.9901	.9374						
.120	.9935	1.0029	1.0227	1.0001	.9400						
.160	.9836	.9975	1.0060	.9990	.9951						
.200	.9312	.9441	.9444	.9406	.9419						
.240	.9757	.9735	.9647	.9313	.9274						
.360	.9737	.9752	.9904	.9779	.9791						
.460	.9759	.9731	.9751	.9743	.9775						
.540	.9784	.9771	.9798	.9901	.9831						
.740	.9896	.9422	.9841	.9846	.9843						
.820	.9932	.9357	.9434	.9493	.9428						
.900	.9917	.9393	.9424	.9261	.9177						
.580	.9940	.9912	.9951	1.0114	1.0118						
1.100	.9955	.9953	1.0024	1.0364	1.0359						
1.200	.9931	.9352	1.0032	1.0057	1.0062						
1.400	1.0023	.9324	1.0018	1.0054	1.0068						
1.500	1.0012	.9952	1.0016	1.0053	1.0040						

$\frac{z}{\delta}$						$\frac{z}{\delta}$	1	2	3	4	5
	1	2	3	4	5						

TABLE IV.- MEASUREMENTS OBTAINED FOR PLATE WITH FAIRING - Continued

(b) Static-pressure ratio - Continued

 $x = 6.875 \text{ in. (} 0.175 \text{ m);}$
 $M = 4.44; R = 3.00 \times 10^6 \text{ per ft (} 9.83 \times 10^6 \text{ per m)}$

$\frac{z}{\delta}$	$\frac{p_l}{p_\infty}$ for probe -				
	1	2	3	4	5
.000	1.1977	.9264	.7569	1.0053	1.0237
.010	1.2033	.9197	.7355	.9967	1.0204
.020	1.1886	.9064	.7076	.9903	1.0204
.030	1.1775	.9030	.6884	.9860	1.0171
.040	1.1628	.9030	.6669	.9817	1.0171
.060	1.1479	.8876	.6486	.9745	1.0152
.080	1.1295	.8676	.6314	.9681	1.0118
.100	1.1151	.8597	.6198	.9625	1.0071
.120	1.0946	.8542	.6057	.9552	.9985
.140	1.0747	.8530	.5963	.9496	.9937
.160	1.0563	.8497	.5856	.9432	.9871
.180	1.0431	.8375	.5800	.9445	.9451
.200	1.0306	.8130	.5727	.9432	.9338
.240	1.0140	.7529	.5663	.9475	.9871
.280	.9934	.6738	.5585	.9574	.9851
.320	.9658	.6170	.5554	.9702	.9318
.360	.9222	.5761	.5556	.9796	.9771
.400	.8922	.5568	.5607	.9831	.9785
.460	.7487	.5167	.5971	.9724	1.0018
.520	.6080	.4860	.6391	.9475	1.0471
.580	.5610	.4800	.6572	.9467	1.0852
.660	.5316	.4933	.6893	.9810	1.1586
.740	.5364	.5527	.7633	1.0652	1.3102
.820	.5915	.6428	.8404	1.1637	1.4335
.900	.6833	.7429	.9196	1.2815	1.5301
.980	.7844	.8430	1.0331	1.4271	1.3102
1.100	.9314	.9998	1.2237	1.5942	1.0637
1.200	1.1353	1.2100	1.4378	1.3329	.9937
1.400	1.3466	1.2300	1.1659	1.1466	.9771
1.500	1.0872	1.0647	1.0453	1.1053	.9751

 $x = 15.000 \text{ in. (} 0.381 \text{ m);}$
 $M = 4.44; R = 3.00 \times 10^6 \text{ per ft (} 9.83 \times 10^6 \text{ per m)}$

$\frac{z}{\delta}$	$\frac{p_l}{p_\infty}$ for probe -				
	1	2	3	4	5
.000	1.0324	1.0198	1.0245	1.0995	.8838
.010	1.0342	1.0165	1.0245	1.0995	.8305
.020	1.0324	1.0098	1.0267	1.1016	.8388
.030	1.0287	1.0098	1.0238	1.1038	.8405
.040	1.0232	1.0098	1.0310	1.1038	.8771
.060	1.0159	1.0098	1.0374	1.1038	.8705
.080	1.0159	1.0132	1.0374	1.1016	.8638
.100	1.0067	1.0098	1.0310	1.0909	.8472
.120	.9993	1.0065	1.0224	1.0824	.8372
.140	.9920	.9998	1.0096	1.0717	.8205
.160	.9883	.9998	1.0031	1.0674	.8105
.180	.9865	.9998	1.0010	1.0631	.8038
.200	.9846	.9998	.9989	1.0610	.7872
.240	.9828	.9998	1.0010	1.0567	.7772
.280	.9846	1.0065	1.0096	1.0417	.7539
.320	.9883	1.0098	1.0224	1.0224	.7405
.360	.9971	.1.0179	1.0410	.9724	.7316
.400	1.0030	1.0265	1.0631	.9004	.7272
.460	1.0140	1.0399	1.0888	.8211	.7339
.520	1.0177	1.0432	1.0802	.8061	.7372
.580	1.0269	1.0565	.9657	.7933	.7572
.660	1.0306	1.0432	.7078	.8061	.7972
.740	.9424	.8830	.6477	.8318	.8138
.820	.6392	.6328	.6348	.8704	.8205
.900	.6025	.6128	.6434	.8811	.8305
.980	.5952	.6128	.6605	.8982	.8538
1.100	.6466	.6728	.7452	.9646	.9504
1.200	.7366	.7696	.8554	1.0481	1.0637
1.400	.8487	.8864	.9860	1.1980	1.2569
1.500	.9608	1.0065	1.1059	1.3158	1.3769

 $x = 10.000 \text{ in. (} 0.254 \text{ m);}$
 $M = 4.44; R = 3.00 \times 10^6 \text{ per ft (} 9.83 \times 10^6 \text{ per m)}$

$\frac{z}{\delta}$	$\frac{p_l}{p_\infty}$ for probe -				
	1	2	3	4	5
.000	1.1371	1.0098	.9689	.9153	.9105
.010	1.1334	.9798	.9710	.9111	.9005
.020	1.1298	.9731	.9732	.9111	.9005
.030	1.1206	.9598	.9753	.9089	.8971
.040	1.1151	.9698	.9753	.9068	.8971
.060	1.1040	.9731	.9732	.9004	.8938
.080	1.0967	.9798	.9582	.8939	.8905
.100	1.0912	.9865	.9453	.8854	.8838
.120	1.0820	.9931	.9260	.8704	.8771
.140	1.0710	.9931	.9046	.8618	.8738
.160	1.0618	.9998	.9789	.8532	.8671
.180	1.0544	1.0098	.8554	.8468	.8638
.200	1.0508	1.0198	.8318	.8425	.8605
.240	1.0471	1.0432	.7697	.8361	.8605
.280	1.0439	1.0632	.7012	.8297	.8605
.320	1.0544	1.0799	.6541	.8275	.8605
.360	1.0581	1.0866	.6220	.8297	.8638
.400	1.0630	1.0699	.5984	.8340	.8705
.460	1.0287	.9431	.5770	.8532	.8805
.520	.9277	.7696	.5727	.8854	.8805
.580	.7579	.6404	.5885	.9166	.8817
.660	.5915	.5660	.6220	.9218	.9105
.740	.5658	.5560	.6327	.9218	.9338
.820	.5658	.5861	.6926	.9625	1.0371
.900	.6034	.6404	.7644	1.0196	1.1319
.980	.6696	.7172	.8394	1.0946	1.2387
1.100	.7671	.8174	.9445	1.2297	1.3988
1.200	.8499	.9043	1.0496	1.3519	1.4589
1.400	1.1702	1.2334	1.3886	1.3993	1.4037
1.500	1.3632	1.4356	1.4677	1.589	.9885

 $x = 22.500 \text{ in. (} 0.572 \text{ m);}$
 $M = 4.44; R = 3.00 \times 10^6 \text{ per ft (} 9.83 \times 10^6 \text{ per m)}$

$\frac{z}{\delta}$	$\frac{p_l}{p_\infty}$ for probe -				
	1	2	3	4	5
.000	.9718	.9865	.9989	1.1081	.9804
.010	.9736	.9898	1.0031	1.1102	.9834
.020	.9754	.9898	1.0053	1.1123	.9838
.030	.9754	.9893	1.0074	1.1145	.9838
.040	.9754	.9898	1.0096	1.1166	.9871
.060	.9736	.9898	1.0096	1.1166	.9838
.080	.9699	.9865	1.0374	1.1166	.9804
.100	.9626	.9798	1.0331	1.1145	.9771
.120	.9534	.9698	.9924	1.1059	.9671
.140	.9442	.9631	.9774	1.0909	.9571
.160	.9424	.9598	.9710	1.0845	.9538
.180	.9424	.9598	.9689	1.0824	.9538
.200	.9424	.9598	.9667	1.0802	.9538
.240	.9424	.9598	.9667	1.0781	.9538
.280	.9424	.9598	.9689	1.0759	.9538
.320	.9424	.7598	.9689	1.0759	.9571
.360	.9424	.9593	.9732	1.0781	.9604
.400	.9442	.9631	.9796	1.0824	.9671
.460	.9479	.9664	.9839	1.0866	.9738
.520	.9534	.9731	.9903	1.0952	.9804
.540	.9589	.9798	1.0010	1.1059	.9771
.660	.9718	.9931	1.0181	1.1316	.8838
.740	.9833	1.0051	1.0317	1.1471	.7728
.820	.9975	1.0198	1.0481	1.1166	.7306
.900	1.0159	1.0399	1.0695	.9303	.7172
.980	1.0232	1.0465	1.0096	.8747	.7339
1.100	.8579	.8497	.7804	.8639	.7739
1.200	.6790	.6778	.6995	.7076	.8811
1.400	.7091	.7295	.7612	.9410	.8671
1.500	.7734	.7929	.8383	1.0031	.9404

TABLE IV.- MEASUREMENTS OBTAINED FOR PLATE WITH FAIRING - Continued

(b) Static-pressure ratio - Concluded

$x = 30.000$ in. (0.762 m);
 $M = 4.44$; $R = 3.00 \times 10^6$ per ft (9.83×10^6 per m)

$\frac{z}{\delta}$	$\frac{p_l}{p_\infty}$ for probe -				
	1	2	3	4	5
.000	.9750	.9945	1.0045	1.1096	.9885
.010	.9768	.9979	1.0048	1.1096	.9885
.020	.9737	.9979	1.0110	1.1118	.9885
.030	.9787	.9979	1.0153	1.1139	.9918
.040	.9773	.9965	1.0138	1.1145	.9904
.060	.9754	.9931	1.0138	1.1145	.9871
.080	.9750	.9912	1.0153	1.1161	.9851
.100	.9681	.9831	1.0074	1.1123	.9804
.120	.9621	.9745	1.0033	1.1053	.9751
.140	.9547	.9678	.9852	1.0946	.9651
.160	.9492	.9611	.9745	1.0839	.9584
.180	.9461	.9564	.9639	1.0781	.9538
.200	.9429	.9518	.9554	1.0744	.9524
.240	.9432	.9524	.9652	1.0768	.9531
.280	.9374	.9451	.9590	1.0680	.9458
.320	.9363	.9464	.9582	1.0674	.9471
.360	.9350	.9464	.9582	1.0652	.9471
.400	.9332	.9464	.9582	1.0652	.9471
.460	.9332	.9498	.9625	1.0652	.9504
.520	.9359	.9531	.9689	1.0695	.9571
.580	.9405	.9504	.9753	1.0759	.9638
.660	.9461	.9664	.9939	1.0866	.9738
.740	.9571	.9765	.9989	1.0995	.9904
.820	.9626	.9831	1.0053	1.1081	1.0004
.900	.9681	.9865	1.0096	1.1123	1.0104
.980	.9736	.9931	1.0160	1.1209	1.0237
1.100	.9920	1.0132	1.0395	1.1423	.9205
1.200	1.0104	1.0332	1.0584	1.1188	.7705
1.400	.8873	.8830	.8104	.9175	.7805
1.500	.7182	.7362	.7440	.9025	.8038

$\frac{z}{\delta}$					
	1	2	3	4	5

$\frac{z}{\delta}$					
	1	2	3	4	5

$\frac{z}{\delta}$					
	1	2	3	4	5

TABLE IV.- MEASUREMENTS OBTAINED FOR PLATE WITH FAIRING - Continued

(c) Total-temperature ratio

$x = 6.875 \text{ in. (} 0.175 \text{ m);}$ $M = 2.49; R = 1.50 \times 10^6 \text{ per ft (} 4.92 \times 10^6 \text{ per m)}$						$x = 10.000 \text{ in. (} 0.254 \text{ m);}$ $M = 2.49; R = 1.50 \times 10^6 \text{ per ft (} 4.92 \times 10^6 \text{ per m)}$					
$\frac{z}{\delta}$	$\frac{T_{t,L}}{T_{t,\infty}}$ for probe -					$\frac{T_{t,L}}{T_{t,\infty}}$ for probe -	1	2	3	4	5
	1	2	3	4	5						
.000	.9458	.9606	.9335	.9310	.9371	.910	.9427	.9515	.9437	.9339	.9324
.010	.9496	.9629	.9373	.9439	.9394	.010	.9518	.9539	.9553	.9349	.9339
.020	.9488	.9612	.9412	.9525	.9471	.020	.9554	.9577	.9514	.9388	.9420
.030	.9457	.9611	.9484	.9571	.9523	.030	.9592	.9611	.9467	.9433	.9493
.040	.9449	.9625	.9546	.9590	.9563	.040	.9626	.9628	.9428	.9474	.9534
.060	.9447	.9638	.9631	.9597	.9582	.060	.9642	.9632	.9480	.9547	.9591
.080	.9509	.9651	.9637	.9631	.9617	.080	.9658	.9657	.9578	.9598	.9616
.100	.9560	.9658	.9661	.9678	.9631	.100	.9653	.9659	.9631	.9608	.9638
.120	.9503	.9635	.9671	.9678	.9653	.140	.9616	.9664	.9684	.9671	.9690
.140	.9492	.9653	.9700	.9711	.9670	.150	.9628	.9649	.9688	.9667	.9679
.160	.9512	.9660	.9722	.9722	.9697	.180	.9637	.9661	.9722	.9711	.9704
.180	.9509	.9659	.9724	.9719	.9700	.200	.9644	.9681	.9745	.9723	.9733
.200	.9546	.9675	.9752	.9743	.9715	.240	.9734	.9709	.9788	.9755	.9765
.240	.9630	.9708	.9784	.9776	.9741	.280	.9800	.9720	.9792	.9786	.9786
.280	.9675	.9731	.9803	.9784	.9754	.320	.9839	.9756	.9833	.9796	.9799
.320	.9757	.9733	.9844	.9789	.9778	.360	.9839	.9744	.9837	.9804	.9817
.360	.9858	.9781	.9875	.9823	.9804	.400	.9888	.9780	.9868	.9828	.9837
.400	.9876	.9785	.9885	.9826	.9810	.460	.9912	.9921	.9894	.9887	.9861
.460	.9893	.9816	.9881	.9856	.9846	.520	.9926	.9937	.9921	.9883	.9872
.520	.9907	.9831	.9916	.9883	.9871	.580	.9938	.9951	.9933	.9905	.9900
.580	.9933	.9868	.9946	.9918	.9910	.660	.9990	.9913	.9947	.9964	.9950
.660	.9925	.9871	.9940	.9928	.9927	.740	.9988	.9921	.9973	.9970	.9957
.740	.9973	.9889	.9965	.9941	.9950	.820	.9963	.9926	.9977	.9980	.9977
.820	.9979	.9901	.9959	.9954	.9951	.900	.9973	.9912	.9961	.9964	.9959
.900	.9969	.9903	.9963	.9956	.9956	.980	.9969	.9913	.9961	.9962	.9968
.980	.9974	.9917	.9956	.9971	.9971	1.100	.9974	.9919	.9959	.9964	.9967
1.100	.9971	.9919	.9959	.9959	.9958	1.200	.9965	.9918	.9950	.9957	.9958
1.200	.9966	.9919	.9962	.9959	.9961	1.400	.9971	.9927	.9956	.9965	.9967
1.400	.9977	.9931	.9964	.9968	.9967	1.500	.9967	.9921	.9950	.9962	.9964
1.500	.9973	.9931	.9959	.9968	.9969						

$x = 15.000 \text{ in. (} 0.381 \text{ m);}$ $M = 2.49; R = 1.50 \times 10^6 \text{ per ft (} 4.92 \times 10^6 \text{ per m)}$						$x = 22.500 \text{ in. (} 0.572 \text{ m);}$ $M = 2.49; R = 1.50 \times 10^6 \text{ per ft (} 4.92 \times 10^6 \text{ per m)}$					
$\frac{z}{\delta}$	$\frac{T_{t,L}}{T_{t,\infty}}$ for probe -					$\frac{T_{t,L}}{T_{t,\infty}}$ for probe -	1	2	3	4	5
	1	2	3	4	5						
.000	.9409	.9411	.9482	.9374	.9374	.000	.9442	.9389	.9447	.9419	.9389
.010	.9542	.9418	.9596	.9400	.9376	.010	.9490	.9391	.9489	.9436	.9381
.020	.9642	.9461	.9662	.9424	.9410	.020	.9631	.9429	.9563	.9480	.9432
.030	.9704	.9502	.9667	.9435	.9438	.030	.9630	.9455	.9592	.9500	.9459
.040	.9711	.9539	.9663	.9445	.9483	.040	.9762	.9508	.9662	.9530	.9492
.060	.9751	.9554	.9652	.9459	.9539	.060	.9783	.9532	.9705	.9528	.9521
.080	.9722	.9560	.9646	.9489	.9569	.080	.9786	.9545	.9701	.9511	.9557
.100	.9697	.9570	.9661	.9519	.9594	.100	.9782	.9550	.9732	.9514	.9590
.120	.9678	.9580	.9681	.9582	.9622	.120	.9789	.9554	.9732	.9514	.9606
.140	.9711	.9615	.9718	.9613	.9649	.140	.9749	.9563	.9728	.9533	.9633
.160	.9683	.9602	.9706	.9625	.9655	.150	.9769	.9571	.9739	.9558	.9623
.180	.9751	.9645	.9738	.9661	.9688	.180	.9805	.9596	.9755	.9593	.9668
.200	.9718	.9654	.9734	.9687	.9694	.200	.9791	.9598	.9754	.9605	.9668
.240	.9790	.9683	.9766	.9745	.9744	.240	.9820	.9646	.9767	.9682	.9704
.280	.9862	.9698	.9799	.9755	.9734	.280	.9862	.9688	.9782	.9733	.9745
.320	.9875	.9728	.9808	.9798	.9784	.320	.9928	.9733	.9822	.9770	.9759
.360	.9894	.9744	.9837	.9794	.9785	.360	.9920	.9739	.9851	.9802	.9782
.400	.9897	.9772	.9854	.9831	.9821	.400	.9927	.9764	.9858	.9839	.9828
.460	.9921	.9805	.9894	.9881	.9865	.460	.9943	.9801	.9901	.9873	.9853
.520	.9940	.9849	.9911	.9906	.9889	.520	.9945	.9826	.9915	.9867	.9858
.580	.9954	.9865	.9939	.9911	.9902	.580	.9943	.9848	.9935	.9911	.9910
.660	.9979	.9897	.9976	.9935	.9923	.660	.9981	.9904	.9973	.9944	.9934
.740	.9974	.9903	.9979	.9952	.9931	.740	.9983	.9911	.9973	.9960	.9960
.820	.9984	.9919	.9974	.9964	.9952	.820	.9985	.9925	.9971	.9978	.9971
.900	.9990	.9936	.9976	.9970	.9971	.900	.9975	.9918	.9960	.9965	.9963
.980	.9975	.9925	.9963	.9939	.9960	.980	.9976	.9927	.9966	.9967	.9967
1.100	.9976	.9929	.9950	.9962	.9964	1.100	.9980	.9932	.9966	.9966	.9964
1.200	.9954	.9913	.9957	.9954	.9955	1.200	.9977	.9932	.9964	.9970	.9971
1.400	.9959	.9913	.9943	.9961	.9964	1.400	.9971	.9926	.9957	.9962	.9965
1.500	.9966	.9916	.9953	.9958	.9962	1.500	.9976	.9931	.9963	.9965	.9955

TABLE IV.- MEASUREMENTS OBTAINED FOR PLATE WITH FAIRING - Continued

(c) Total-temperature ratio - Continued

 $x = 30.000$ in. (0.762 m); $M = 2.49; R = 1.50 \times 10^6$ per ft (4.92×10^6 per m)

$\frac{z}{\delta}$	$\frac{T_{t,l}}{T_{t,\infty}}$ for probe -				
	1	2	3	4	5
.000	.9428	.9404	.9438	.9404	.9389
.010	.9511	.9395	.9489	.9451	.9419
.020	.9633	.9440	.9545	.9502	.9455
.030	.9717	.9475	.9586	.9521	.9482
.040	.9901	.9518	.9629	.9554	.9508
.060	.9817	.9547	.9696	.9566	.9533
.080	.9821	.9558	.9697	.9553	.9563
.100	.9812	.9561	.9731	.9546	.9580
.120	.9799	.9562	.9727	.9525	.9587
.140	.9934	.9570	.9739	.9542	.9616
.160	.9793	.9563	.9734	.9537	.9620
.180	.9812	.9573	.9750	.9551	.9653
.200	.9808	.9591	.9760	.9577	.9653
.240	.9855	.9631	.9789	.9649	.9684
.280	.9886	.9672	.9802	.9697	.9715
.320	.9902	.9700	.9826	.9739	.9745
.360	.9930	.9739	.9851	.9785	.9791
.400	.9929	.9755	.9858	.9812	.9811
.460	.9933	.9785	.9889	.9837	.9831
.520	.9942	.9815	.9900	.9980	.9869
.580	.9957	.9862	.9936	.9899	.9883
.660	.9980	.9875	.9959	.9951	.9941
.740	.9975	.9904	.9961	.9963	.9958
.820	.9987	.9926	.9985	.9976	.9973
.900	.9990	.9933	.9975	.9983	.9986
.980	.9986	.9937	.9973	.9976	.9974
1.100	.9973	.9930	.9959	.9967	.9967
1.200	.9967	.9923	.9957	.9959	.9960
1.400	.9971	.9928	.9956	.9960	.9963
1.500	.9980	.9935	.9967	.9973	.9976

 $x = 10.000$ in. (0.254 m); $M = 2.49; R = 3.00 \times 10^6$ per ft (9.83×10^6 per m)

$\frac{z}{\delta}$	$\frac{T_{t,l}}{T_{t,\infty}}$ for probe -				
	1	2	3	4	5
.000	.9539	.9388	.9468	.9306	.9302
.010	.9606	.9417	.9590	.9311	.9300
.020	.9727	.9483	.9515	.9356	.9407
.030	.9771	.9517	.9393	.9395	.9477
.040	.9796	.9538	.9300	.9455	.9533
.060	.9817	.9565	.9332	.9454	.9593
.080	.9798	.9585	.9452	.9587	.9604
.100	.9778	.9637	.9582	.9616	.9634
.120	.9753	.9656	.9632	.9642	.9652
.140	.9790	.9661	.9675	.9661	.9672
.160	.9809	.9681	.9709	.9693	.9701
.180	.9864	.9692	.9730	.9742	.9737
.200	.9851	.9659	.9725	.9721	.9711
.240	.9889	.9686	.9783	.9755	.9769
.280	.9896	.9732	.9814	.9797	.9780
.320	.9871	.9741	.9808	.9795	.9781
.360	.9873	.9769	.9830	.9782	.9798
.400	.9898	.9796	.9858	.9839	.9826
.460	.9915	.9835	.9901	.9886	.9859
.520	.9930	.9866	.9930	.9919	.9900
.580	.9922	.9859	.9925	.9919	.9893
.660	.9928	.9881	.9912	.9928	.9912
.740	.9958	.9904	.9961	.9951	.9926
.820	.9930	.9910	.9958	.9946	.9945
.900	.9932	.9899	.9937	.9925	.9925
.980	.9956	.9924	.9951	.9960	.9961
1.100	.9968	.9943	.9957	.9965	.9967
1.200	.9955	.9926	.9947	.9945	.9945
1.400	.9976	.9949	.9969	.9955	.9955
1.500	.9971	.9945	.9958	.9962	.9960

 $x = 6.875$ in. (0.175 m); $M = 2.49; R = 3.00 \times 10^6$ per ft (9.83×10^6 per m)

$\frac{z}{\delta}$	$\frac{T_{t,l}}{T_{t,\infty}}$ for probe -				
	1	2	3	4	5
.000	.9573	.9650	.9293	.9314	.9351
.010	.9545	.9710	.9328	.9462	.9398
.020	.9523	.9720	.9357	.9556	.9481
.030	.9511	.9672	.9410	.9597	.9535
.040	.9558	.9656	.9509	.9611	.9567
.060	.9679	.9665	.9644	.9634	.9599
.080	.9737	.9693	.9655	.9671	.9623
.100	.9695	.9685	.9666	.9670	.9635
.120	.9663	.9689	.9688	.9720	.9661
.140	.9705	.9692	.9737	.9746	.9699
.160	.9703	.9690	.9735	.9758	.9719
.180	.9701	.9680	.9740	.9749	.9712
.200	.9769	.9707	.9776	.9782	.9731
.240	.9837	.9734	.9804	.9792	.9760
.280	.9873	.9746	.9847	.9809	.9776
.320	.9862	.9744	.9838	.9807	.9772
.360	.9876	.9774	.9881	.9829	.9813
.400	.9890	.9810	.9888	.9856	.9833
.450	.9919	.9842	.9922	.9885	.9862
.520	.9938	.9878	.9936	.9915	.9892
.580	.9933	.9910	.9962	.9938	.9924
.660	.9964	.9906	.9962	.9949	.9940
.740	.9974	.9926	.9960	.9953	.9952
.820	.9970	.9927	.9960	.9967	.9961
.900	.9960	.9920	.9952	.9955	.9956
.980	.9961	.9922	.9953	.9960	.9948
1.100	.9957	.9930	.9951	.9959	.9960
1.200	.9972	.9943	.9966	.9963	.9963
1.400	.9971	.9947	.9963	.9965	.9963
1.500	.9988	.9960	.9975	.9970	.9964

 $x = 15.000$ in. (0.381 m); $M = 2.49; R = 3.00 \times 10^6$ per ft (9.83×10^6 per m)

$\frac{z}{\delta}$	$\frac{T_{t,l}}{T_{t,\infty}}$ for probe -				
	1	2	3	4	5
.070	.9492	.9357	.9425	.9337	.9273
.010	.9607	.9397	.9533	.9370	.9279
.020	.9789	.9485	.9622	.9399	.9321
.030	.9816	.9503	.9620	.9403	.9370
.040	.9810	.9485	.9627	.9406	.9407
.060	.9833	.9480	.9613	.9417	.9451
.080	.9807	.9448	.9632	.9425	.9525
.120	.9829	.9446	.9654	.9470	.9551
.140	.9830	.9475	.9667	.9477	.9572
.160	.9855	.9516	.9680	.9533	.9604
.180	.9816	.9547	.9677	.9569	.9594
.200	.9848	.9594	.9701	.9613	.9637
.240	.9848	.9627	.9727	.9688	.9674
.280	.9862	.9668	.9757	.9721	.9716
.320	.9898	.9715	.9818	.9790	.9770
.360	.9891	.9733	.9856	.9805	.9802
.400	.9901	.9773	.9868	.9816	.9799
.450	.9919	.9821	.9875	.9868	.9866
.520	.9931	.9858	.9900	.9897	.9877
.580	.9851	.9800	.9892	.9872	.9864
.660	.9950	.9903	.9959	.9948	.9930
.740	.9946	.9910	.9935	.9942	.9914
.820	.9967	.9924	.9962	.9953	.9943
.900	.9961	.9928	.9956	.9922	.9939
.980	.9966	.9943	.9953	.9945	.9940
1.100	.9951	.9913	.9938	.9926	.9933
1.200	.9950	.9932	.9945	.9957	.9957
1.400	.9935	.9915	.9932	.9928	.9930
1.500	.9975	.9949	.9962	.9965	.9962

TABLE IV.- MEASUREMENTS OBTAINED FOR PLATE WITH FAIRING - Continued

(c) Total-temperature ratio - Continued

 $x = 30.000$ in. (0.762 m); $M = 2.49; R = 3.00 \times 10^6$ per ft (9.83×10^6 per m)

$\frac{z}{\delta}$	$\frac{T_{t,l}}{T_{t,\infty}}$ for probe -				
	1	2	3	4	5
.000	.9419	.9355	.9289	.9233	.9219
.010	.9503	.9405	.9365	.9338	.9280
.020	.9618	.9445	.9403	.9407	.9316
.030	.9731	.9502	.9449	.9443	.9339
.040	.9820	.9556	.9487	.9484	.9382
.060	.9860	.9553	.9564	.9486	.9398
.080	.9833	.9516	.9547	.9445	.9408
.100	.9821	.9489	.9547	.9415	.9431
.120	.9753	.9456	.9536	.9367	.9455
.140	.9789	.9453	.9540	.9352	.9436
.160	.9774	.9457	.9555	.9363	.9469
.180	.9735	.9436	.9537	.9342	.9493
.200	.9836	.9511	.9636	.9416	.9533
.240	.9735	.9491	.9605	.9424	.9525
.280	.9873	.9591	.9722	.9557	.9589
.320	.9875	.9650	.9744	.9615	.9644
.360	.9838	.9632	.9741	.9647	.9657
.400	.9849	.9690	.9785	.9724	.9731
.460	.9870	.9713	.9805	.9743	.9725
.520	.9898	.9773	.9859	.9824	.9800
.580	.9895	.9801	.9868	.9813	.9823
.660	.9936	.9853	.9908	.9875	.9862
.740	.9891	.9859	.9888	.9900	.9895
.820	.9951	.9905	.9946	.9949	.9928
.900	.9930	.9987	.9927	.9885	.9881
.980	.9922	.9982	.9935	.9894	.9991
1.100	.9933	.9911	.9917	.9935	.9932
1.200	.9942	.9921	.9935	.9936	.9932
1.400	.9908	.9987	.9910	.9905	.9912
1.500	.9937	.9920	.9924	.9945	.9953

$\frac{z}{\delta}$	1	2	3	4	5

$\frac{z}{\delta}$	1	2	3	4	5

$\frac{z}{\delta}$	1	2	3	4	5

TABLE IV.- MEASUREMENTS OBTAINED FOR PLATE WITH FAIRING - Continued

(c) Total-temperature ratio - Continued

x = 6.875 in. (0.175 m);

 M = 4.44; R = 3.00×10^6 per ft (9.83×10^6 per m)

$\frac{z}{\delta}$	$\frac{T_{t,l}}{T_{t,\infty}}$ for probe -				
	1	2	3	4	5
.000	.9109	.9142	.9031	.9038	.9043
.010	.9249	.9228	.9108	.9179	.9074
.020	.9324	.9218	.9302	.9347	.9203
.030	.9281	.9146	.9381	.9348	.9244
.040	.9246	.9148	.9420	.9322	.9260
.060	.9227	.9311	.9450	.9333	.9280
.080	.9188	.9399	.9452	.9352	.9296
.100	.9166	.9427	.9505	.9425	.9339
.120	.9088	.9425	.9509	.9454	.9391
.140	.9043	.9457	.9539	.9501	.9435
.160	.9008	.9463	.9553	.9514	.9474
.180	.9044	.9489	.9570	.9542	.9518
.200	.9094	.9511	.9592	.9548	.9523
.240	.9249	.9533	.9613	.9581	.9573
.280	.9400	.9569	.9659	.9624	.9617
.320	.9529	.9574	.9662	.9635	.9641
.360	.9695	.9595	.9692	.9663	.9666
.400	.9745	.9634	.9730	.9729	.9737
.460	.9721	.9652	.9729	.9753	.9753
.520	.9751	.9662	.9735	.9783	.9772
.580	.9788	.9670	.9763	.9804	.9804
.660	.9822	.9698	.9793	.9835	.9824
.740	.9845	.9725	.9821	.9857	.9849
.820	.9856	.9731	.9852	.9854	.9849
.900	.9886	.9796	.9878	.9918	.9896
.980	.9931	.9848	.9904	.9943	.9868
1.100	.9963	.9888	.9947	.9968	.9971
1.200	.9949	.9895	.9929	.9904	.9967
1.400	.9903	.9857	.9967	.9970	.9971
1.500	.9977	.9925	.9956	.9971	.9969

x = 10.000 in. (0.254 m);

 M = 4.44; R = 3.00×10^6 per ft (9.83×10^6 per m)

$\frac{z}{\delta}$	$\frac{T_{t,l}}{T_{t,\infty}}$ for probe -				
	1	2	3	4	5
.000	.9042	.9334	.9000	.8943	.8981
.010	.9182	.9487	.9095	.8997	.9016
.020	.9313	.9470	.9094	.9151	.9085
.030	.9361	.9367	.9073	.9239	.9168
.040	.9392	.9296	.9103	.9316	.9235
.060	.9387	.9240	.9237	.9357	.9303
.080	.9346	.9286	.9347	.9368	.9324
.100	.9296	.9338	.9418	.9413	.9336
.120	.9259	.9401	.9462	.9452	.9379
.140	.9223	.9439	.9477	.9485	.9414
.150	.9216	.9465	.9497	.9532	.9478
.180	.9242	.9498	.9535	.9560	.9518
.200	.9291	.9492	.9557	.9564	.9529
.240	.9416	.9535	.9607	.9609	.9583
.280	.9561	.9543	.9656	.9653	.9614
.320	.9635	.9566	.9670	.9661	.9630
.360	.9710	.9599	.9717	.9695	.9671
.400	.9713	.9576	.9708	.9693	.9672
.460	.9752	.9627	.9744	.9740	.9738
.520	.9754	.9658	.9780	.9766	.9782
.580	.9744	.9682	.9765	.9781	.9813
.660	.9839	.9718	.9804	.9819	.9850
.740	.9877	.9751	.9836	.9867	.9869
.820	.9884	.9769	.9854	.9898	.9897
.900	.9886	.9775	.9871	.9893	.9895
.980	.9927	.9835	.9917	.9961	.9961
1.100	.9960	.9882	.9950	.9943	.9968
1.200	.9971	.9911	.9959	.9980	.9952
1.400	.9979	.9927	.9976	.9896	.9968
1.500	.9977	.9933	.9913	.9961	.9963

x = 15.000 in. (0.381 m);

 M = 4.44; R = 3.00×10^6 per ft (9.83×10^6 per m)

$\frac{z}{\delta}$	$\frac{T_{t,l}}{T_{t,\infty}}$ for probe -				
	1	2	3	4	5
.000	.8977	.9179	.9095	.8933	.8917
.010	.9083	.9274	.9324	.8908	.8895
.020	.9246	.9347	.9327	.9194	.8948
.030	.9336	.9384	.9275	.8979	.9047
.040	.9390	.9401	.9208	.9052	.9134
.060	.9383	.9355	.9136	.9136	.9205
.080	.9373	.9373	.9189	.9249	.9296
.100	.9355	.9379	.9280	.9326	.9353
.120	.9299	.9361	.9310	.9319	.9349
.140	.9333	.9411	.9425	.9401	.9444
.160	.9332	.9421	.9449	.9436	.9465
.180	.9358	.9440	.9486	.9451	.9489
.200	.9398	.9450	.9508	.9483	.9532
.240	.9504	.9510	.9583	.9571	.9592
.280	.9581	.9511	.9609	.9591	.9595
.320	.9676	.9567	.9672	.9660	.9660
.360	.9719	.9591	.9688	.9680	.9695
.400	.9763	.9630	.9719	.9748	.9740
.460	.9775	.9643	.9764	.9764	.9769
.520	.9784	.9645	.9742	.9764	.9778
.580	.9801	.9691	.9784	.9790	.9785
.660	.9813	.9737	.9787	.9809	.9911
.740	.9778	.9709	.9807	.9808	.9919
.820	.9834	.9754	.9834	.9838	.9857
.900	.9947	.9839	.9929	.9942	.9947
.980	.9934	.9841	.9913	.9934	.9939
1.100	.9930	.9852	.9908	.9946	.9952
1.200	.9976	.9906	.9964	.9977	.9976
1.400	1.0021	.9960	1.0009	1.0019	1.0021
1.500	.9992	.9937	.9982	.9996	1.0001

x = 22.500 in. (0.572 m);

 M = 4.44; R = 3.00×10^6 per ft (9.83×10^6 per m)

$\frac{z}{\delta}$	$\frac{T_{t,l}}{T_{t,\infty}}$ for probe -				
	1	2	3	4	5
.000	.9006	.9068	.9094	.8940	.8971
.110	.9038	.9106	.9211	.8943	.8971
.220	.9135	.9131	.9310	.8971	.8970
.030	.9299	.9245	.9442	.9070	.9036
.040	.9371	.9305	.9488	.9061	.9083
.060	.9447	.9387	.9531	.9136	.9195
.080	.9404	.9341	.9447	.9128	.9190
.100	.9406	.9385	.9480	.9188	.9274
.120	.9357	.9355	.9449	.9209	.9009
.140	.9377	.9380	.9474	.9260	.9343
.160	.9391	.9396	.9497	.9296	.9366
.180	.9387	.9380	.9483	.9325	.9387
.200	.9452	.9454	.9545	.9391	.9445
.240	.9520	.9476	.9577	.9461	.9509
.280	.9598	.9519	.9609	.9549	.9565
.320	.9631	.9522	.9616	.9581	.9591
.360	.9671	.9522	.9637	.9621	.9622
.400	.9717	.9573	.9669	.9601	.9685
.460	.9752	.9607	.9708	.9729	.9742
.520	.9803	.9672	.9782	.9807	.9802
.580	.9902	.9678	.9783	.9806	.9804
.660	.9816	.9699	.9808	.9820	.9826
.740	.9847	.9734	.9824	.9844	.9855
.820	.9855	.9768	.9841	.9845	.9889
.900	.9853	.9774	.9832	.9834	.9862
.980	.9906	.9823	.9865	.9919	.9917
1.100	.9896	.9845	.9929	.9942	.9942
1.200	.9968	.9903	.9933	.9978	.9976
1.400	.9975	.9908	.9969	.9963	.9967
1.500	.9978	.9918	.9989	.9984	.9990

TABLE IV.- MEASUREMENTS OBTAINED FOR PLATE WITH FAIRING - Continued

(c) Total-temperature ratio - Concluded

 $x = 30.000 \text{ in. (0.762 m)}$ $M = 4.44; R = 3.00 \times 10^6 \text{ per ft (9.83} \times 10^6 \text{ per m)}$

$\frac{z}{\delta}$	$\frac{T_{t,L}}{T_{t,\infty}}$ for probe -				
	1	2	3	4	5
.000	.9040	.9052	.9101	.8982	.9004
.010	.9064	.9053	.9170	.9002	.9007
.020	.9184	.9137	.9301	.9058	.9082
.030	.9249	.9173	.9370	.9058	.9092
.040	.9345	.9269	.9468	.9120	.9152
.060	.9414	.9326	.9539	.9162	.9207
.080	.9443	.9347	.9546	.9173	.9247
.100	.9410	.9330	.9534	.9167	.9242
.120	.9412	.9337	.9543	.9205	.9266
.140	.9392	.9350	.9538	.9212	.9328
.160	.9510	.9462	.9641	.9344	.9439
.180	.9454	.9396	.9579	.9277	.9405
.200	.9520	.9440	.9632	.9356	.9450
.240	.9504	.9448	.9590	.9394	.9477
.280	.9585	.9515	.9639	.9494	.9559
.320	.9629	.9526	.9663	.9556	.9592
.360	.9643	.9524	.9657	.9587	.9618
.400	.9700	.9576	.9690	.9668	.9668
.460	.9720	.9579	.9704	.9690	.9681
.520	.9758	.9621	.9736	.9754	.9761
.580	.9791	.9667	.9767	.9785	.9799
.660	.9796	.9689	.9778	.9804	.9816
.740	.9820	.9721	.9799	.9835	.9849
.820	.9863	.9764	.9854	.9876	.9883
.900	.9927	.9847	.9916	.9951	.9955
.980	.9980	.9811	.9871	.9896	.9900
1.100	.9944	.9882	.9920	.9959	.9920
1.200	.9977	.9920	.9959	.9960	.9972
1.400	.9901	.9848	.9922	.9924	.9927
1.500	.9940	.9880	.9935	.9944	.9949

$\frac{z}{\delta}$					
	1	2	3	4	5

$\frac{z}{\delta}$					
	1	2	3	4	5

$\frac{z}{\delta}$					
	1	2	3	4	5

TABLE IV.- MEASUREMENTS OBTAINED FOR PLATE WITH FAIRING - Continued

(d) Velocity ratio

 $x = 6.875$ in. (0.175 m); $M = 2.49; R = 1.50 \times 10^6$ per ft (4.92×10^6 per m)

$\frac{z}{\delta}$	$\frac{u_l}{u_\infty}$ for probe -				
	1	2	3	4	5
.000	.4954	.5333	.3111	.5177	.5322
.010	.4700	.5983	.4236	.6811	.6537
.020	.4958	.6248	.5227	.7311	.6929
.030	.5175	.6468	.6309	.7635	.7198
.040	.5344	.6695	.6834	.7782	.7357
.060	.5762	.7101	.7310	.7980	.7575
.080	.6181	.7337	.7488	.8150	.7753
.100	.6572	.7491	.7665	.8317	.7921
.120	.6785	.7571	.7809	.8478	.8092
.140	.6982	.7667	.7951	.8530	.8230
.160	.7219	.7751	.8075	.8748	.8345
.180	.7409	.7842	.8176	.8843	.8474
.200	.7606	.7926	.8299	.8918	.8543
.240	.8045	.8163	.8658	.9073	.8715
.280	.8361	.8339	.9113	.9181	.8900
.320	.8621	.8506	.9571	.9274	.8996
.360	.8789	.8663	.9820	.9378	.9009
.400	.8967	.8900	.9458	.9470	.9115
.450	.9173	.9252	1.0090	.9591	.9265
.520	.9425	.9668	1.0161	.9654	.9353
.580	.9783	1.0090	1.0168	.9695	.9508
.660	1.0309	1.0339	1.0149	.9734	.9678
.740	1.0504	1.0380	1.0131	.9790	.9840
.820	1.0460	1.0345	1.0128	.9922	.9933
.900	1.0327	1.0243	1.0104	1.0014	.9940
.980	1.0198	1.0123	1.0057	1.0008	.9895
1.100	1.0039	1.0004	1.0038	.9929	.9808
1.200	1.0037	1.0003	.9992	.9852	.9734
1.400	.9931	.9869	.9810	.9636	.9596
1.500	.9828	.9763	.9707	.9607	.9529

 $x = 10.000$ in. (0.254 m); $M = 2.49; R = 1.50 \times 10^6$ per ft (4.92×10^6 per m)

$\frac{z}{\delta}$	$\frac{u_l}{u_\infty}$ for probe -				
	1	2	3	4	5
.000	.5026	.5270	.4003	.3734	.4737
.010	.6001	.6033	.5088	.4596	.6229
.020	.6403	.6529	.5438	.5355	.6787
.030	.6613	.6771	.5564	.5938	.7103
.040	.6770	.6931	.5683	.6347	.7317
.060	.7004	.7140	.6123	.6864	.7576
.080	.7250	.7331	.6706	.7163	.7771
.100	.7385	.7448	.7096	.7310	.7927
.140	.7661	.7622	.7544	.7633	.8308
.160	.7776	.7705	.7666	.7762	.8474
.180	.7947	.7832	.7816	.7916	.8607
.200	.8158	.7933	.7949	.8062	.8751
.240	.8434	.8151	.8175	.8296	.8967
.280	.8648	.8344	.8347	.8514	.9118
.320	.8813	.8522	.8501	.8701	.9247
.360	.8906	.8653	.8626	.8911	.9360
.400	.9014	.8802	.8763	.9197	.9439
.460	.9139	.8993	.8968	.9545	.9637
.520	.9221	.9128	.9162	.9874	.9712
.580	.9347	.9274	.9487	.9998	.9797
.660	.9516	.9508	.9981	1.0100	.9900
.740	.9771	.9884	1.0335	1.0119	.9939
.820	1.0208	1.0275	1.0357	1.0108	.9961
.900	1.0473	1.0395	1.0305	1.0075	.9990
.980	1.0449	1.0366	1.0250	1.0035	1.0039
1.100	1.0319	1.0264	1.0183	1.0051	1.0076
1.200	1.0195	1.0149	1.0111	1.0060	1.0025
1.400	1.0070	1.0037	1.0045	.9963	.9892
1.500	1.0046	1.0005	.9981	.9888	.9821

 $x = 15.000$ in. (0.381 m); $M = 2.49; R = 1.50 \times 10^6$ per ft (4.92×10^6 per m)

$\frac{z}{\delta}$	$\frac{u_l}{u_\infty}$ for probe -				
	1	2	3	4	5
.000	.5341	.5048	.4948	.3420	.4357
.010	.6536	.5730	.6048	.4702	.5427
.020	.7142	.6326	.6551	.5222	.5927
.030	.7366	.6667	.6692	.5572	.6330
.040	.7471	.6796	.6702	.5768	.6548
.060	.7649	.7021	.6745	.6198	.6971
.080	.7765	.7182	.6851	.6563	.7214
.100	.7883	.7312	.7045	.6883	.7411
.120	.7991	.7407	.7222	.7125	.7550
.140	.8093	.7561	.7427	.7327	.7686
.160	.8186	.7679	.7598	.7503	.7818
.180	.8339	.7823	.7760	.7656	.7935
.200	.8461	.7964	.7917	.7825	.8062
.240	.8679	.8164	.8124	.8071	.8260
.280	.8863	.8365	.8345	.8310	.8467
.320	.8945	.8543	.8493	.8498	.8630
.360	.9092	.8706	.8655	.8644	.8766
.400	.9142	.8843	.8796	.8791	.8906
.460	.9263	.9038	.9493	.8972	.9772
.520	.9340	.9193	.9152	.9148	.9252
.580	.9442	.9331	.9298	.9274	.9376
.660	.9556	.9471	.9454	.9419	.9551
.740	.9646	.9577	.9579	.9552	.9769
.820	.9716	.9657	.9667	.9654	1.0041
.900	.9739	.9685	.9684	.9799	1.0181
.980	.9737	.9639	.9723	1.0010	1.0236
1.100	.9822	.9463	1.0107	1.0236	1.0196
1.200	1.0250	1.0233	1.0309	1.0187	1.0120
1.400	1.0303	1.0267	1.0221	1.0097	1.0094
1.500	1.0245	1.0201	1.0173	1.0070	1.0112

 $x = 22.500$ in. (0.572 m); $M = 2.49; R = 1.50 \times 10^6$ per ft (4.92×10^6 per m)

$\frac{z}{\delta}$	$\frac{u_l}{u_\infty}$ for probe -				
	1	2	3	4	5
.000	.5419	.5047	.4895	.4169	.4450
.010	.6758	.5334	.5054	.5162	.5531
.020	.7393	.6435	.6532	.5625	.5928
.030	.7672	.6729	.6857	.5924	.6226
.040	.7817	.6907	.7007	.6093	.6408
.060	.8007	.7129	.7190	.6333	.6736
.080	.8109	.7262	.7286	.6498	.7008
.100	.8174	.7335	.7366	.6642	.7235
.120	.8275	.7433	.7428	.6800	.7387
.140	.8359	.7568	.7532	.6993	.7554
.160	.8448	.7681	.7651	.7163	.7665
.180	.8541	.7801	.7764	.7359	.7782
.200	.8613	.7914	.7900	.7544	.7913
.240	.8800	.8183	.8143	.7924	.8165
.280	.8938	.8374	.8323	.8183	.8366
.320	.9062	.7555	.8485	.8390	.8525
.360	.9144	.8690	.8630	.8575	.8638
.400	.9218	.8835	.8775	.8738	.8836
.460	.9318	.9019	.8957	.8924	.9016
.520	.9414	.9183	.9135	.9093	.9185
.580	.9455	.9304	.9271	.9247	.9329
.660	.9622	.9516	.9483	.9442	.9516
.740	.9711	.9626	.9609	.9569	.9636
.820	.9758	.9691	.9691	.9671	.9731
.900	.9772	.9737	.9743	.9730	.9790
.980	.9824	.9770	.9780	.9759	.9806
1.100	.9858	.9810	.9823	.9803	.9834
1.200	.9869	.9827	.9837	.9815	.9841
1.400	.9874	.9829	.9831	.9807	.9857
1.500	.9874	.9829	.9830	.9813	.9915

TABLE IV.- MEASUREMENTS OBTAINED FOR PLATE WITH FAIRING - Continued

(d) Velocity ratio - Continued

$x = 30.000$ in. (0.762 m);
 $M = 2.49; R = 1.50 \times 10^6$ per ft (4.92×10^6 per m)

$\frac{z}{\delta}$	$\frac{u_l}{u_\infty}$ for probe -				
	1	2	3	4	5
.000	.5493	.5100	.4697	.4154	.4781
.010	.6464	.5780	.5841	.5281	.5573
.020	.7255	.6371	.6375	.5767	.5952
.030	.7664	.6751	.6728	.6080	.6203
.040	.7891	.6956	.6934	.6283	.6425
.060	.8145	.7251	.7216	.6549	.6714
.080	.8248	.7378	.7354	.6697	.6956
.100	.8328	.7483	.7463	.6815	.7128
.120	.8378	.7567	.7518	.6876	.7297
.140	.8465	.7649	.7587	.6968	.7416
.160	.8510	.7737	.7677	.7085	.7553
.180	.8596	.7857	.7794	.7239	.7702
.200	.8651	.7961	.7898	.7397	.7822
.240	.8818	.8175	.8111	.7736	.8076
.280	.8955	.8365	.8307	.8036	.8271
.320	.9033	.8506	.8454	.8263	.8442
.360	.9138	.8666	.8623	.8488	.8631
.400	.9223	.8815	.8749	.8665	.8774
.460	.9336	.9008	.8967	.8897	.8989
.520	.9414	.9157	.9108	.9061	.9146
.580	.9531	.9328	.9276	.9214	.9280
.660	.9618	.9481	.9445	.9416	.9492
.740	.9688	.9594	.9586	.9564	.9637
.820	.9782	.9722	.9722	.9691	.9749
.900	.9818	.9767	.9775	.9756	.9812
.980	.9842	.9795	.9809	.9786	.9834
1.100	.9860	.9818	.9829	.9811	.9857
1.200	.9886	.9842	.9852	.9829	.9865
1.400	.9906	.9863	.9868	.9841	.9872
1.500	.9918	.9873	.9879	.9849	.9881

$x = 10.000$ in. (0.254 m);
 $M = 2.49; R = 3.00 \times 10^6$ per ft (9.83×10^6 per m)

$x = 6.875$ in. (0.175 m);
 $M = 2.49; R = 3.00 \times 10^6$ per ft (9.83×10^6 per m)

$\frac{z}{\delta}$	$\frac{u_l}{u_\infty}$ for probe -				
	1	2	3	4	5
.000	.5223	.5751	.3150	.6048	.5665
.010	.5909	.6607	.4094	.7261	.6613
.020	.6131	.6795	.5186	.7884	.7182
.030	.6399	.6391	.6151	.8087	.7397
.040	.6676	.7049	.6876	.8203	.7552
.060	.7228	.7383	.7585	.8362	.7766
.080	.7658	.7620	.7822	.8502	.7949
.100	.7916	.7737	.8029	.8642	.8124
.120	.8046	.7772	.8221	.8820	.8278
.140	.8150	.7802	.8399	.8945	.8415
.160	.8270	.7889	.8521	.9072	.8554
.180	.8375	.7943	.8679	.9118	.8631
.200	.8536	.8080	.8893	.9209	.8710
.240	.8712	.8261	.9346	.9324	.8859
.280	.8871	.8503	.9807	.9450	.8954
.320	.8903	.8624	1.0033	.9533	.9046
.360	.8984	.8800	1.0154	.9622	.9149
.400	.9100	.9093	1.0230	.9705	.9279
.460	.9385	.9655	1.0344	.9804	.9407
.520	.9636	1.0183	1.0353	.9835	.9523
.580	.9976	1.0477	1.0354	.9869	.9661
.660	1.0631	1.0569	1.0305	.9884	.9854
.740	1.0675	1.0543	1.0248	.9954	.9978
.820	1.0567	1.0473	1.0231	1.0100	1.0025
.900	1.0410	1.0343	1.0187	1.0139	1.0030
.980	1.0257	1.0290	1.0160	1.0119	.9953
1.100	1.0094	1.0077	1.0127	1.0028	.9870
1.200	1.0114	1.0087	1.0064	.9925	.9769
1.400	.9995	.9947	.9878	.9767	.9654
1.500	.9901	.9844	.9785	.9681	.9592

$x = 15.000$ in. (0.381 m);
 $M = 2.49; R = 3.00 \times 10^6$ per ft (9.83×10^6 per m)

$x = 15.000$ in. (0.381 m);
 $M = 2.49; R = 3.00 \times 10^6$ per ft (9.83×10^6 per m)

$\frac{z}{\delta}$	$\frac{u_l}{u_\infty}$ for probe -				
	1	2	3	4	5
.000	.5934	.5435	.4670	.4086	.5278
.010	.6947	.6119	.5644	.5004	.6653
.020	.7360	.6614	.5864	.5759	.7180
.030	.7528	.6811	.5797	.6264	.7455
.040	.7674	.6964	.5751	.6702	.7633
.060	.7926	.7211	.6068	.7177	.7873
.080	.8074	.7404	.6679	.7410	.8047
.100	.8207	.7577	.7297	.7587	.8226
.120	.8299	.7677	.7611	.7758	.8418
.140	.8435	.7734	.7789	.7904	.9608
.160	.8588	.7850	.7965	.8053	.8782
.180	.8703	.7945	.8056	.8157	.8875
.200	.8800	.8045	.8199	.8321	.9006
.240	.8959	.8264	.8416	.8538	.9186
.280	.9014	.8446	.8551	.8767	.9328
.320	.9049	.8617	.8680	.8954	.9434
.360	.9125	.8820	.8831	.9249	.9557
.400	.9179	.8963	.8969	.9643	.9671
.460	.9265	.9128	.9140	1.0037	.9795
.520	.9310	.9230	.9310	1.0140	.9853
.580	.9396	.9339	.9668	1.0178	.9881
.660	.9525	.9577	1.0286	1.0231	.9942
.740	.9931	1.0068	1.0486	1.0252	.9985
.820	1.0427	1.0455	1.0459	1.0230	1.0025
.900	1.0558	1.0503	1.0398	1.0181	1.0053
.980	1.0492	1.0447	1.0322	1.0126	1.0124
1.100	1.0358	1.0343	1.0266	1.0164	1.0138
1.200	1.0224	1.0199	1.0170	1.0138	1.0064
1.400	1.0093	1.0076	1.0104	1.0023	.9921
1.500	1.0085	1.0063	1.0042	.9957	.9855

$\frac{z}{\delta}$	$\frac{u_l}{u_\infty}$ for probe -				
	1	2	3	4	5
.000	.5972	.5381	.5547	.4321	.4558
.010	.7299	.6126	.6709	.5094	.5638
.020	.7835	.6737	.7057	.5528	.6190
.030	.8056	.6939	.7065	.5762	.6501
.040	.8159	.7030	.7029	.5961	.6763
.060	.8337	.7140	.7016	.6324	.7162
.080	.8436	.7246	.7094	.6668	.7419
.100	.8512	.7359	.7223	.6962	.7570
.120	.8631	.7493	.7406	.7235	.7733
.140	.8770	.7696	.7624	.7475	.7868
.160	.8819	.7825	.7775	.7614	.7947
.180	.8864	.7951	.7967	.7808	.8078
.200	.8931	.8057	.8093	.7976	.8233
.240	.9040	.8289	.8344	.8279	.8425
.280	.9149	.8500	.8563	.8530	.8653
.320	.9182	.8639	.8688	.8684	.8775
.360	.9229	.8790	.8833	.8831	.8927
.400	.9252	.8925	.8945	.8960	.9060
.460	.9355	.9136	.9121	.9123	.9204
.520	.9404	.9272	.9244	.9255	.9326
.580	.9471	.9367	.9370	.9351	.9437
.660	.9617	.9542	.9546	.9534	.9679
.740	.9687	.9617	.9625	.9608	.9933
.820	.9729	.9679	.9697	.9715	1.0168
.900	.9749	.9709	.9731	.9957	1.0288
.980	.9759	.9736	.9820	1.0253	1.0280
1.100	.9898	1.0017	1.0310	1.0311	1.0192
1.200	1.0360	1.0349	1.0357	1.0250	1.0125
1.400	1.0322	1.0313	1.0264	1.0149	1.0114
1.500	1.0269	1.0257	1.0230	1.0149	1.0136

TABLE IV.- MEASUREMENTS OBTAINED FOR PLATE WITH FAIRING - Continued

(d) Velocity ratio - Continued

$x = 30.000 \text{ in. (} 0.762 \text{ m);}$
 $M = 2.49; R = 3.00 \times 10^6 \text{ per ft} (9.83 \times 10^6 \text{ per m)}$

$\frac{z}{\delta}$	$\frac{u_z}{u_\infty}$ for probe -				
	1	2	3	4	5
.000	.5982	.5570	.5153	.4822	.4568
.010	.6092	.5772	.5788	.5536	.5529
.020	.7649	.6785	.6625	.6257	.6021
.040	.8402	.7427	.7189	.6807	.6481
.080	.8634	.7690	.7509	.6925	.6978
.120	.9699	.7760	.7652	.6921	.7311
.160	.8833	.7925	.7890	.7072	.7584
.200	.8916	.8033	.8086	.7367	.7340
.280	.9134	.8468	.8494	.8091	.8351
.360	.9247	.8751	.8757	.8586	.8693
.460	.9399	.9051	.9036	.8979	.9020
.580	.9565	.9364	.9345	.9308	.9366
.740	.9689	.9621	.9614	.9609	.9658
.820	.9775	.9727	.9742	.9728	.9749
.900	.9796	.9756	.9785	.9756	.9783
.980	.9811	.9775	.9818	.9785	.9798
1.100	.9849	.9830	.9843	.9850	.9865
1.200	.9881	.9858	.9872	.9867	.9874
1.400	.9889	.9867	.9884	.9872	.9880
1.500	.9918	.9895	.9900	.9899	.9904

$\frac{z}{\delta}$					
	1	2	3	4	5

$\frac{z}{\delta}$					
	1	2	3	4	5

$\frac{z}{\delta}$					
	1	2	3	4	5

TABLE IV.- MEASUREMENTS OBTAINED FOR PLATE WITH FAIRING - Continued

(d) Velocity ratio - Continued

$x = 6.875$ in. (0.175 m);
 $M = 4.44; R = 3.00 \times 10^6$ per ft (9.83×10^6 per m)

$\frac{z}{\delta}$	$\frac{u_l}{u_\infty}$ for probe -				
	1	2	3	4	5
.000	.4688	.2890	.2883	.3486	.4169
.010	.5673	.4273	.6659	.6094	.5782
.020	.5881	.4922	.7422	.6694	.6318
.030	.6001	.5602	.7673	.6887	.6584
.040	.6079	.6039	.7808	.6962	.6725
.060	.6285	.7168	.7975	.7166	.6997
.080	.6480	.7746	.8115	.7338	.7218
.100	.6645	.8001	.8288	.7582	.7481
.120	.6755	.8162	.8435	.7762	.7716
.140	.6843	.8280	.8545	.7920	.7912
.160	.6981	.8398	.8697	.8093	.8125
.180	.7167	.8470	.8767	.8189	.8265
.200	.7430	.8541	.8843	.8289	.8385
.240	.7904	.8603	.8953	.8452	.8556
.280	.8328	.8724	.9075	.8610	.8719
.320	.8654	.8860	.9183	.8742	.8863
.360	.8900	.8985	.9290	.8836	.8976
.400	.8969	.9084	.9384	.8931	.9104
.460	.9106	.9261	.9457	.9045	.9207
.520	.9277	.9410	.9458	.9154	.9306
.580	.9389	.9543	.9525	.9273	.9422
.660	.9602	.9687	.9620	.9406	.9524
.740	.9769	.9759	.9688	.9517	.9583
.820	.9853	.9784	.9743	.9592	.9714
.900	.9894	.9804	.9781	.9662	.9714
.980	.9901	.9828	.9818	.9707	.9785
1.100	.9959	.9885	.9856	.9764	.9832
1.200	.9936	.9866	.9823	.9714	.9940
1.400	.9957	.9948	.9785	.9795	.9940
1.500	.9875	.9857	.9898	.9836	.9937

$x = 15.000$ in. (0.381 m);
 $M = 4.44; R = 3.00 \times 10^6$ per ft (9.83×10^6 per m)

$x = 10.000$ in. (0.254 m);
 $M = 4.44; R = 3.00 \times 10^6$ per ft (9.83×10^6 per m)

$\frac{z}{\delta}$	$\frac{u_l}{u_\infty}$ for probe -				
	1	2	3	4	5
.000	.5003	.4786	.3166	.3197	.4209
.010	.6408	.6789	.4337	.5640	.5868
.020	.6651	.6801	.5498	.6452	.6465
.030	.6825	.6717	.6192	.6849	.6797
.040	.6912	.6672	.6590	.7028	.6992
.060	.7059	.6795	.7229	.7295	.7292
.080	.7165	.7115	.7548	.7460	.7448
.100	.7262	.7499	.7787	.7655	.7716
.120	.7331	.7744	.7982	.7851	.7918
.140	.7427	.7942	.8144	.8016	.8086
.160	.7547	.8086	.8298	.8166	.8268
.180	.7685	.8190	.8427	.8299	.8417
.200	.7873	.8276	.8518	.8396	.8531
.240	.8192	.8415	.8666	.8571	.8726
.280	.8532	.8567	.8840	.8747	.8876
.320	.8755	.8697	.9012	.8863	.8996
.360	.8893	.8801	.9161	.8962	.9112
.400	.8989	.8912	.9279	.9060	.9221
.460	.9138	.8998	.9434	.9184	.9313
.520	.9218	.9065	.9573	.9275	.9429
.580	.9312	.9329	.9634	.9331	.9482
.660	.9573	.9548	.9679	.9411	.9579
.740	.9720	.9691	.9774	.9529	.9616
.820	.9854	.9790	.9929	.9631	.9722
.900	.9945	.9867	.9880	.9708	.9804
.980	1.0002	.9931	.9926	.9790	.9841
1.100	1.0057	.9980	.9961	.9818	.9882
1.200	1.0053	.9984	.9955	.9823	.9901
1.400	.9952	.9882	.9860	.9861	.9903
1.500	.9902	.9830	.9855	.9784	.9939

$x = 22.500$ in. (0.572 m);

$M = 4.44; R = 3.00 \times 10^6$ per ft (9.83×10^6 per m)

$\frac{z}{\delta}$	$\frac{u_l}{u_\infty}$ for probe -				
	1	2	3	4	5
.000	.5430	.4749	.3216	.3276	.4146
.010	.6774	.6916	.5116	.4772	.5739
.020	.7139	.7227	.5648	.5490	.6469
.030	.7337	.7338	.5891	.5930	.6849
.040	.7438	.7386	.6043	.6229	.7070
.060	.7580	.7458	.6333	.6739	.7407
.080	.7605	.7503	.6607	.7045	.7625
.100	.7693	.7621	.7035	.7329	.7865
.120	.7759	.7758	.7374	.7539	.8038
.140	.7867	.7909	.7704	.7748	.8227
.160	.7958	.8033	.7928	.7920	.8372
.180	.8077	.8126	.8081	.8038	.8445
.200	.8200	.8239	.8267	.8210	.8625
.240	.8442	.8406	.8493	.8449	.8779
.280	.8667	.8532	.8676	.8640	.8914
.320	.8832	.8668	.8818	.8780	.9037
.360	.8945	.8773	.8907	.8911	.9155
.400	.9048	.8890	.9009	.9047	.9262
.460	.9143	.9014	.9141	.9199	.9458
.520	.9242	.9138	.9262	.9291	.9493
.580	.9329	.9241	.9392	.9403	.9585
.660	.9438	.9379	.9598	.9506	.9611
.740	.9568	.9503	.9759	.9600	.9708
.820	.9818	.9757	.9884	.9661	.9822
.900	.9947	.9882	.9974	.9764	.9853
.980	1.0058	.9988	1.0031	.9819	.9951
1.100	1.0115	1.0051	1.0052	.9875	.9964
1.200	1.0100	1.0037	1.0019	.9865	.9946
1.400	1.0069	1.0009	.9982	.9852	.9913
1.500	1.0011	.9947	.9927	.9815	.9889

$\frac{z}{\delta}$	$\frac{u_l}{u_\infty}$ for probe -				
	1	2	3	4	5
.000	.5015	.4518	.3689	.3225	.4179
.010	.6708	.6506	.5550	.4605	.5453
.020	.7126	.6961	.6224	.5346	.6085
.030	.7381	.7187	.6512	.5665	.6400
.040	.7582	.7377	.6669	.5927	.6643
.060	.7766	.7560	.6815	.6322	.7012
.080	.7851	.7654	.6886	.6601	.7283
.100	.7918	.7762	.6977	.6876	.7536
.120	.7996	.7856	.7141	.7123	.7722
.140	.8095	.7976	.7394	.7401	.7915
.160	.8172	.8069	.7614	.7582	.8081
.180	.8253	.8157	.7824	.7759	.8196
.200	.8344	.8253	.8037	.7911	.8353
.240	.8538	.8418	.8361	.8196	.8573
.280	.8716	.8564	.8594	.8434	.8774
.320	.8864	.8683	.8773	.8637	.8934
.360	.8984	.8789	.8906	.8802	.9077
.400	.9091	.8903	.9016	.8947	.9157
.460	.9201	.9045	.9164	.9112	.9355
.520	.9285	.9162	.9277	.9232	.9409
.580	.9369	.9270	.9378	.9340	.9519
.660	.9466	.9382	.9496	.9452	.9642
.740	.9574	.9499	.9603	.9562	.9756
.820	.9696	.9640	.9728	.9681	.9881
.900	.9799	.9739	.9798	.9751	.9848
.980	.9914	.9849	.9898	.9838	.9862
1.100	.9997	.9908	.9978	.9922	1.0016
1.200	1.0122	1.0058	1.0097	.9944	1.0026
1.400	1.0180	1.0120	1.0136	.9953	1.0101
1.500	1.0163	1.0108	1.0103	.9954	1.0035

TABLE IV.- MEASUREMENTS OBTAINED FOR PLATE WITH FAIRING - Concluded

(d) Velocity ratio - Concluded

 $x = 30.000 \text{ in. (} 0.762 \text{ m)}$ $M = 4.44; R = 3.00 \times 10^6 \text{ per ft (} 9.83 \times 10^6 \text{ per m)}$

$\frac{z}{\delta}$	$\frac{u_l}{u_\infty}$ for probe -				
	1	2	3	4	5
.000	.4214	.4470	.3583	.2950	.3922
.010	.6402	.6174	.5498	.4665	.5527
.020	.6922	.6738	.6187	.5387	.6127
.030	.7209	.7000	.6485	.5681	.6386
.040	.7457	.7229	.6718	.5939	.6612
.060	.7729	.7500	.6972	.6289	.6971
.080	.7877	.7648	.7073	.6536	.7221
.100	.7973	.7757	.7164	.6754	.7436
.120	.8063	.7864	.7281	.6996	.7608
.140	.8123	.7952	.7407	.7194	.7785
.160	.8178	.8008	.7518	.7348	.7901
.180	.8257	.8095	.7678	.7528	.8083
.200	.8357	.8191	.7861	.7697	.8179
.240	.8483	.8340	.8154	.7479	.8374
.280	.8651	.8510	.8447	.8251	.8599
.320	.8781	.8637	.8660	.8467	.8789
.360	.8906	.8753	.8830	.8663	.8996
.400	.9001	.8850	.8954	.8822	.9064
.460	.9127	.8975	.9102	.9004	.9204
.520	.9227	.9096	.9211	.9142	.9341
.580	.9304	.9203	.9306	.9245	.9445
.660	.9397	.9315	.9420	.9367	.9492
.740	.9517	.9453	.9548	.9503	.9691
.820	.9643	.9578	.9680	.9622	.9806
.900	.9770	.9710	.9774	.9712	.9840
.980	.9836	.9777	.9819	.9743	.9832
1.100	.9939	.9881	.9894	.9821	.9960
1.200	.9973	.9916	.9927	.9860	.9979
1.400	1.0020	.9953	.9977	.9841	.9964
1.500	1.0068	1.0016	1.0053	.9881	.9967

$\frac{z}{\delta}$	1	2	3	4	5

$\frac{z}{\delta}$	1	2	3	4	5

$\frac{z}{\delta}$	1	2	3	4	5

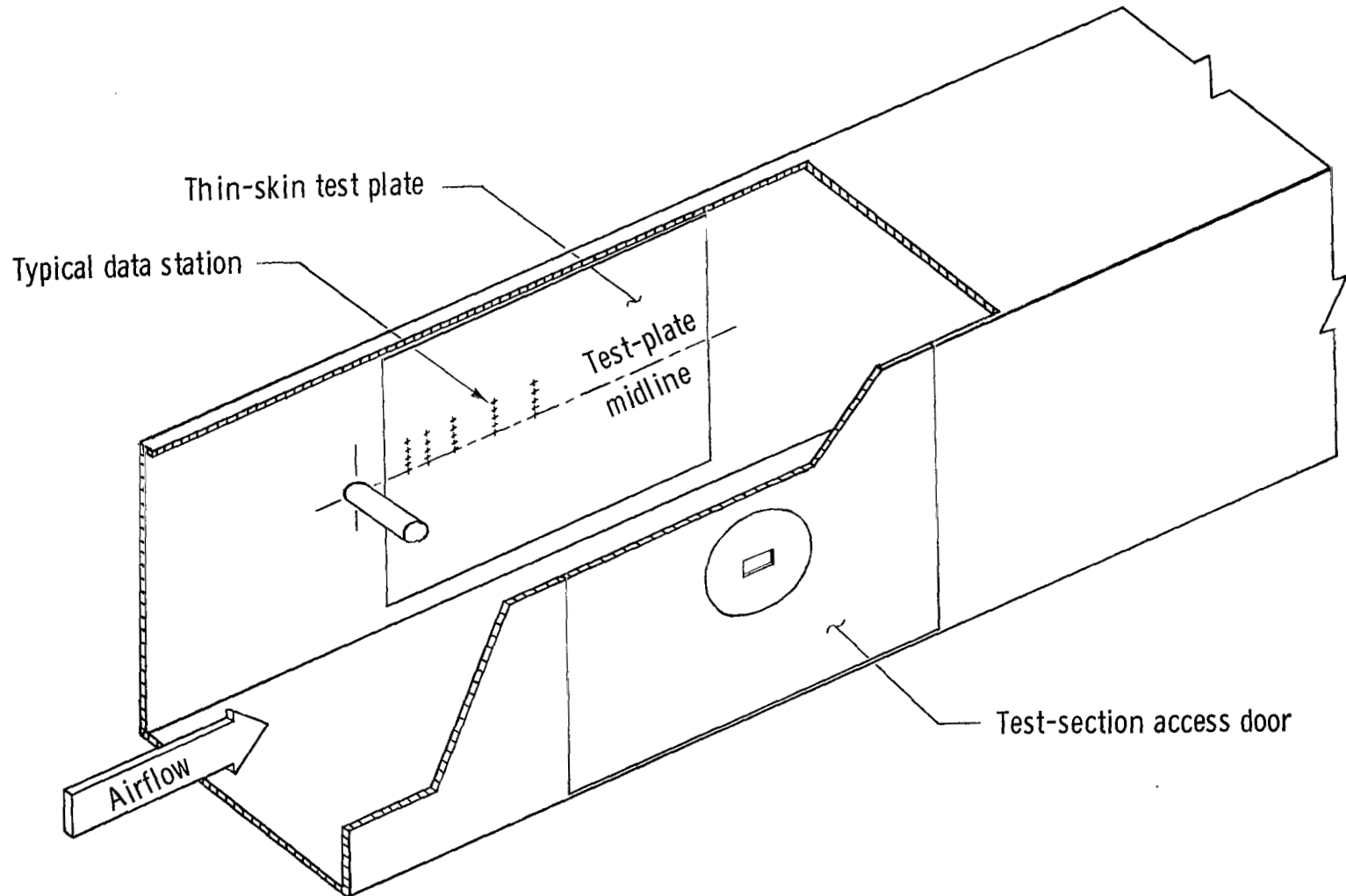
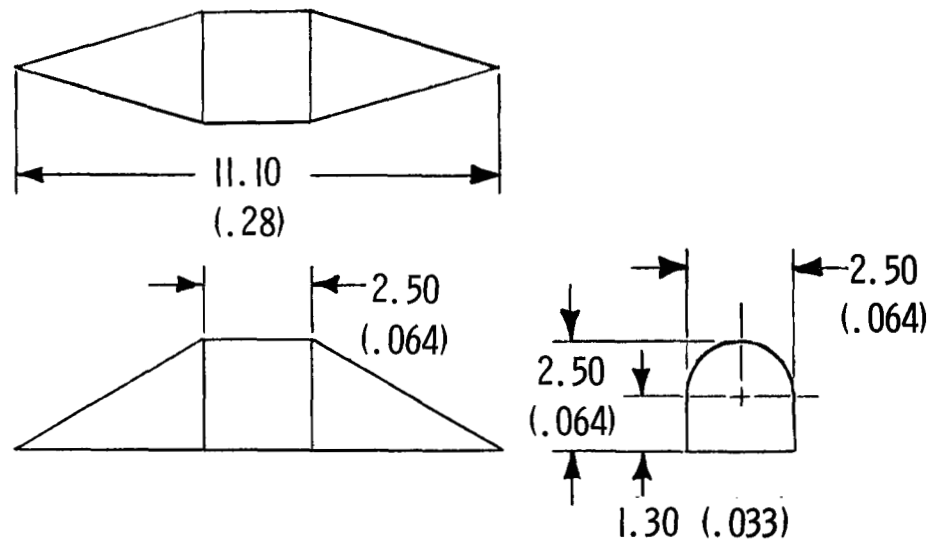
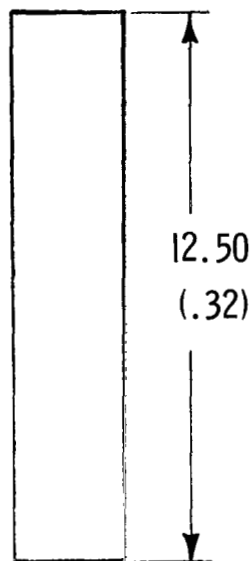
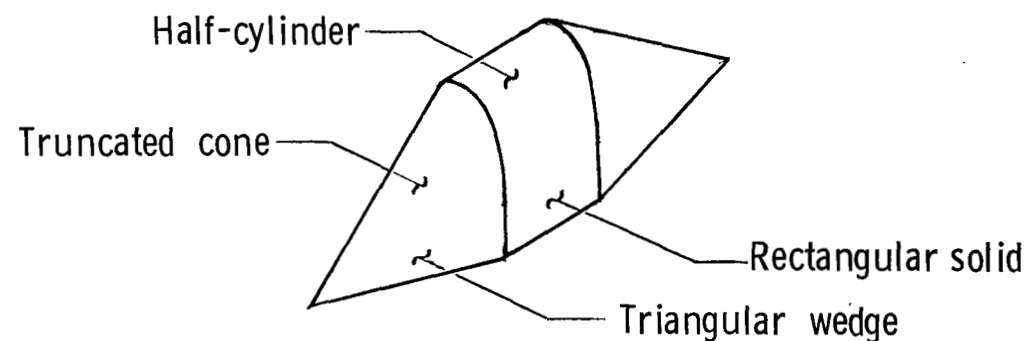
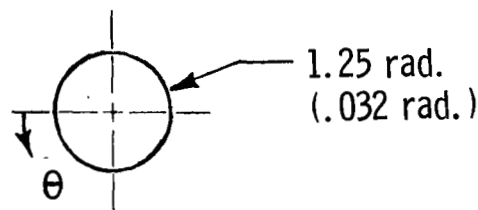


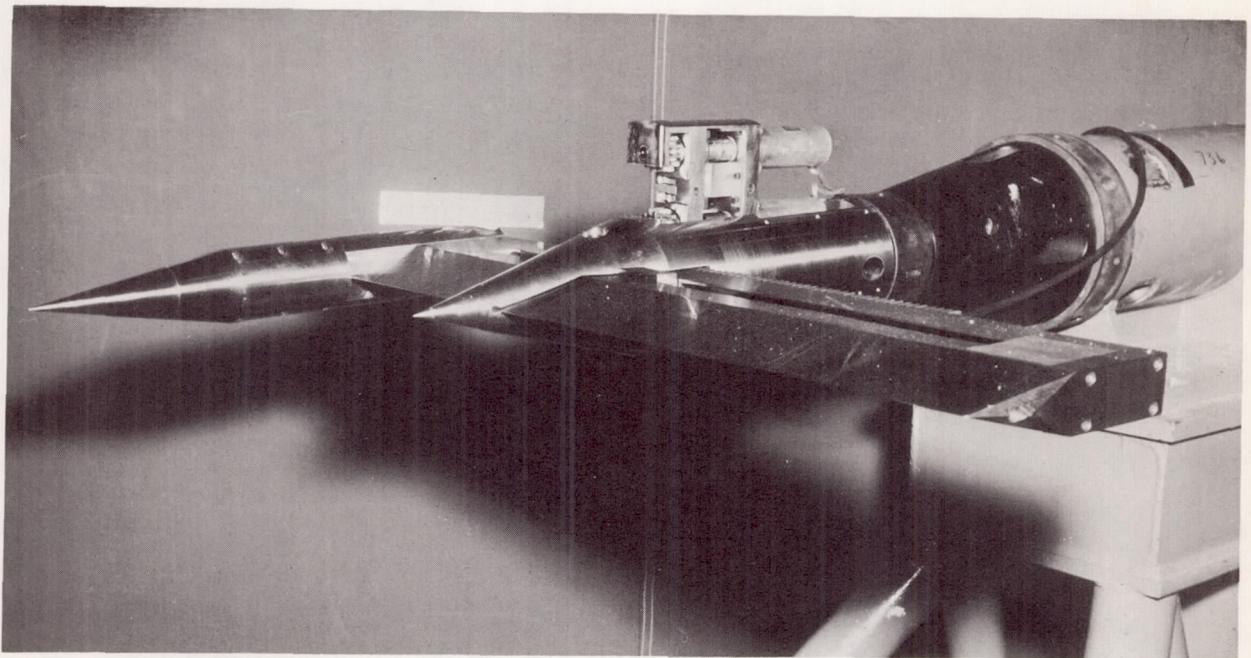
Figure 1.- Cylinder installed in test section.



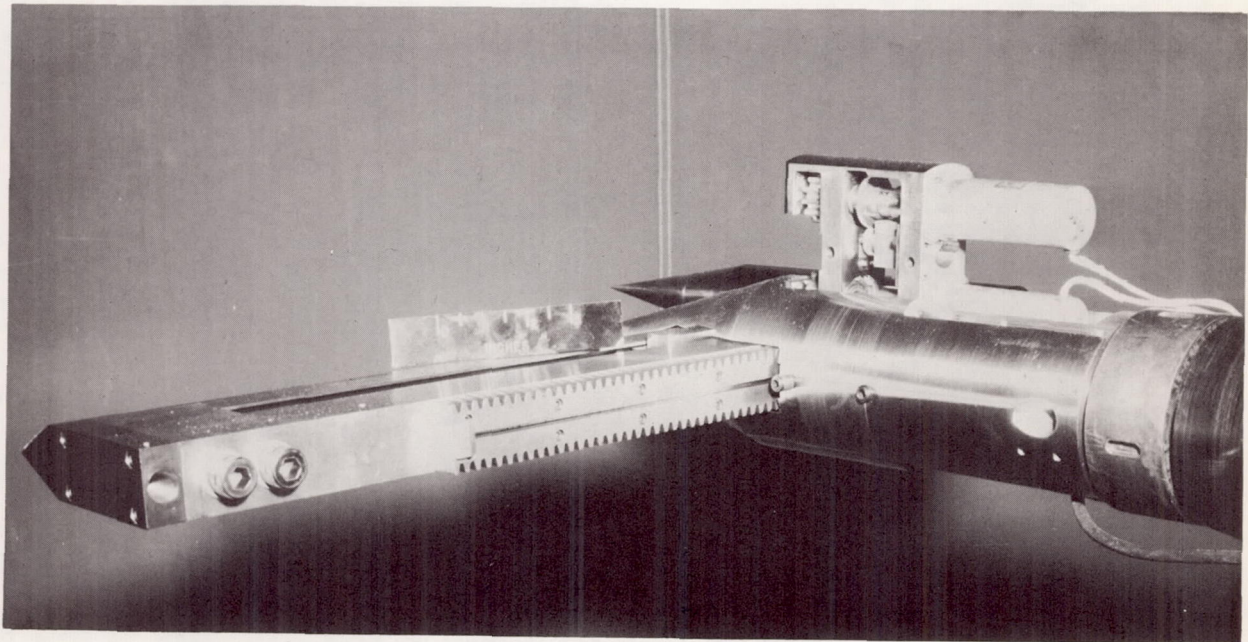
(a) Cylinder.

(b) Fairing.

Figure 2.- Models. Dimensions are in inches (meters).



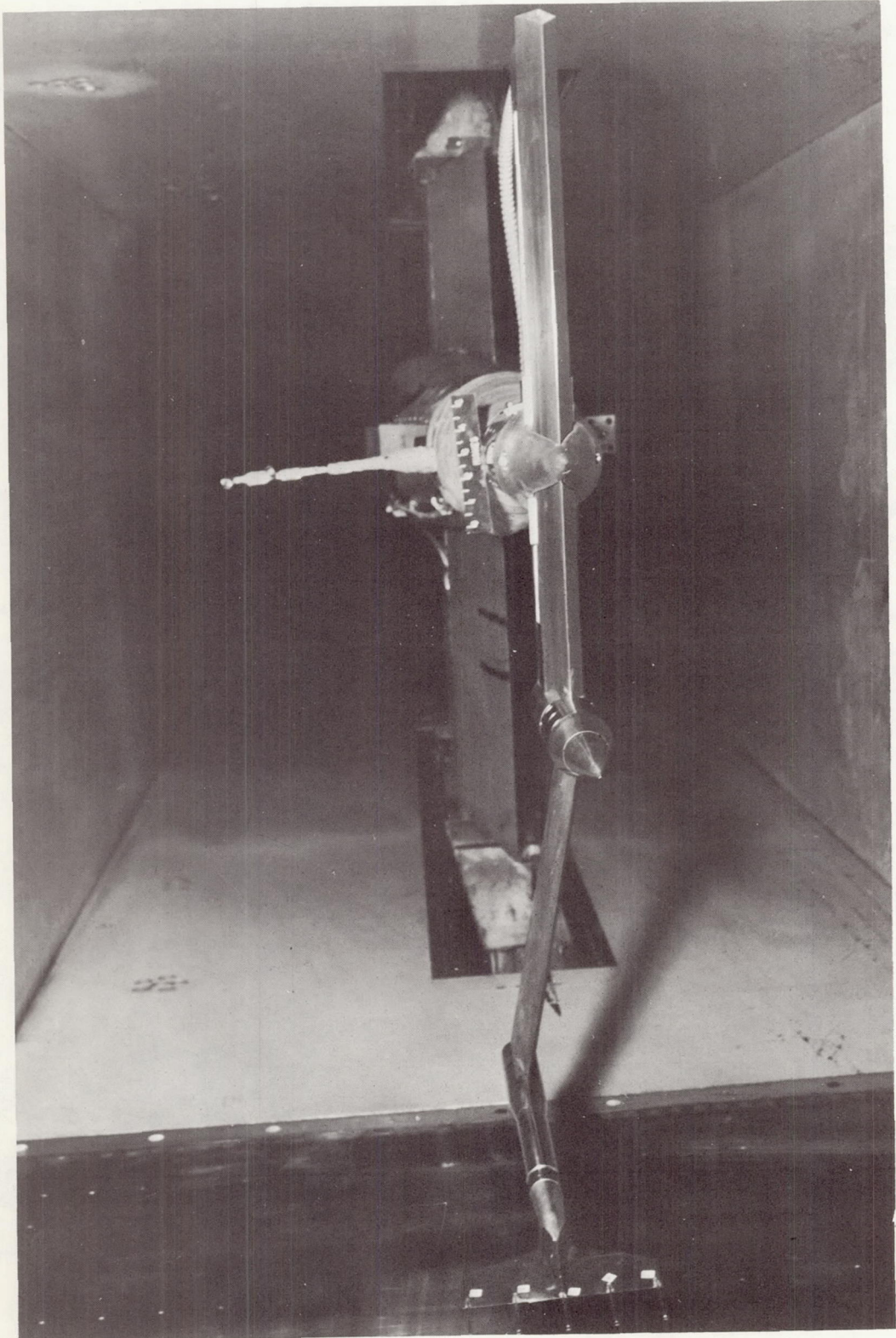
L-65-7175



(a) Traversing assembly.

L-65-7174

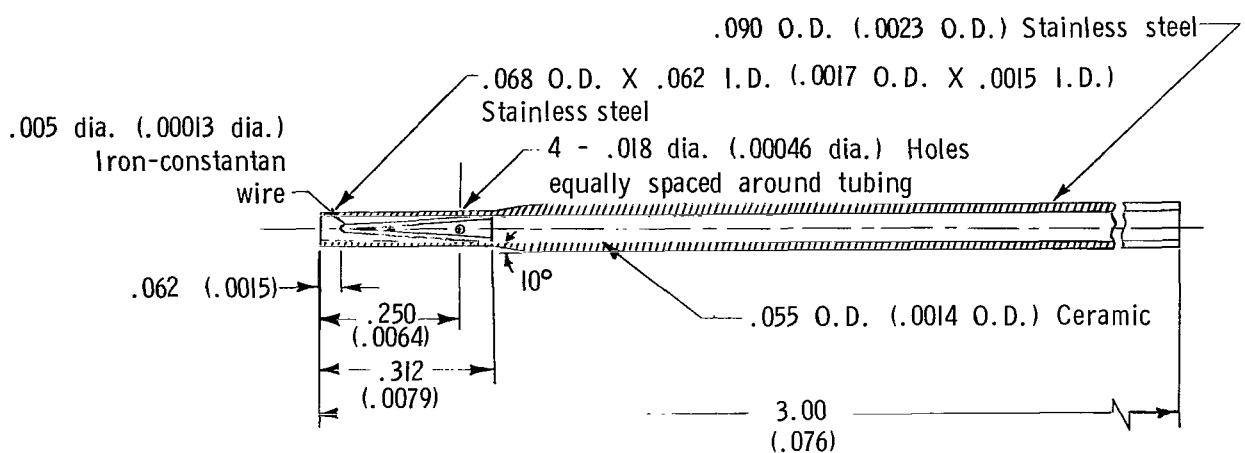
Figure 3.- Rake and traversing assembly.



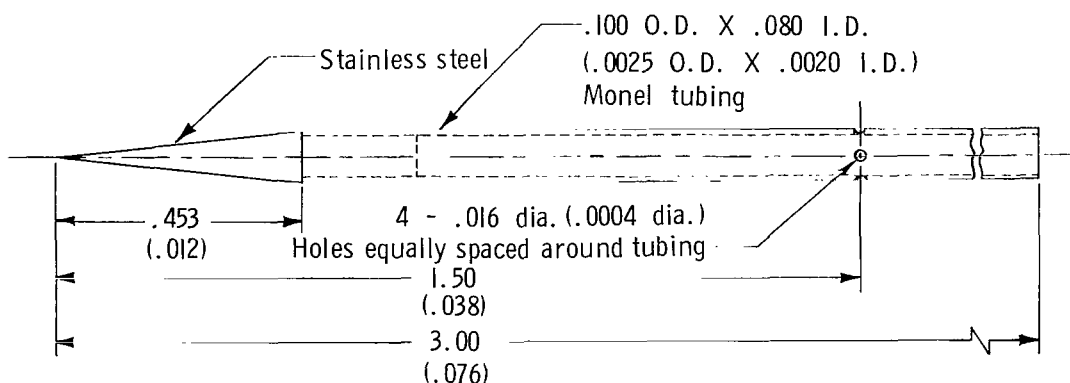
(b) Rake and traversing assembly installed in test section.

L-66-1526

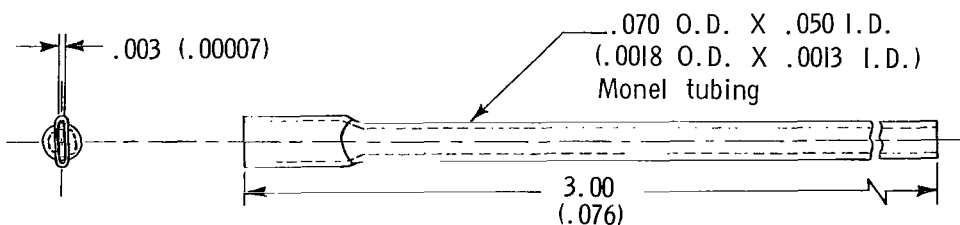
Figure 3.- Concluded.



(a) Total-temperature probe.



(b) Static-pressure probe.



(c) Pitot-pressure probe.

Figure 4.- Instrumentation. Dimensions are in inches (meters).

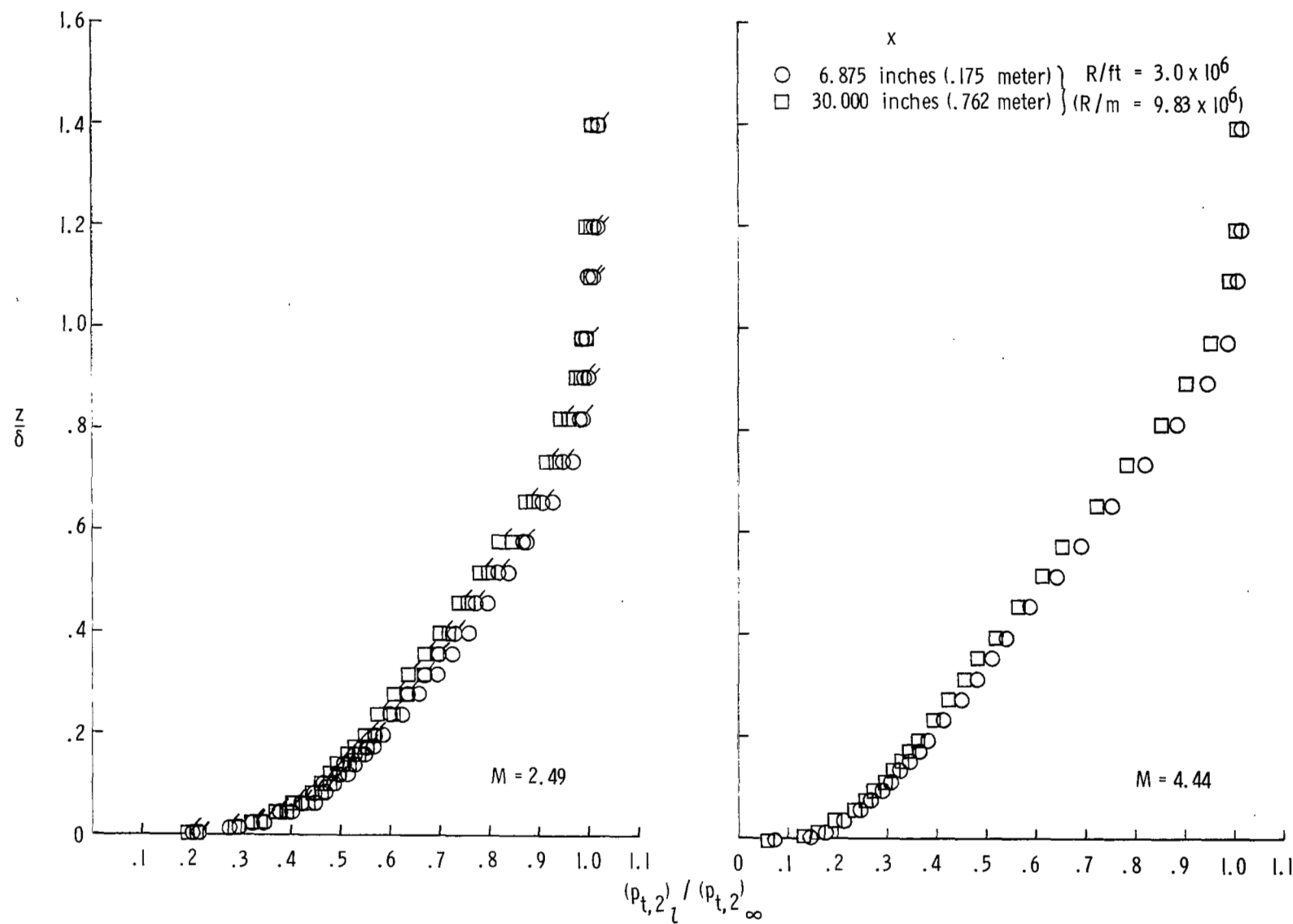


Figure 5.- Pitot-pressure distributions through the boundary layer on the flat plate at two longitudinal stations. $y = 0$ inch. Flagged symbols indicate data for $R/ft = 1.5 \times 10^6$ ($R/m = 4.92 \times 10^6$).

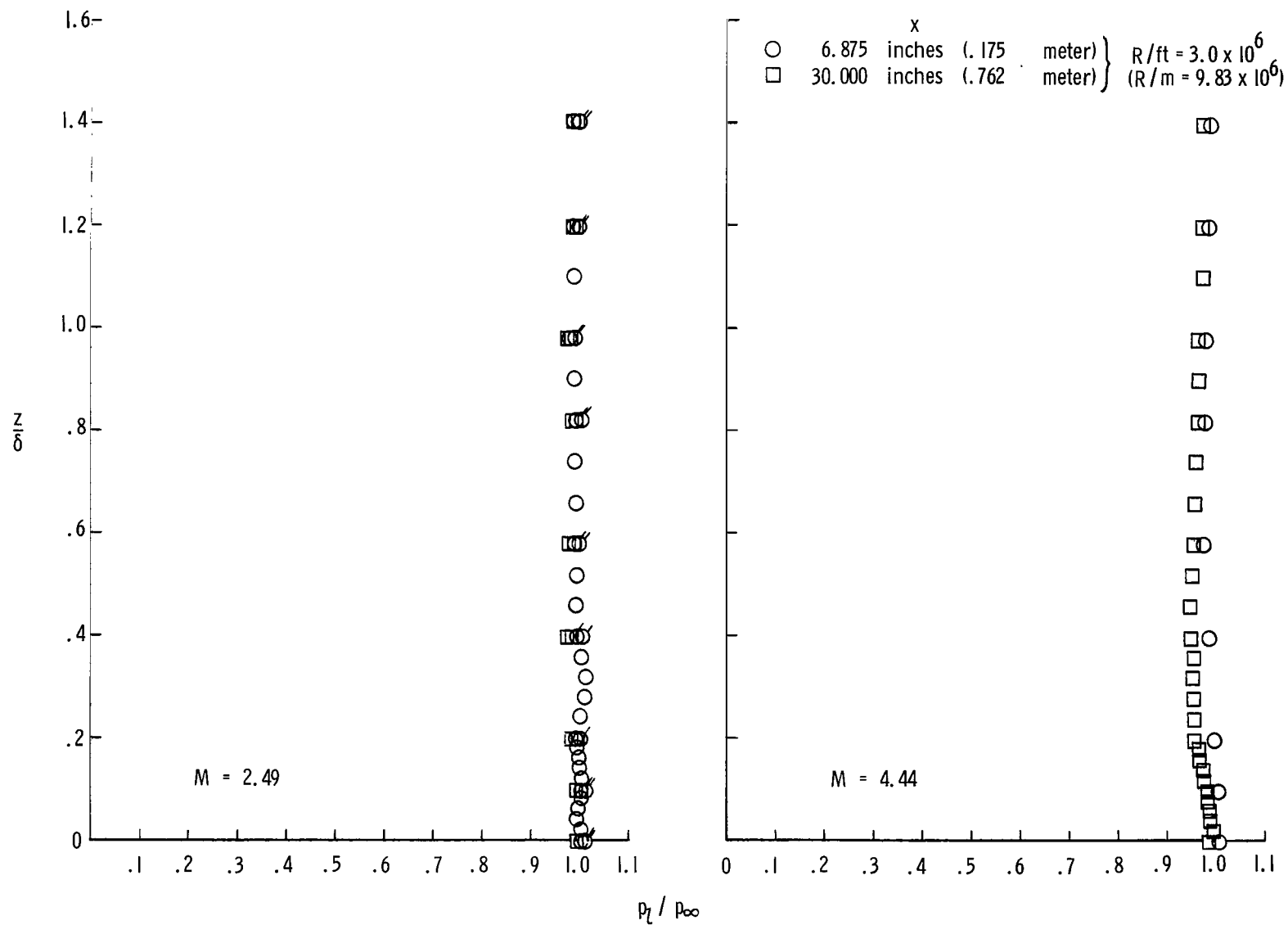


Figure 6.- Static-pressure distributions through the boundary layer on the flat plate at two longitudinal stations. $y = 0$ inch. Flagged symbols indicate data for $R/\text{ft} = 1.5 \times 10^6$ ($R/\text{m} = 4.92 \times 10^6$).

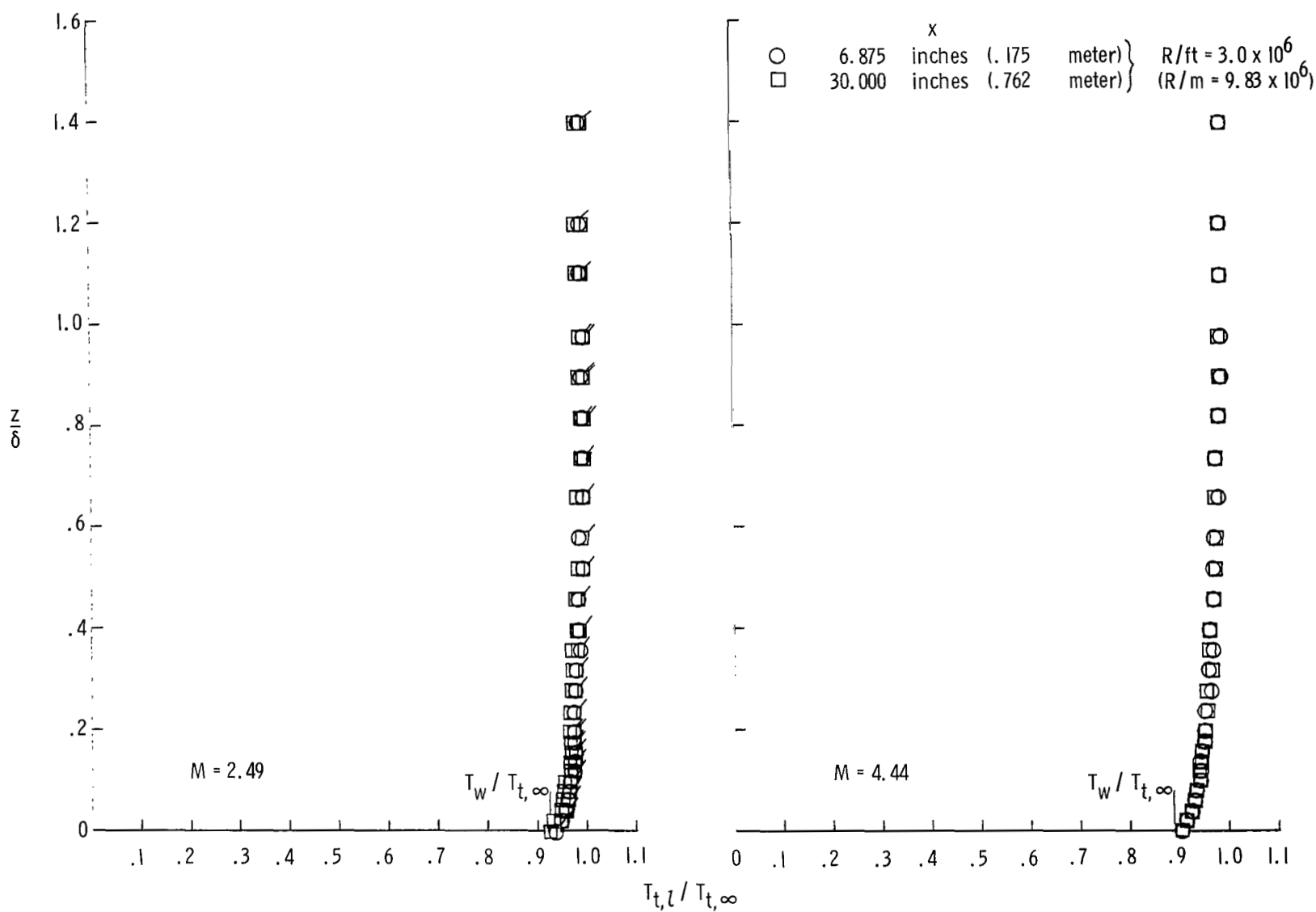


Figure 7.- Total-temperature distributions through the boundary layer on the flat plate at two longitudinal stations. $y = 0$ inch. Flagged symbols indicate data for $R/\text{ft} = 1.5 \times 10^6$ ($R/\text{m} = 4.92 \times 10^6$).

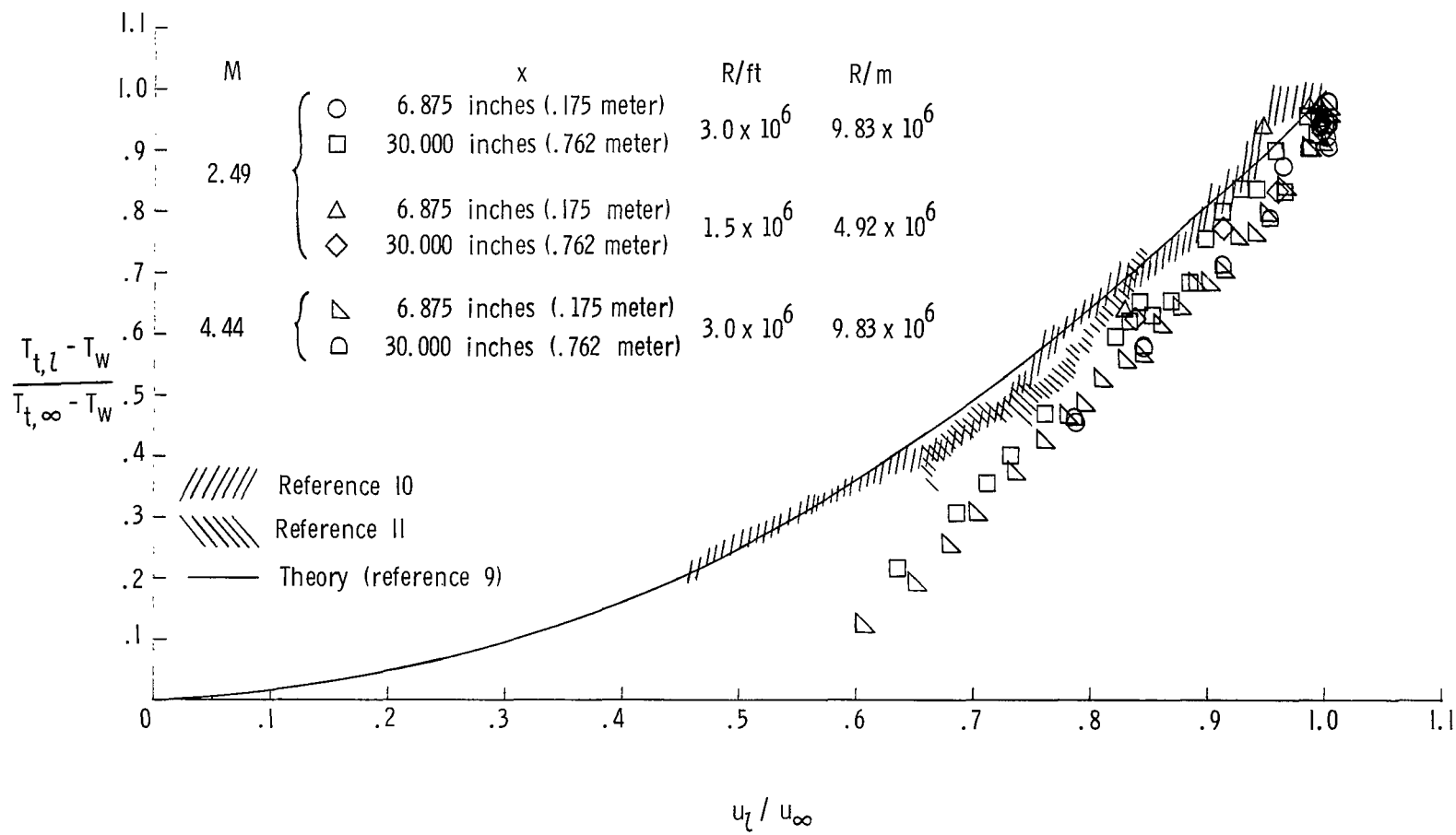


Figure 8.- Correlation of temperature ratios.

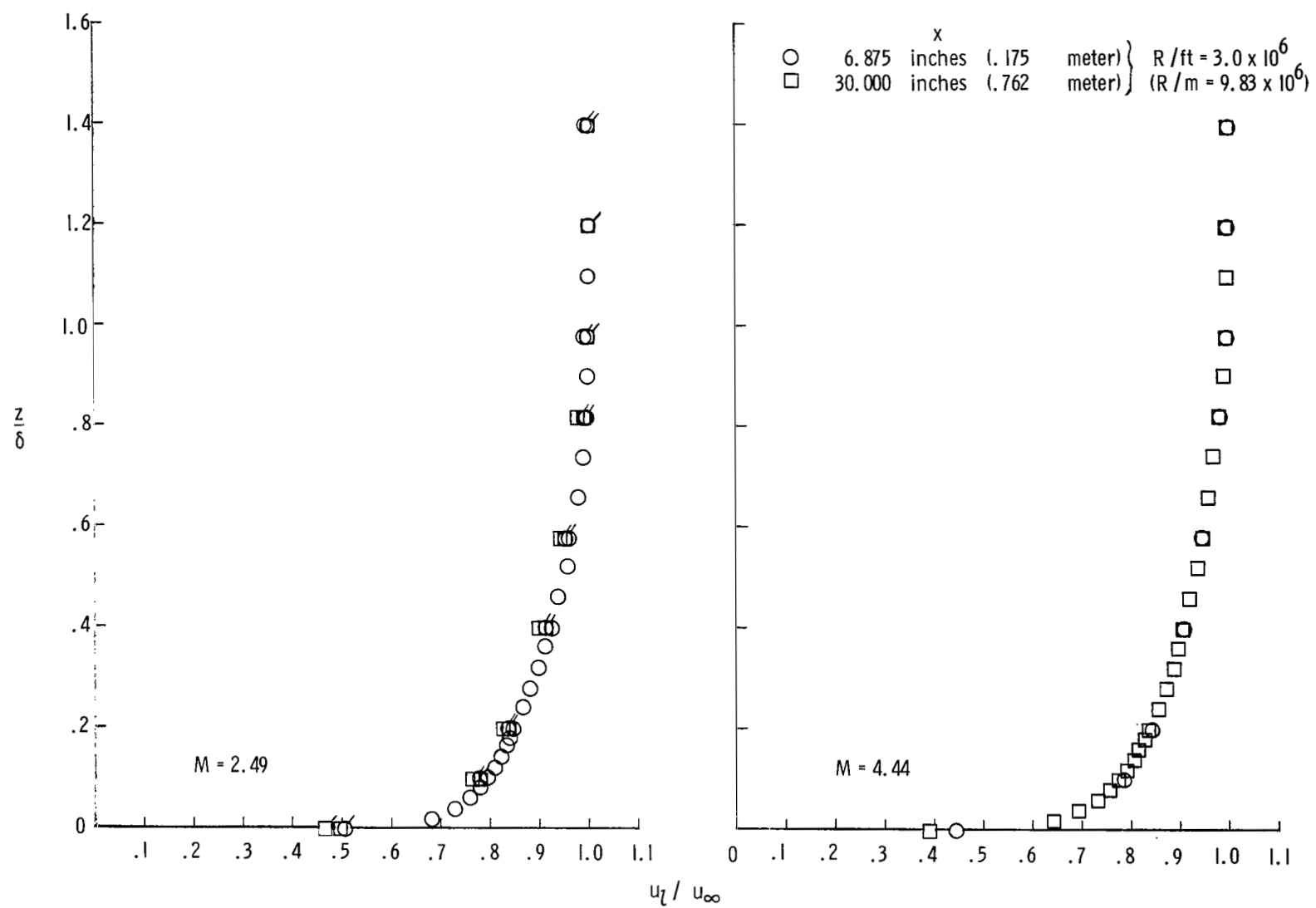
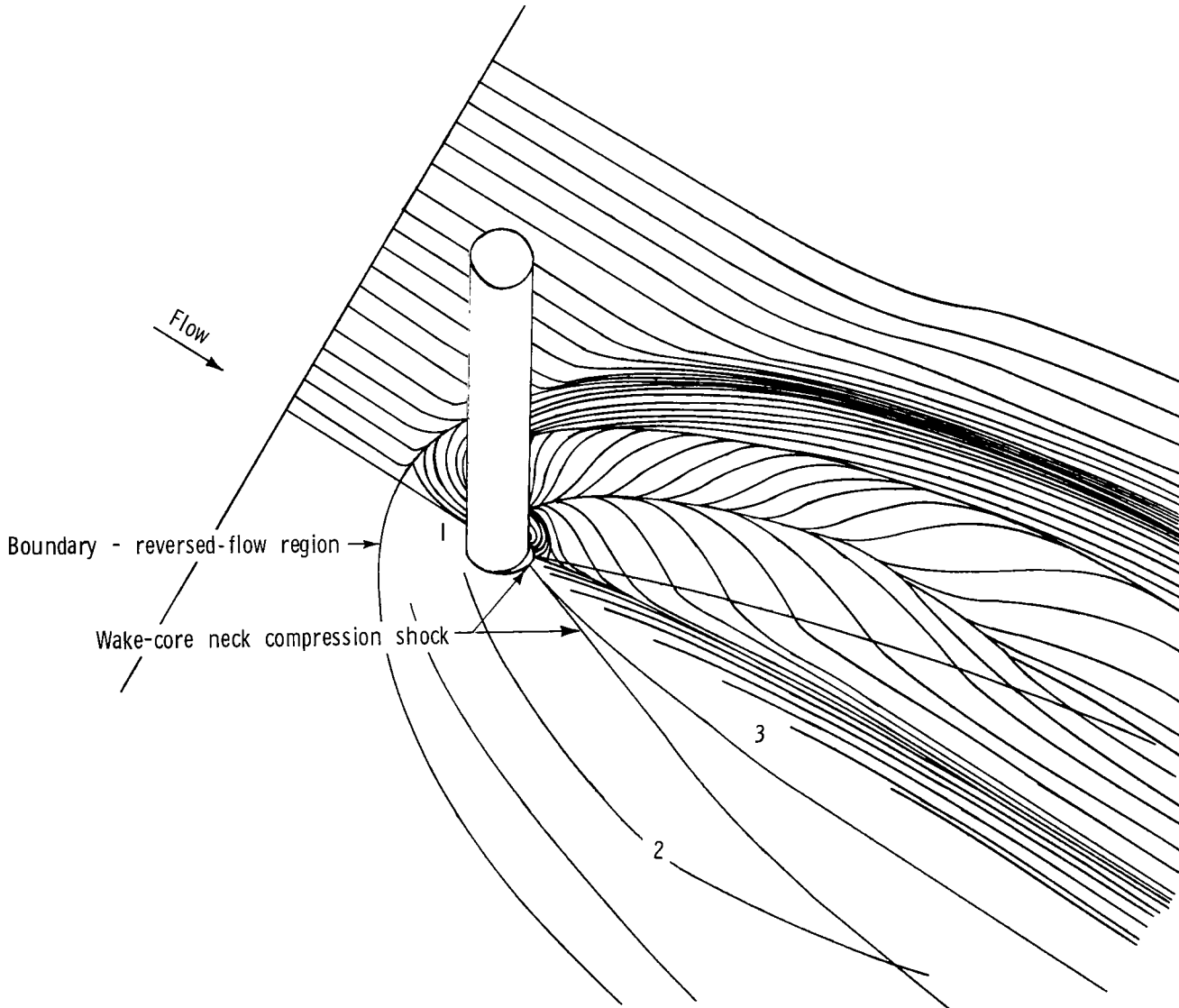
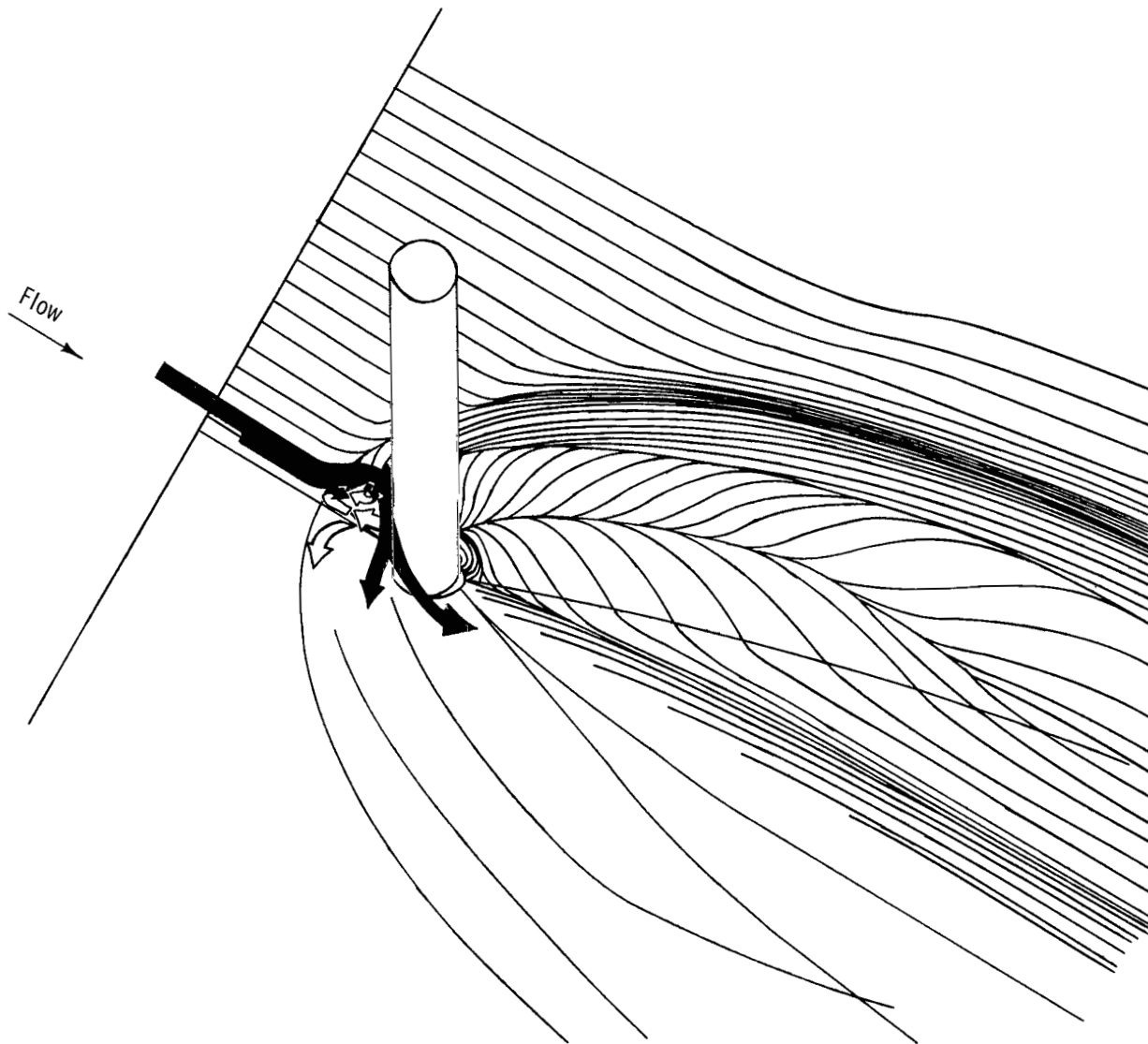


Figure 9.- Velocity distributions through the boundary layer on the flat plate at two longitudinal stations. $y = 0$ inch. Flagged symbols indicate data for $R/\text{ft} = 1.5 \times 10^6$ ($R/\text{m} = 4.92 \times 10^6$).



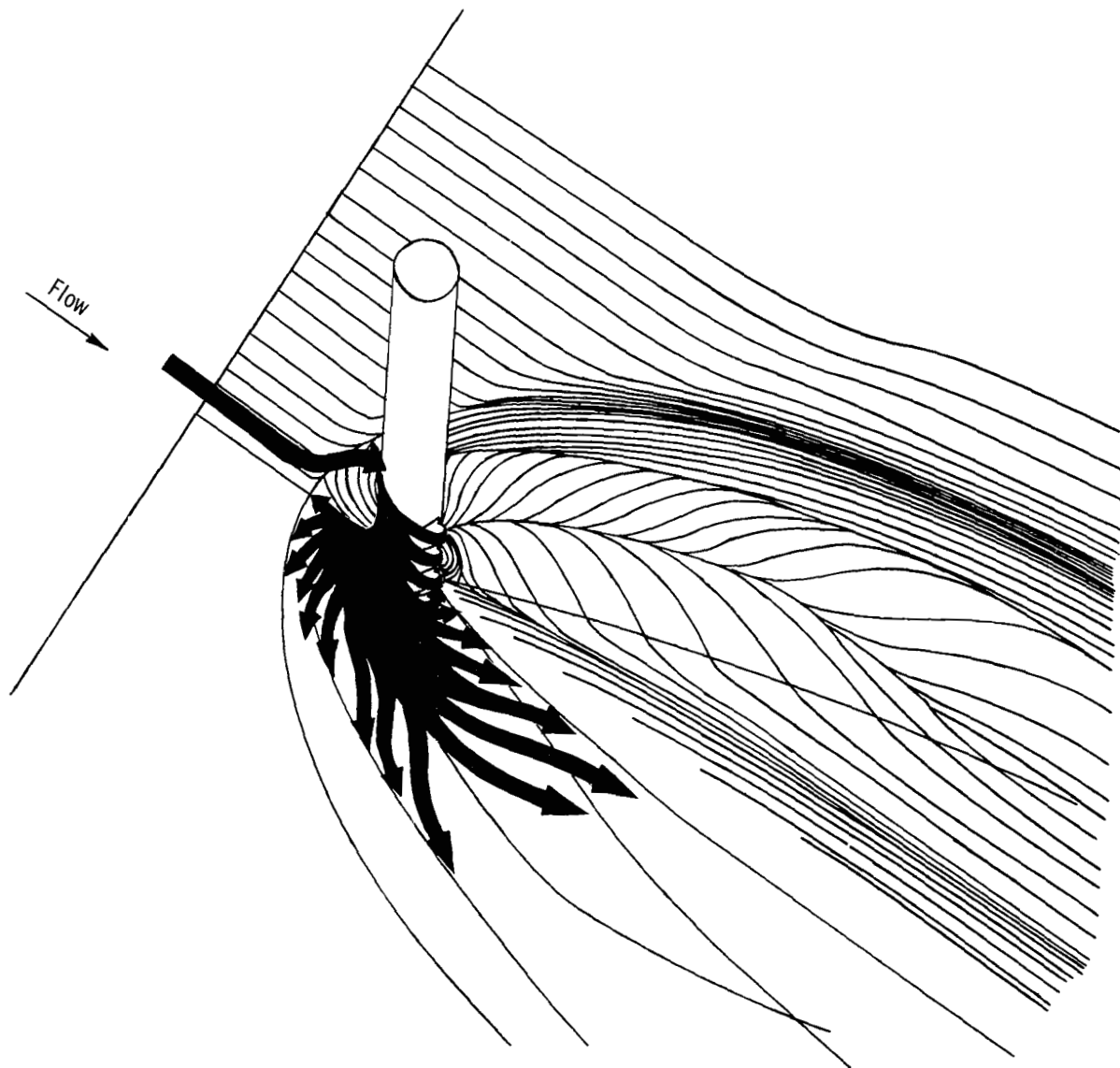
(a) Flow on plate. 1, 2, and 3 indicate distinct regions of flow.

Figure 10.- Flow model of flat plate with attached cylinder.



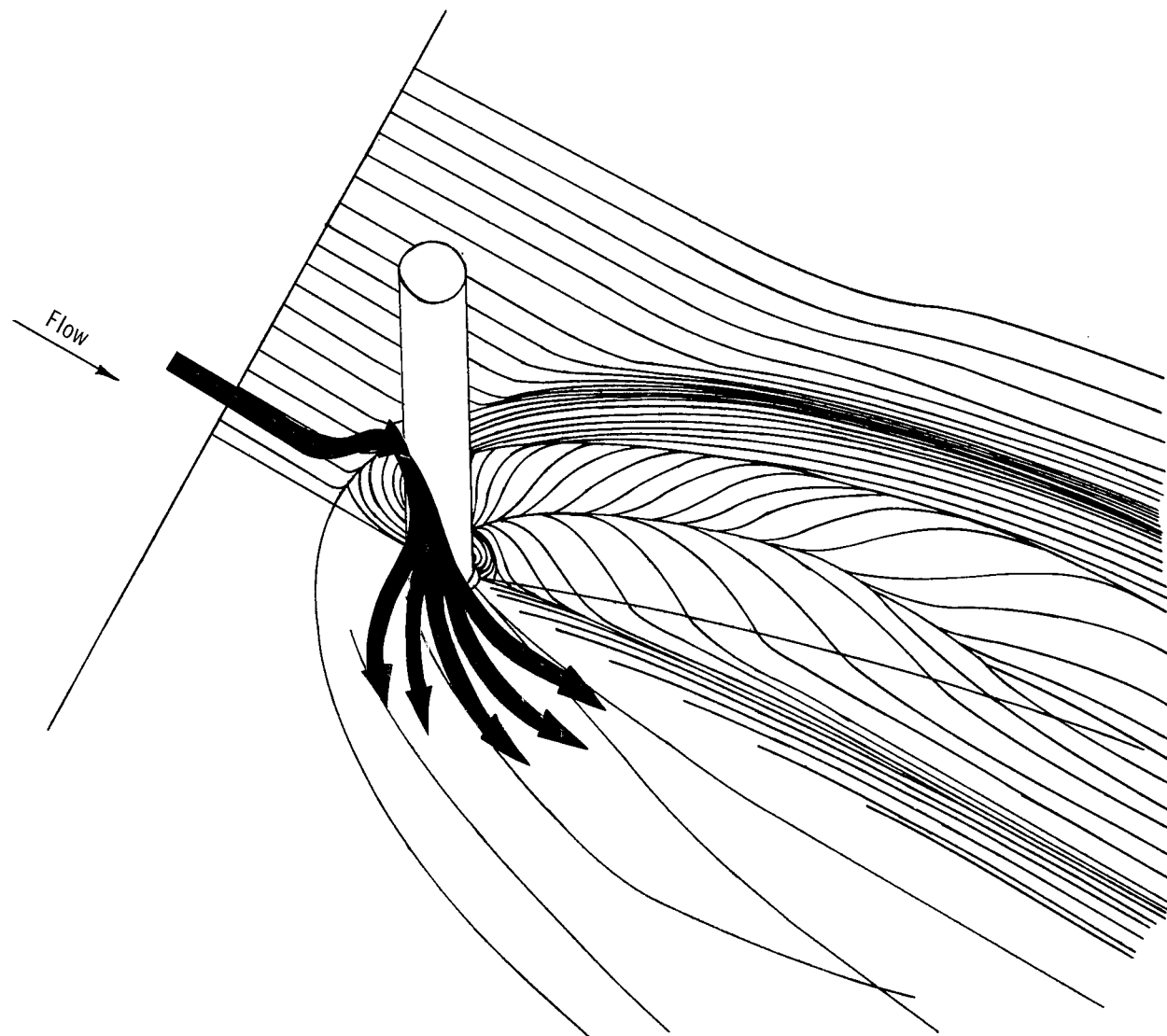
(b) Upstream reversed-flow region.

Figure 10.- Continued.



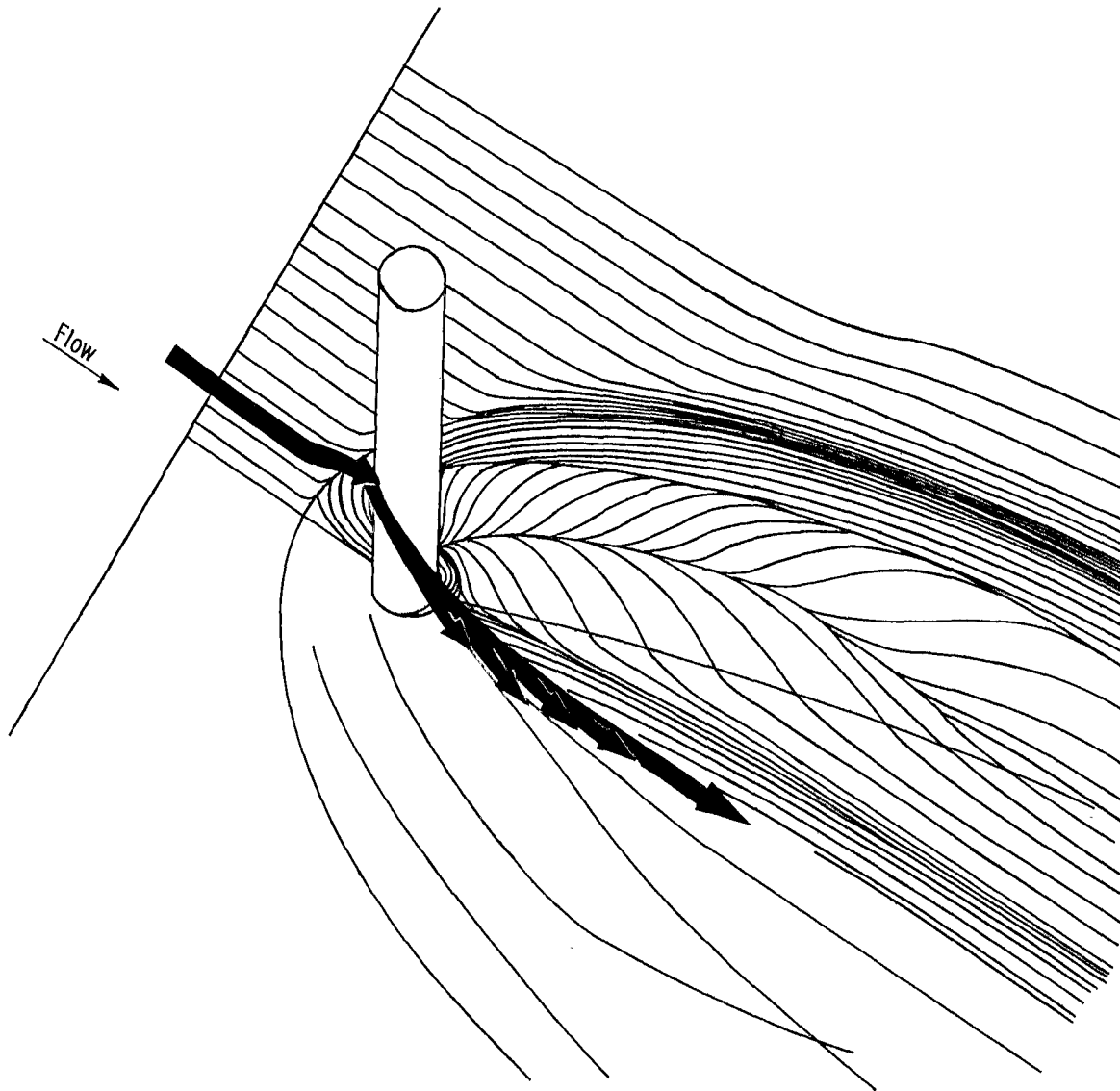
(c) Radial flow away from cylinder.

Figure 10.- Continued.



(d) Flow-impingement region.

Figure 10.- Continued.



(e) Wake-core region.

Figure 10.- Concluded.

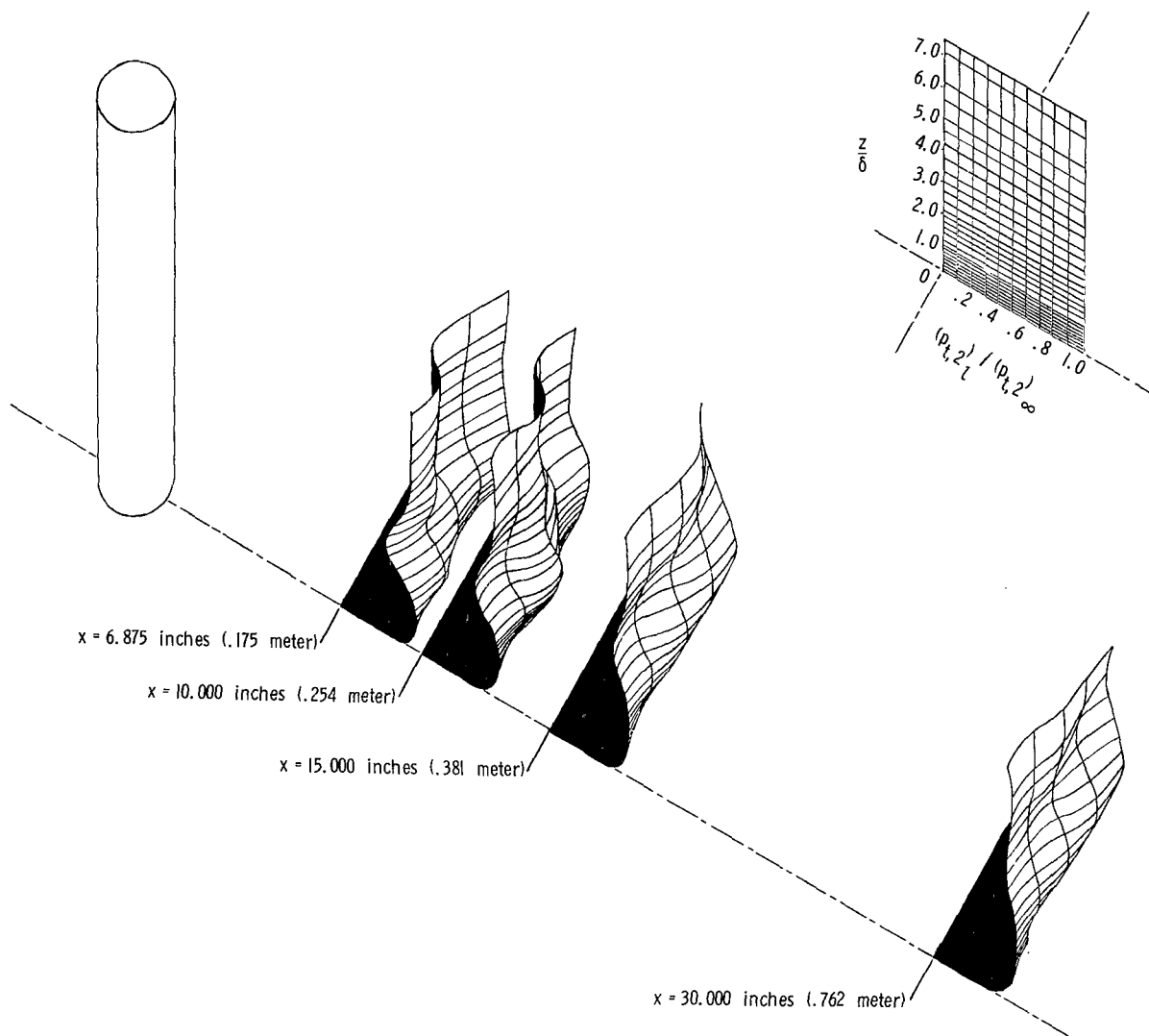
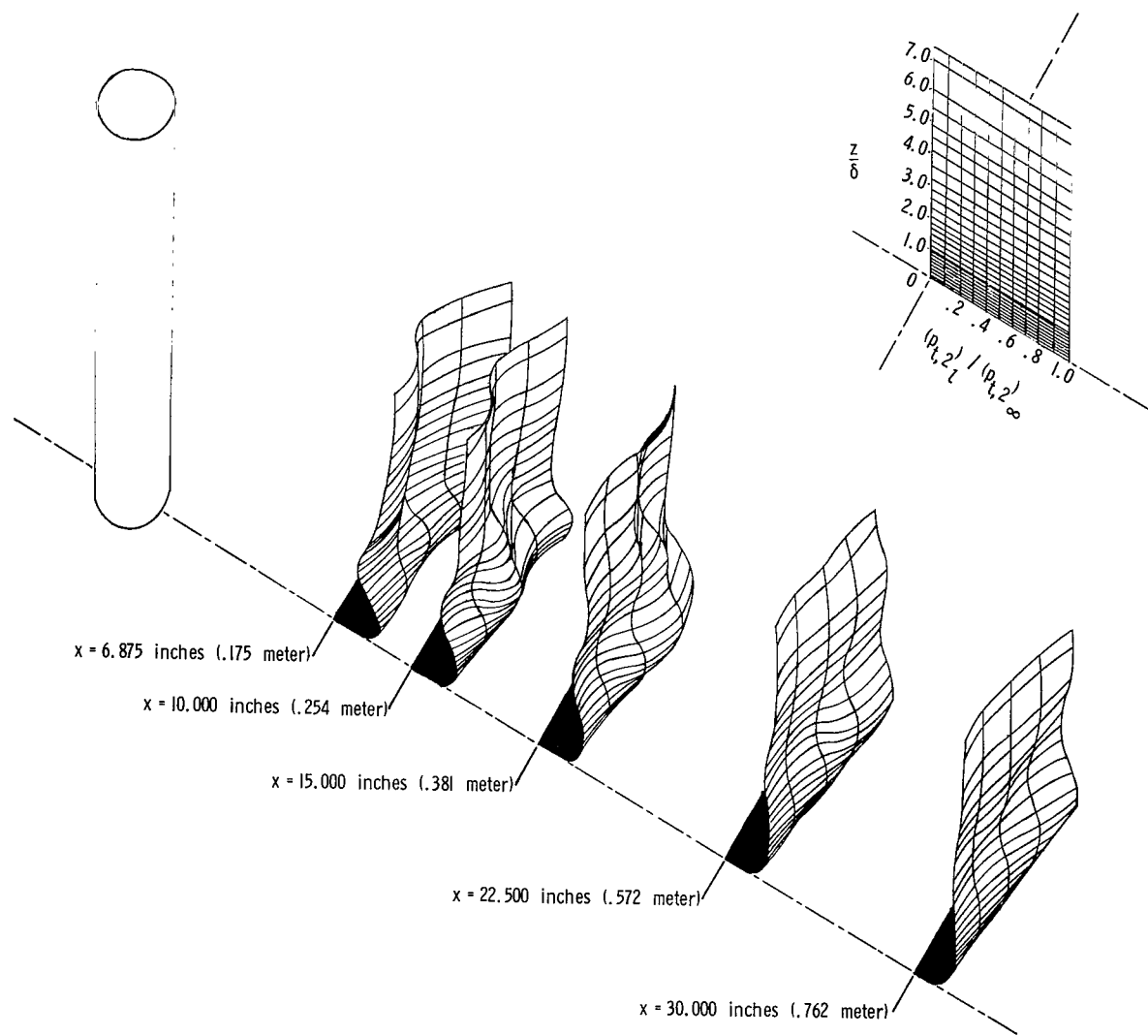
(a) $M = 2.49$.

Figure 11.- Isometric pitot-pressure distributions downstream of attached cylinder.



(b) $M = 4.44$.

Figure 11.- Concluded.

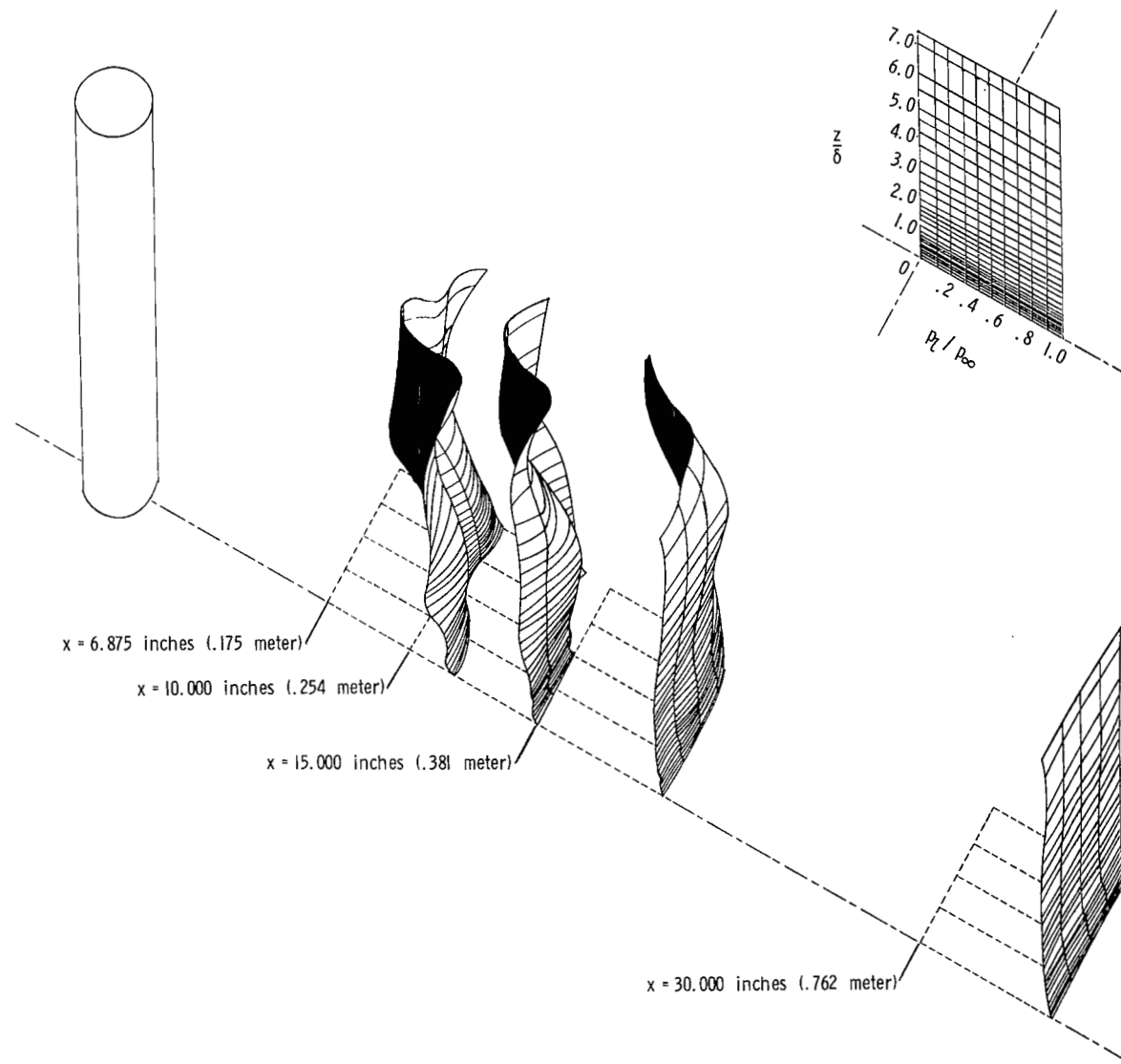
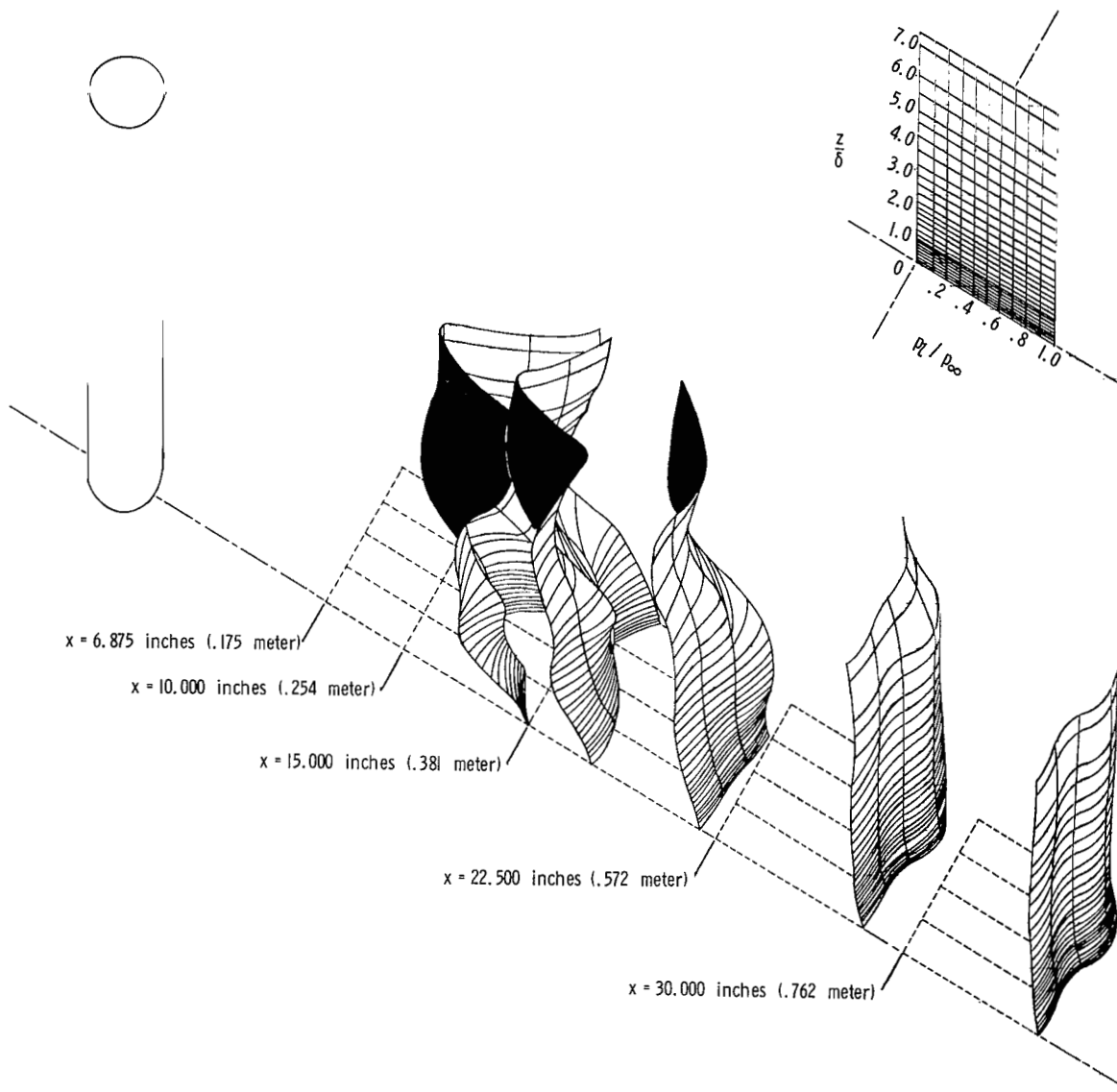
(a) $M = 2.49$.

Figure 12.- Isometric static-pressure distributions downstream of attached cylinder.



(b) $M = 4.44$.

Figure 12.- Concluded.

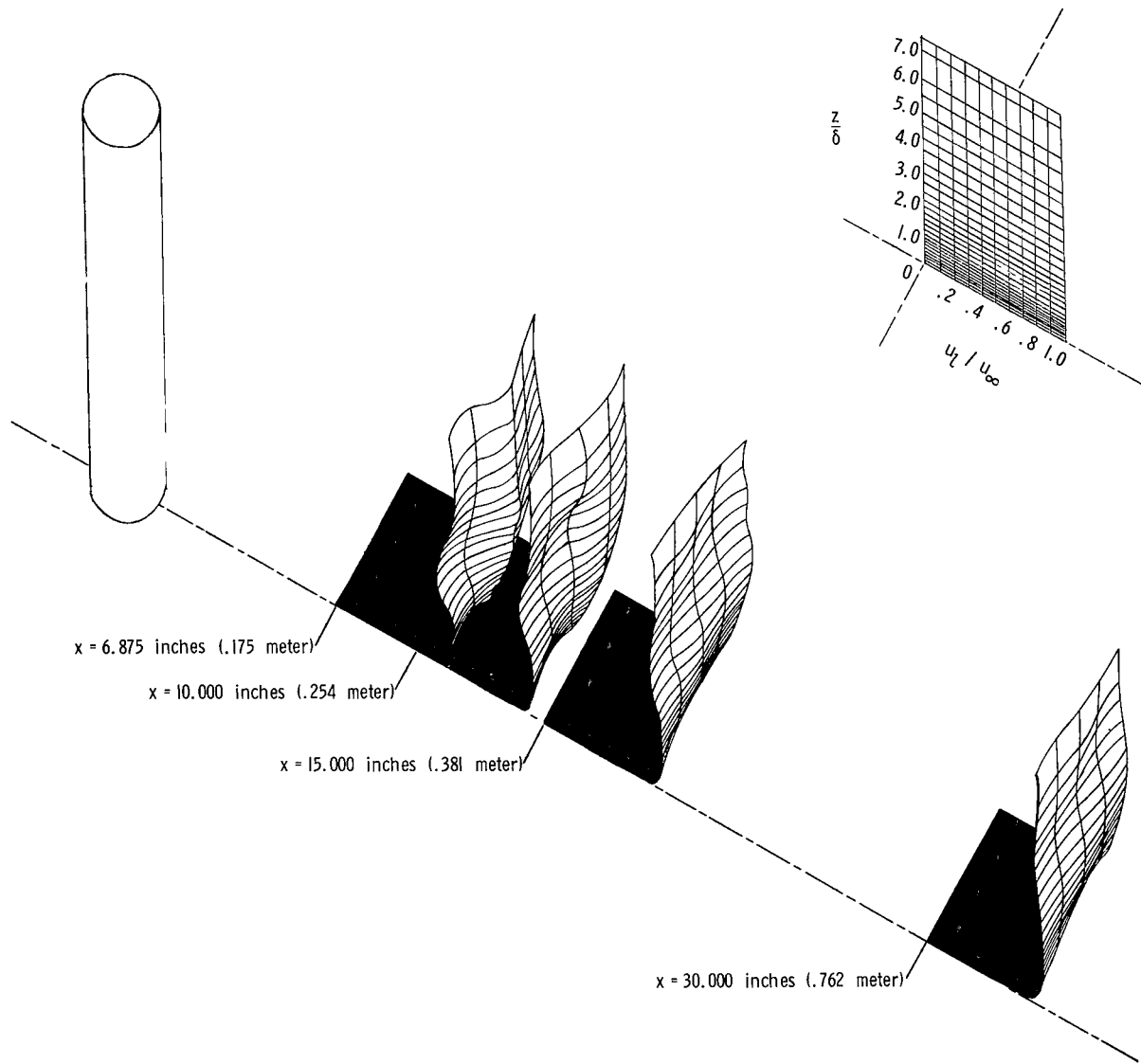
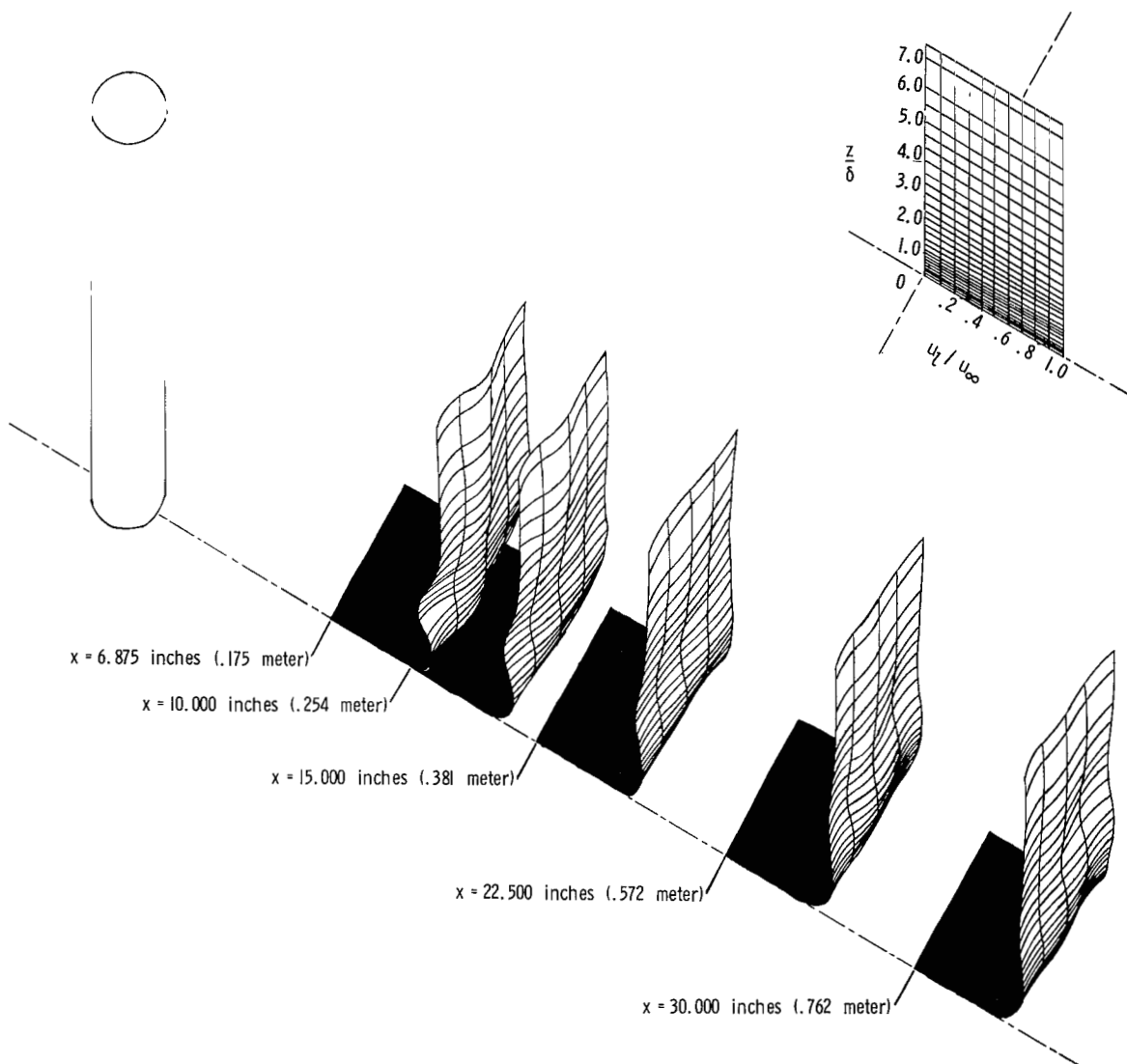
(a) $M = 2.49$.

Figure 13.- Isometric velocity distributions downstream of attached cylinder.



(b) $M = 4.44$.

Figure 13.- Concluded.

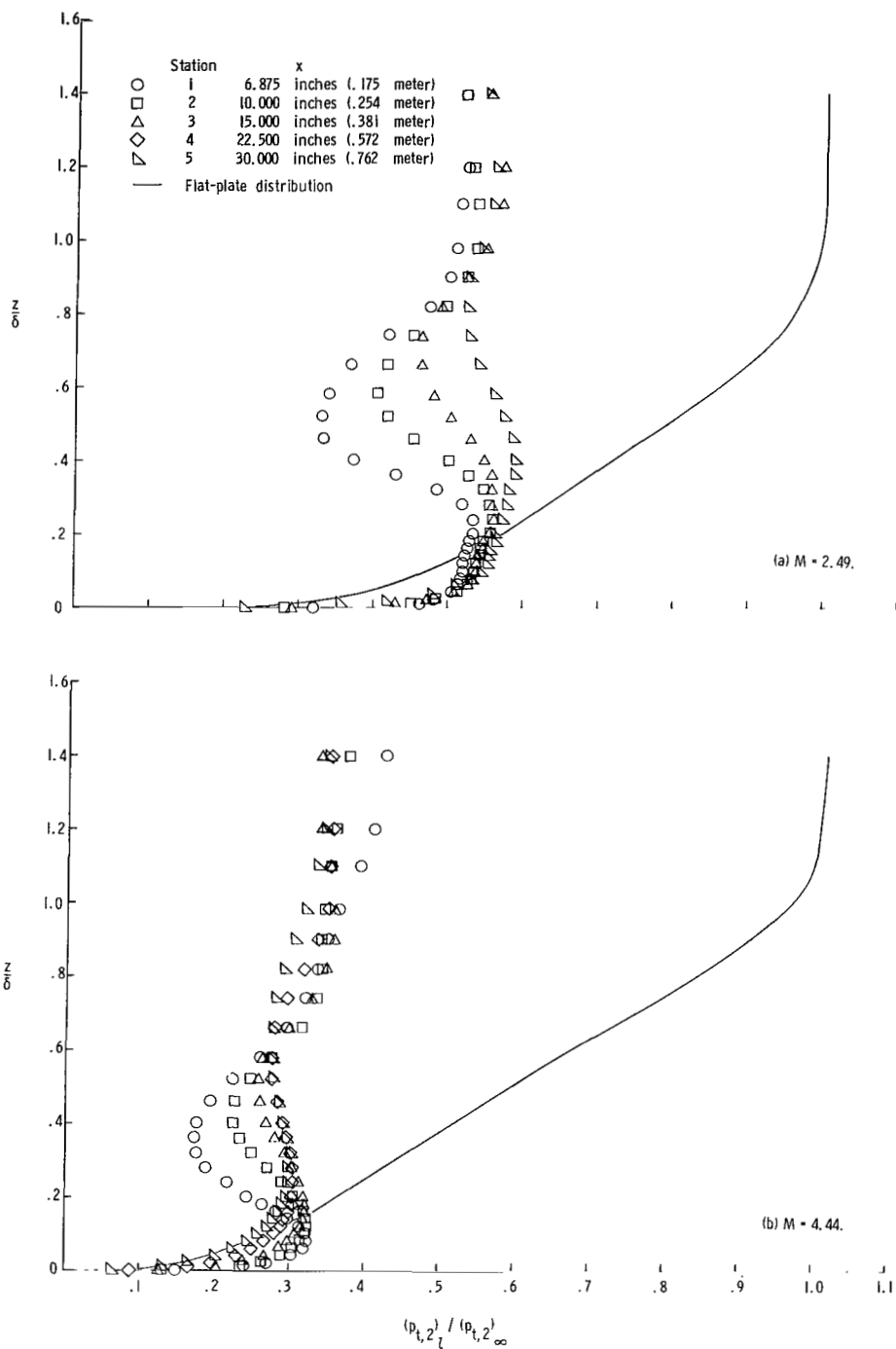


Figure 14.- Pitot-pressure distributions downstream of cylinder at longitudinal stations, $y = 0$ inch.

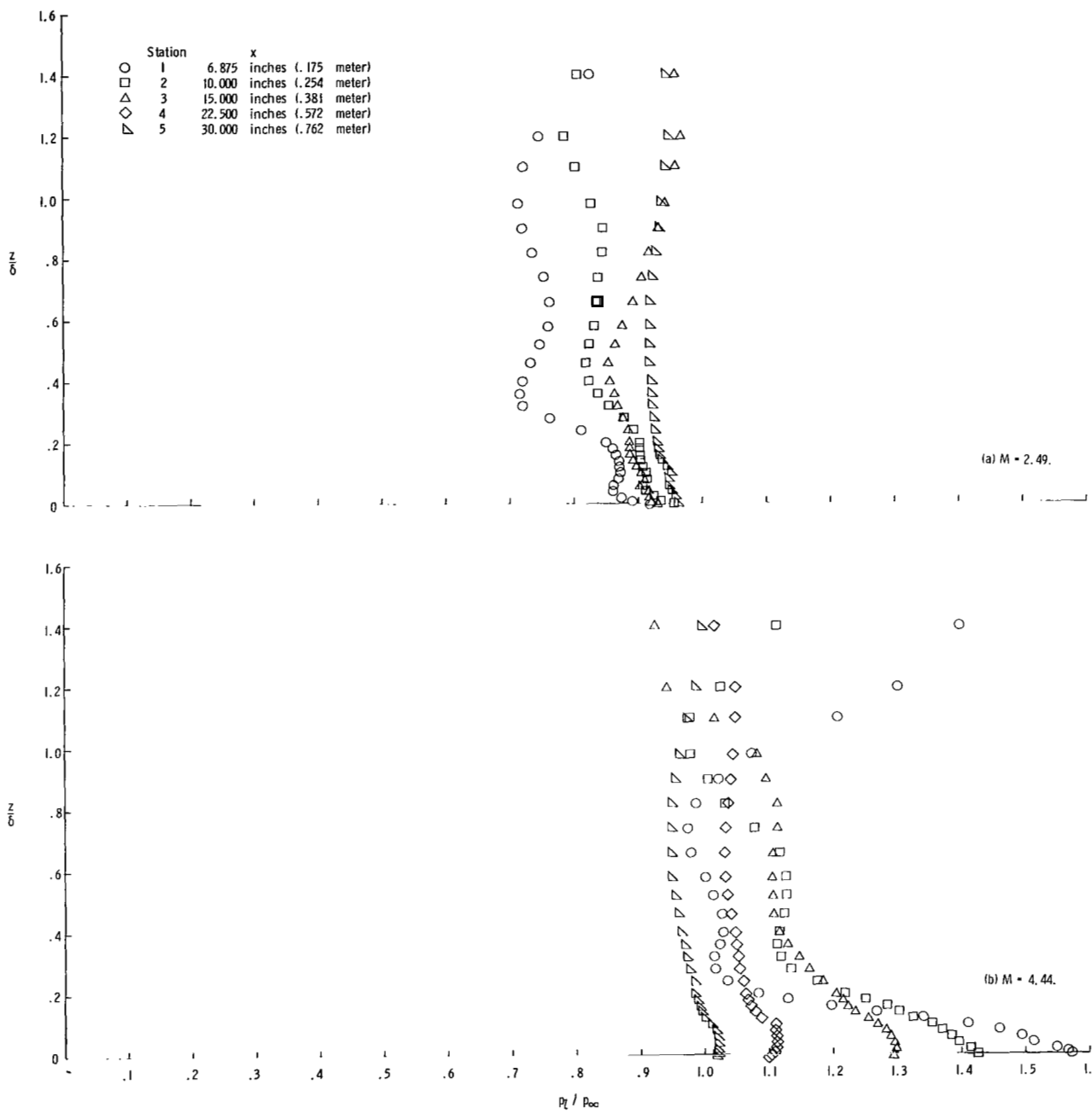


Figure 15.- Static-pressure distributions downstream of cylinder at longitudinal stations. $y = 0$ inch.

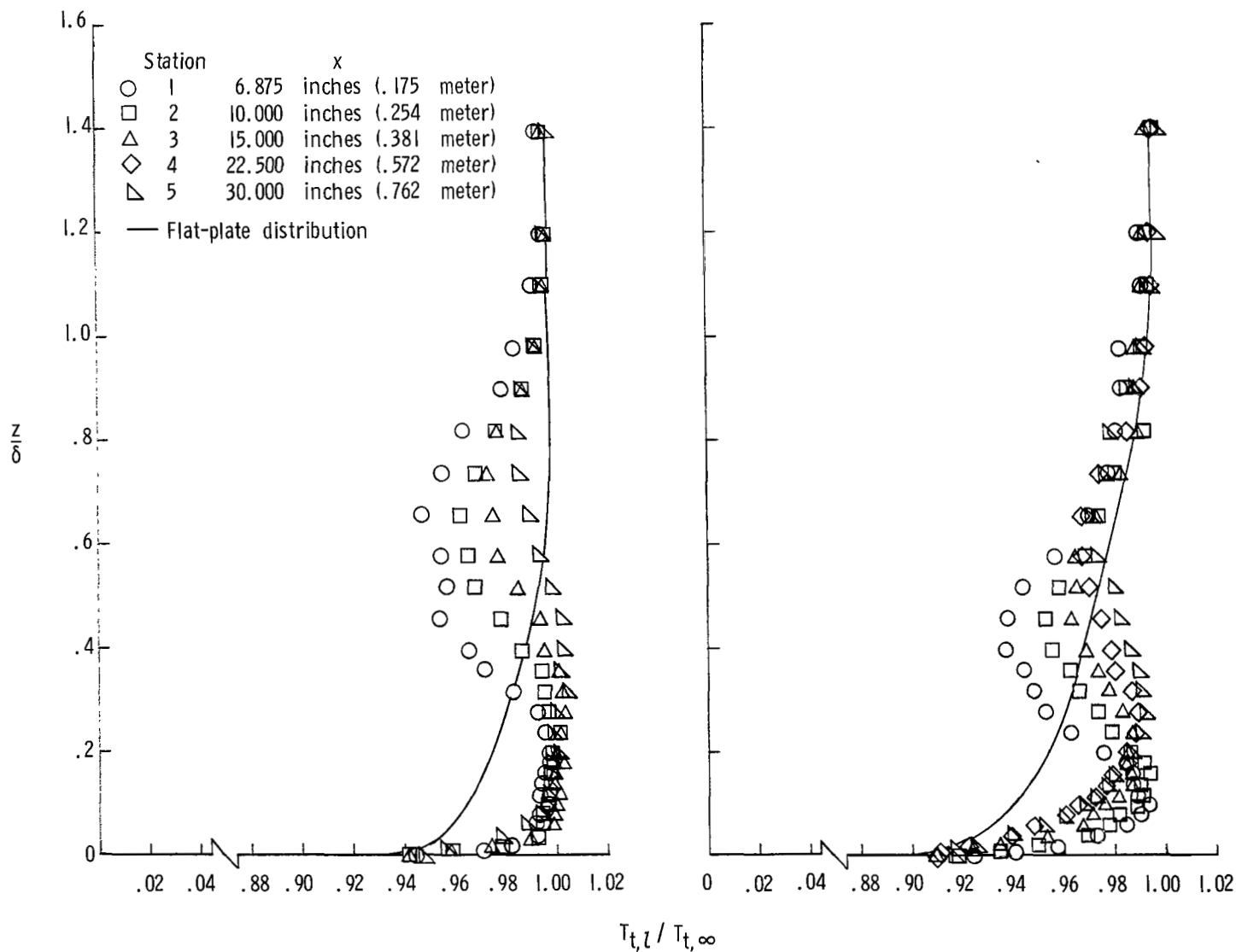
(a) $M = 2.49.$ (b) $M = 4.44.$

Figure 16.- Total-temperature distributions downstream of cylinder at longitudinal stations. $y = 0$ inch.

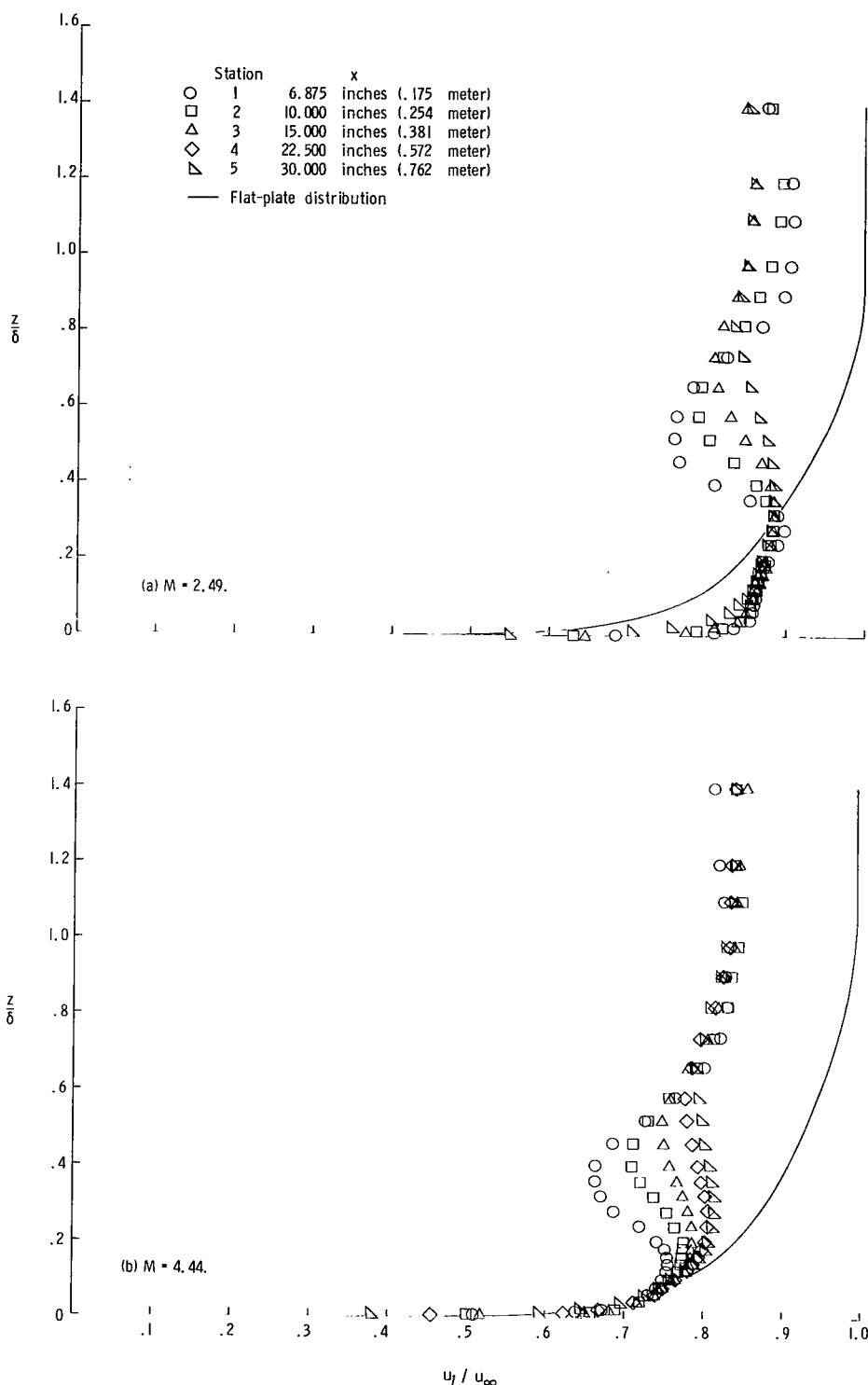
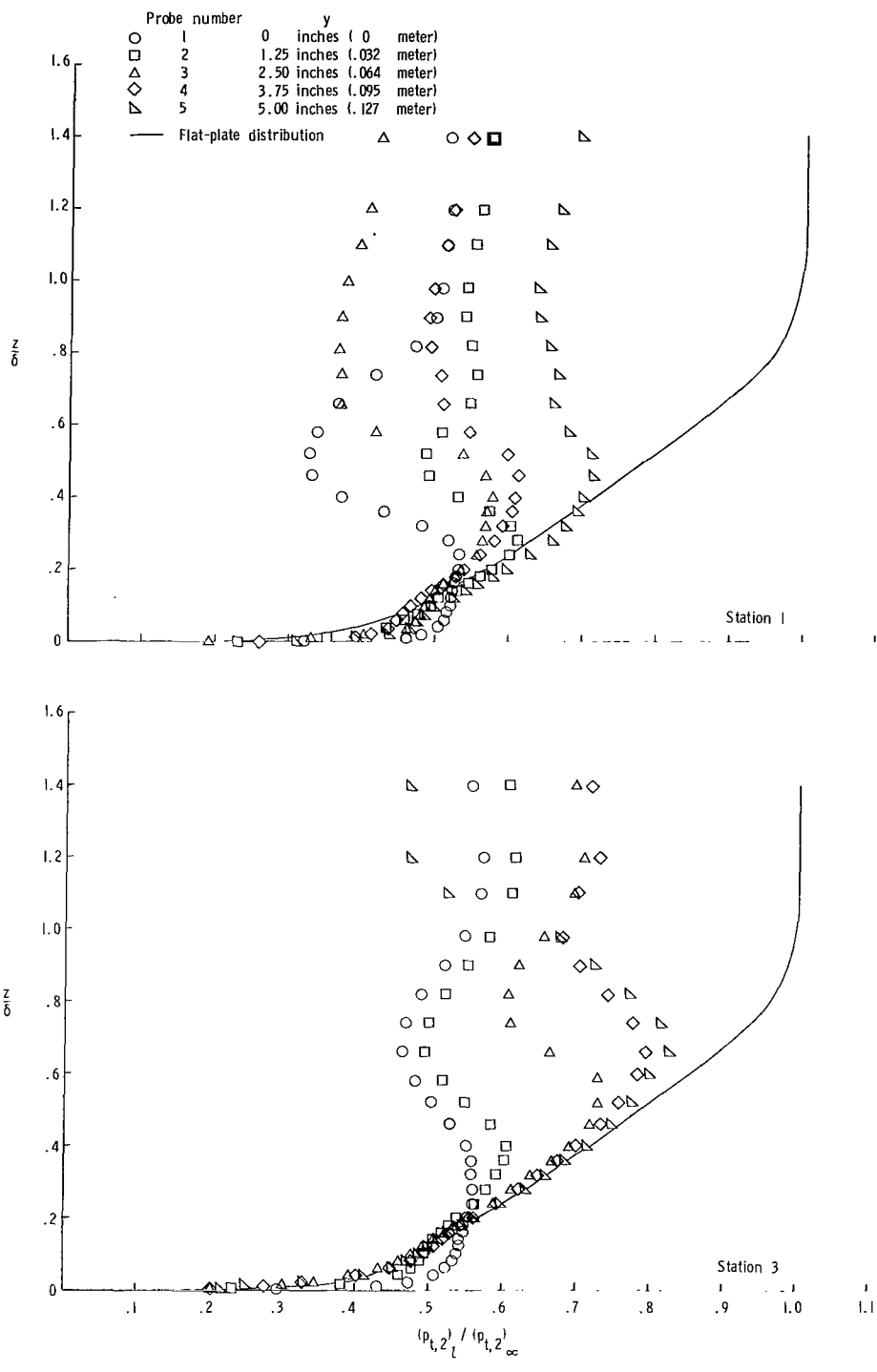
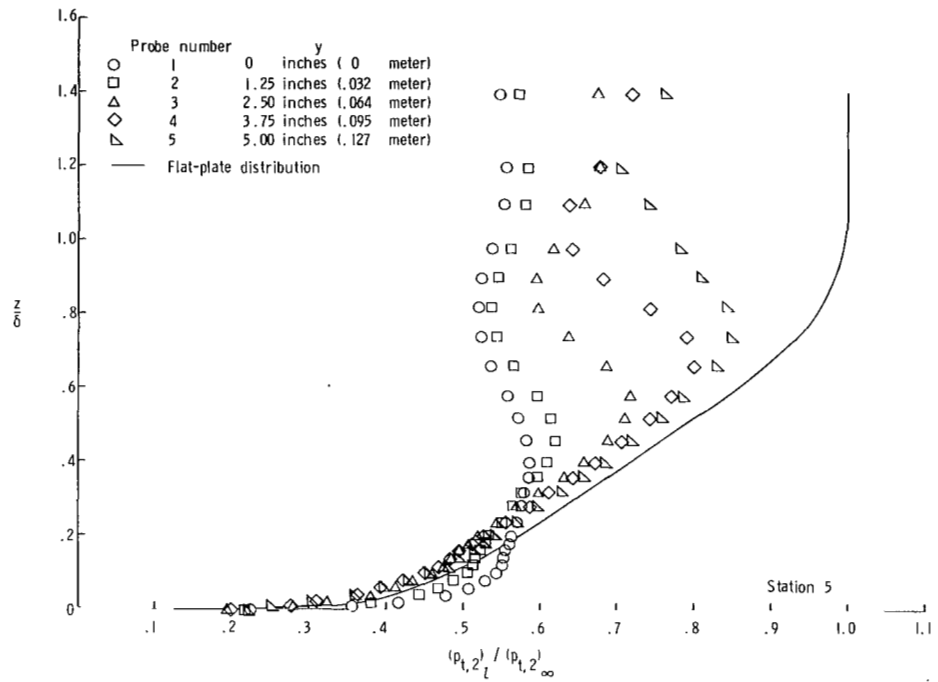


Figure 17.- Velocity distributions downstream of cylinder at longitudinal stations. $y = 0$ inch.



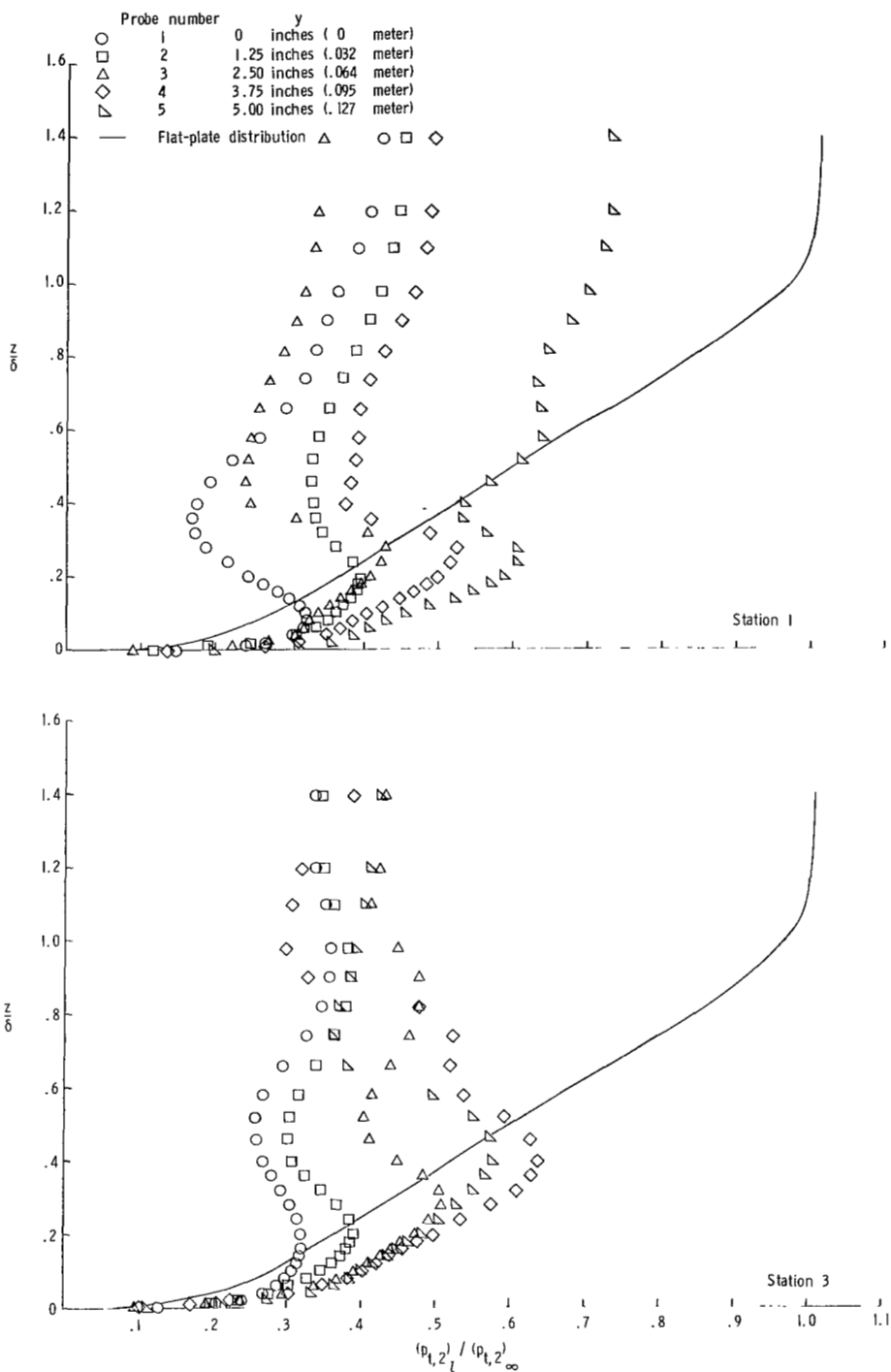
(a) $M = 2.49$.

Figure 18.- Pitot-pressure distributions downstream of cylinder at spanwise stations at three longitudinal stations.



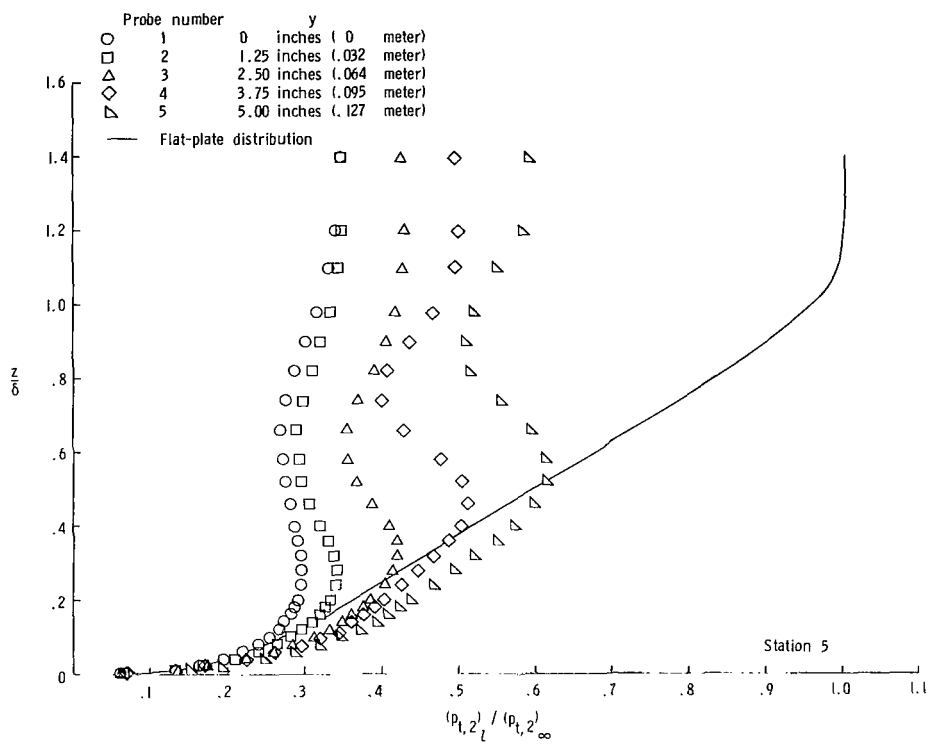
(a) Concluded.

Figure 18.- Continued.



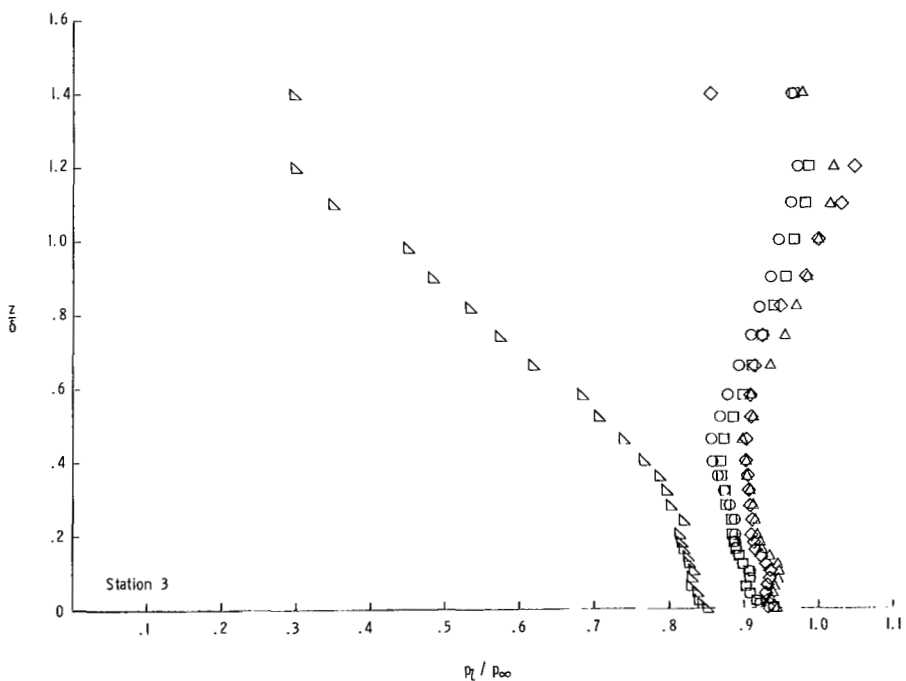
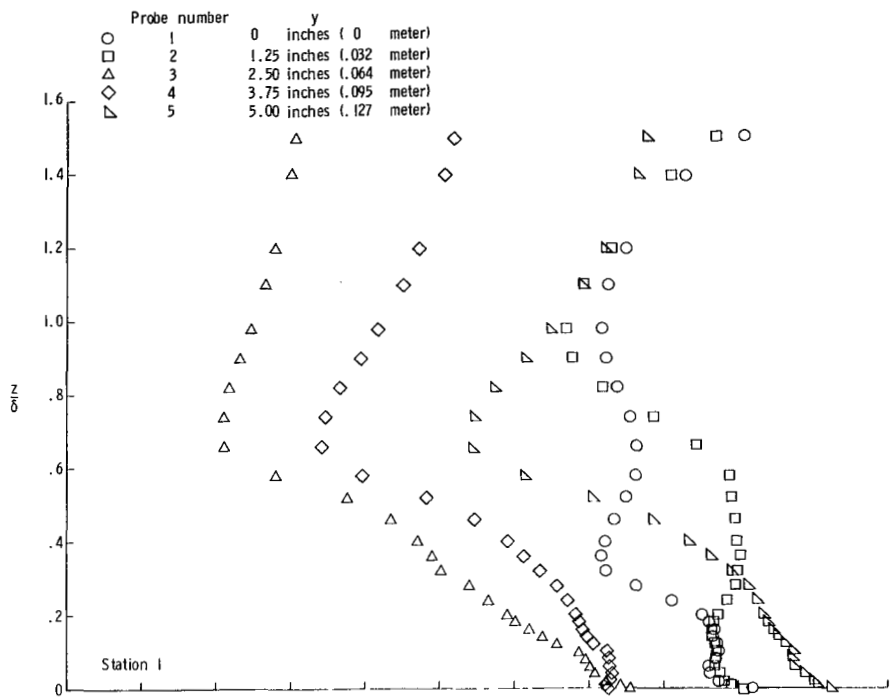
(b) $M = 4.44$.

Figure 18.- Continued.



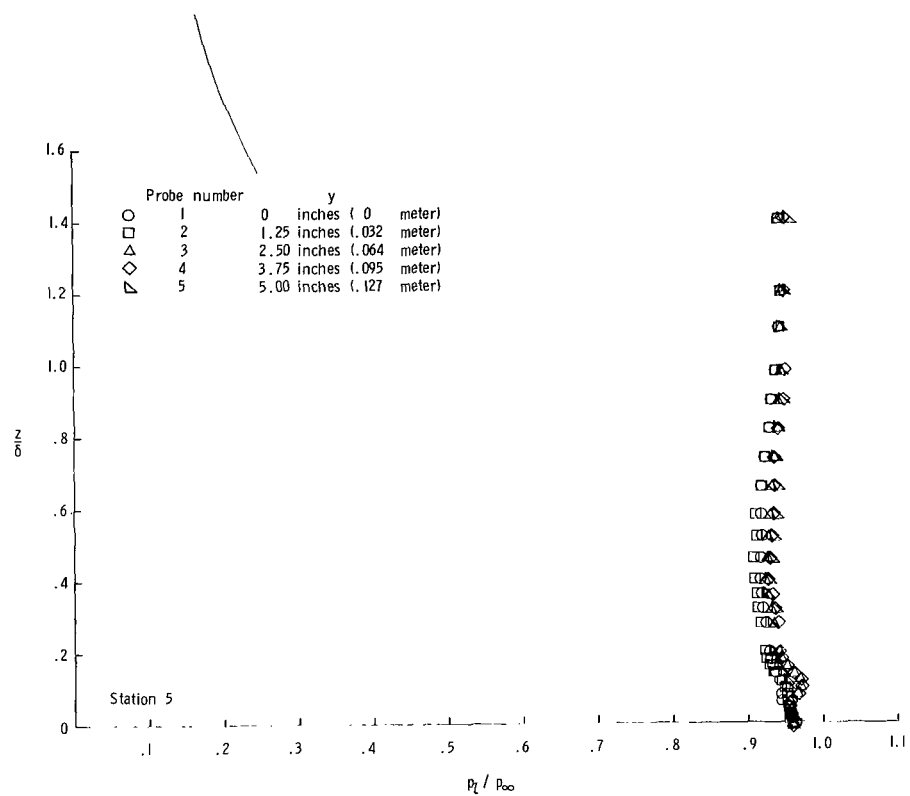
(b) Concluded.

Figure 18.- Concluded.



(a) $M = 2.49$.

Figure 19.- Static-pressure distributions downstream of cylinder at spanwise stations at three longitudinal stations.



(a) Concluded.

Figure 19.- Continued.

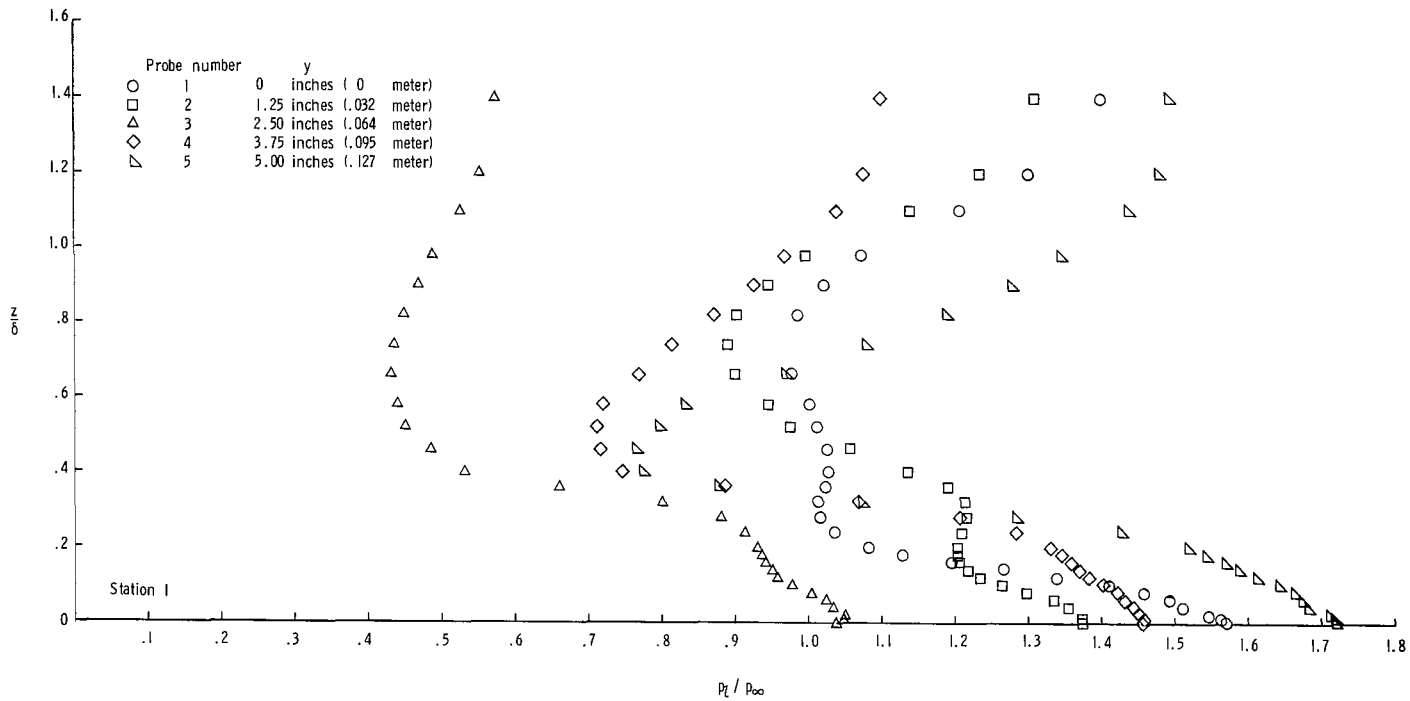
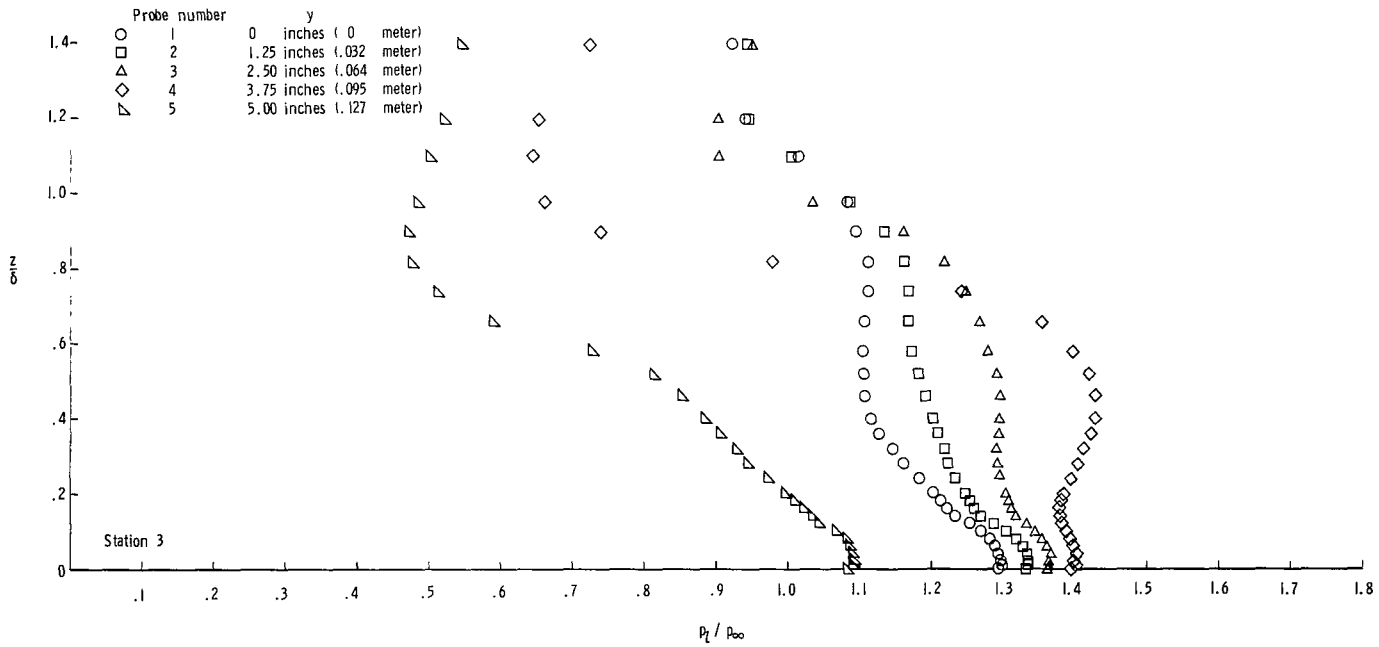
(b) $M = 4.44$.

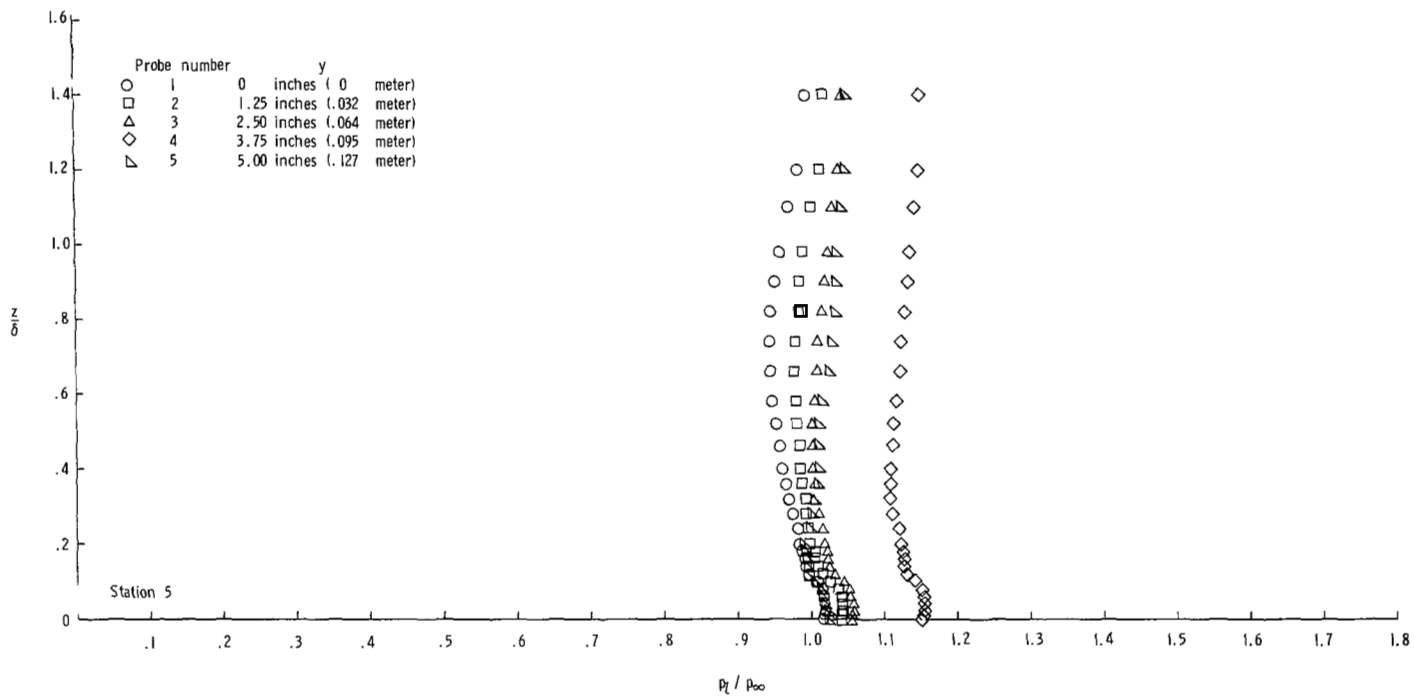
Figure 19.- Continued.

1.6 -



(b) Continued.

Figure 19.- Continued.



(b) Concluded.

Figure 19.- Concluded.

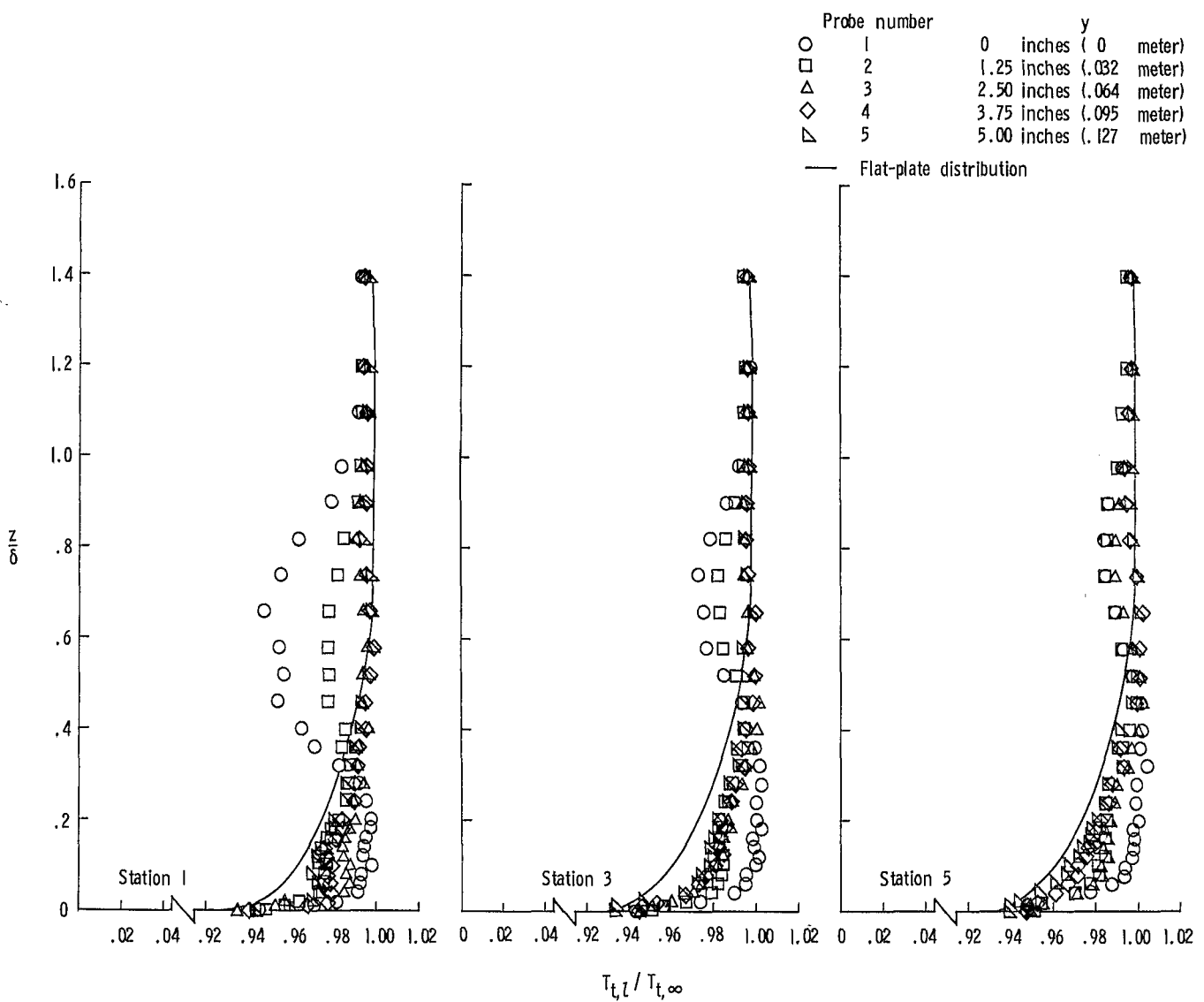


Figure 20.- Total-temperature distributions downstream of cylinder at spanwise stations at three longitudinal stations.

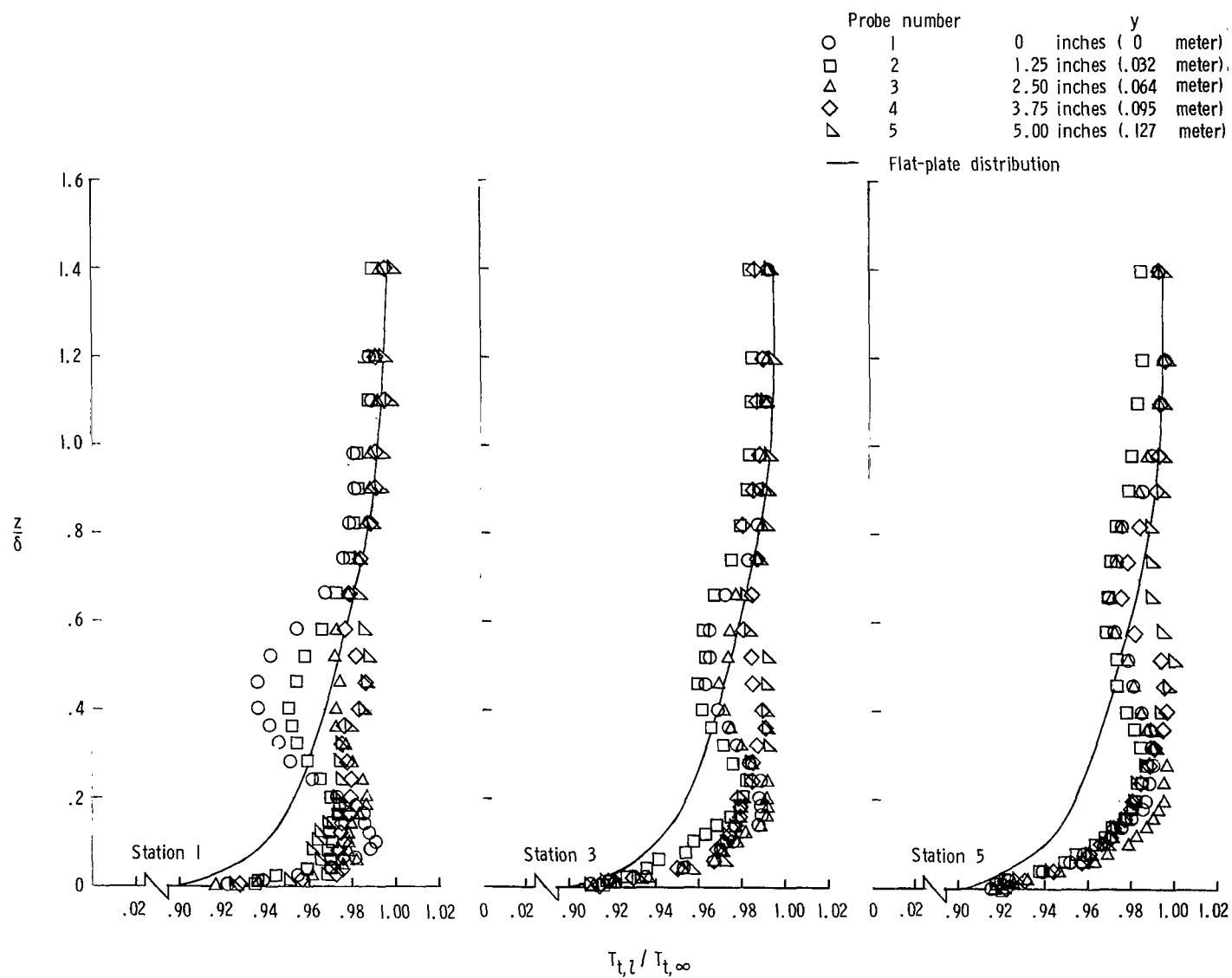
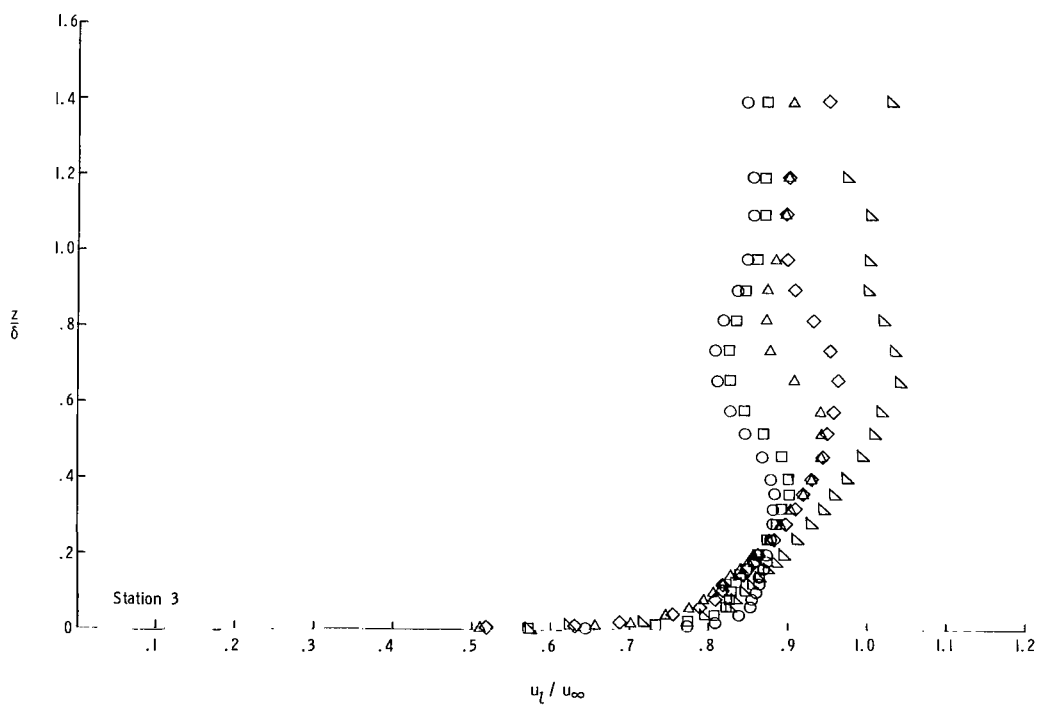
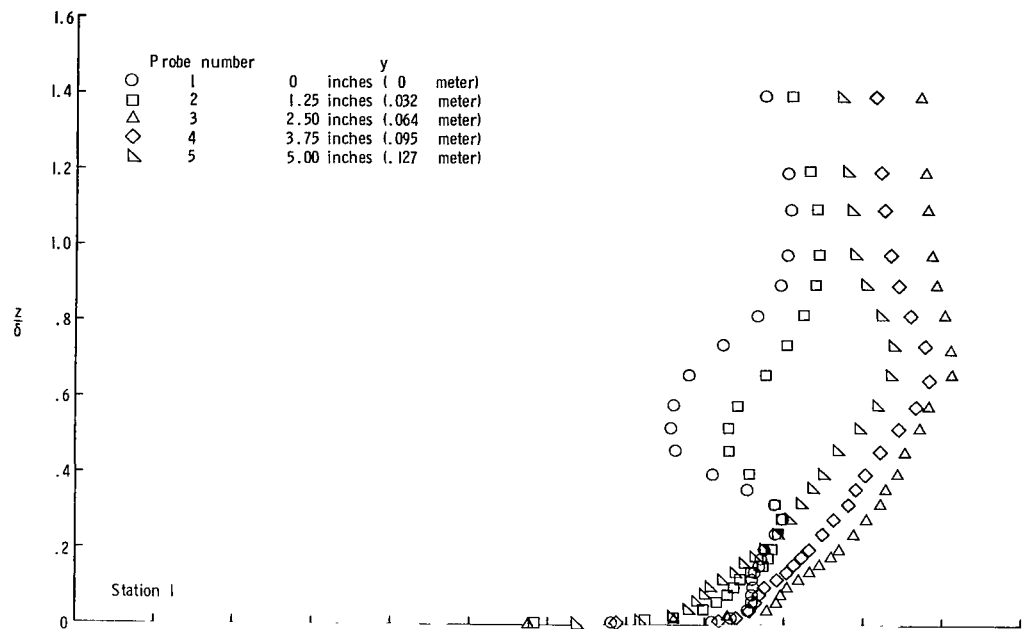
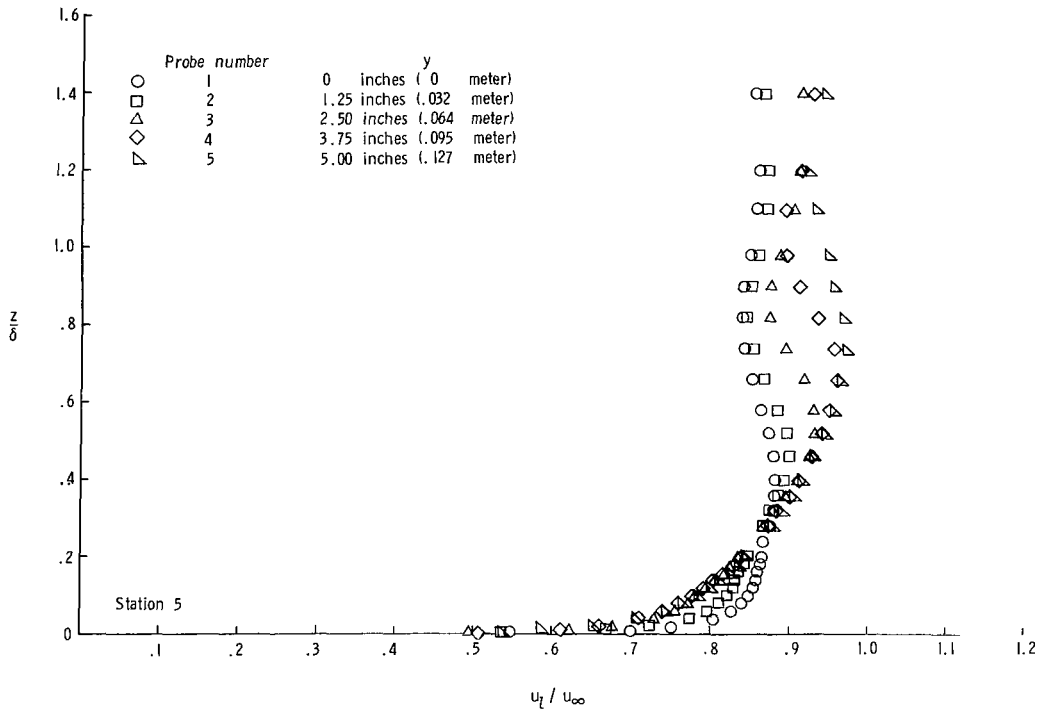
(b) $M = 4.44$.

Figure 20.- Concluded.



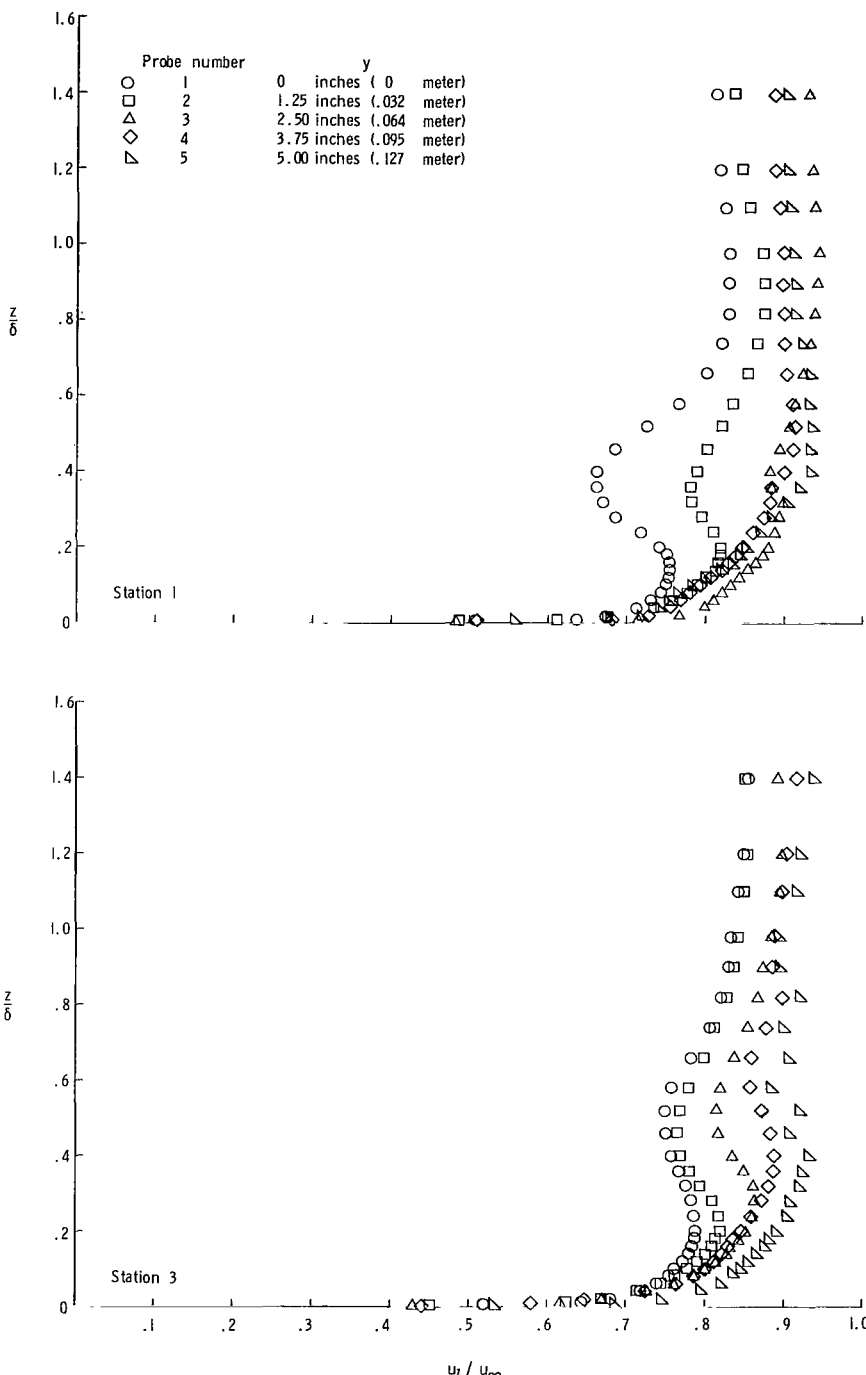
(a) $M = 2.49$.

Figure 21.- Velocity distributions downstream of cylinder at spanwise stations at three longitudinal stations.



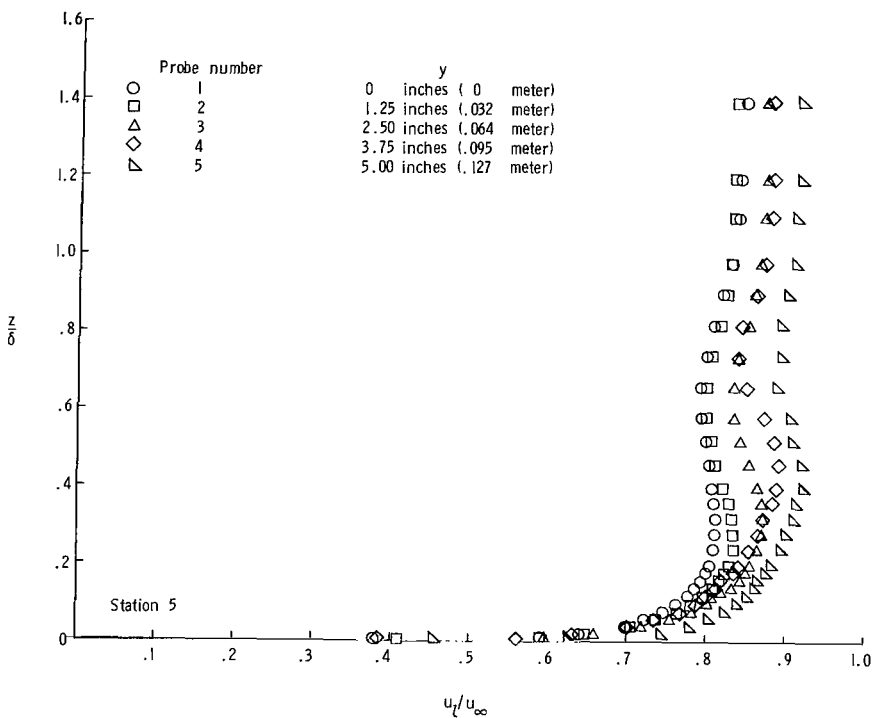
(a) Concluded.

Figure 21.- Continued.



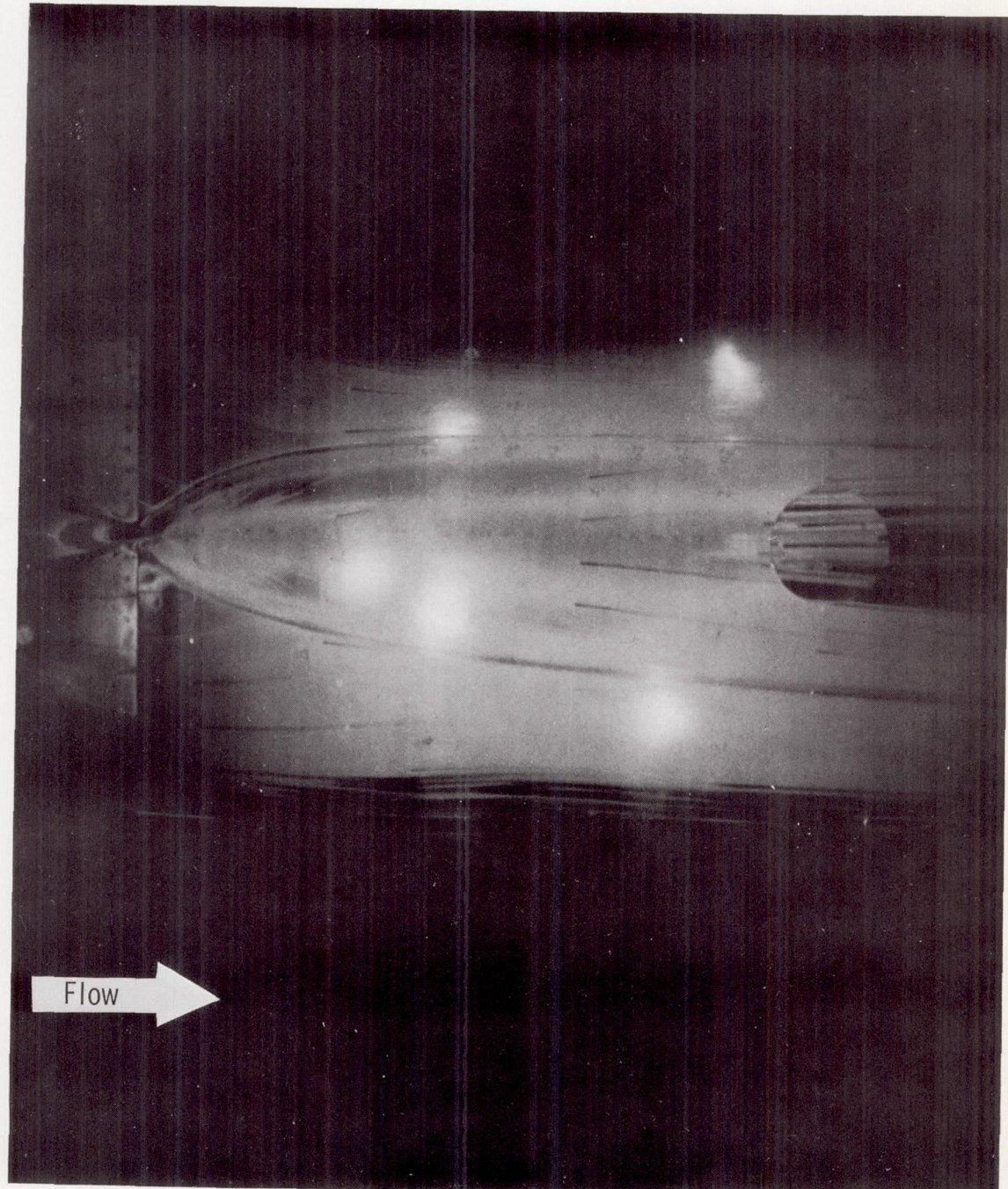
(b) $M = 4.44$.

Figure 21.- Continued.



(b) Concluded.

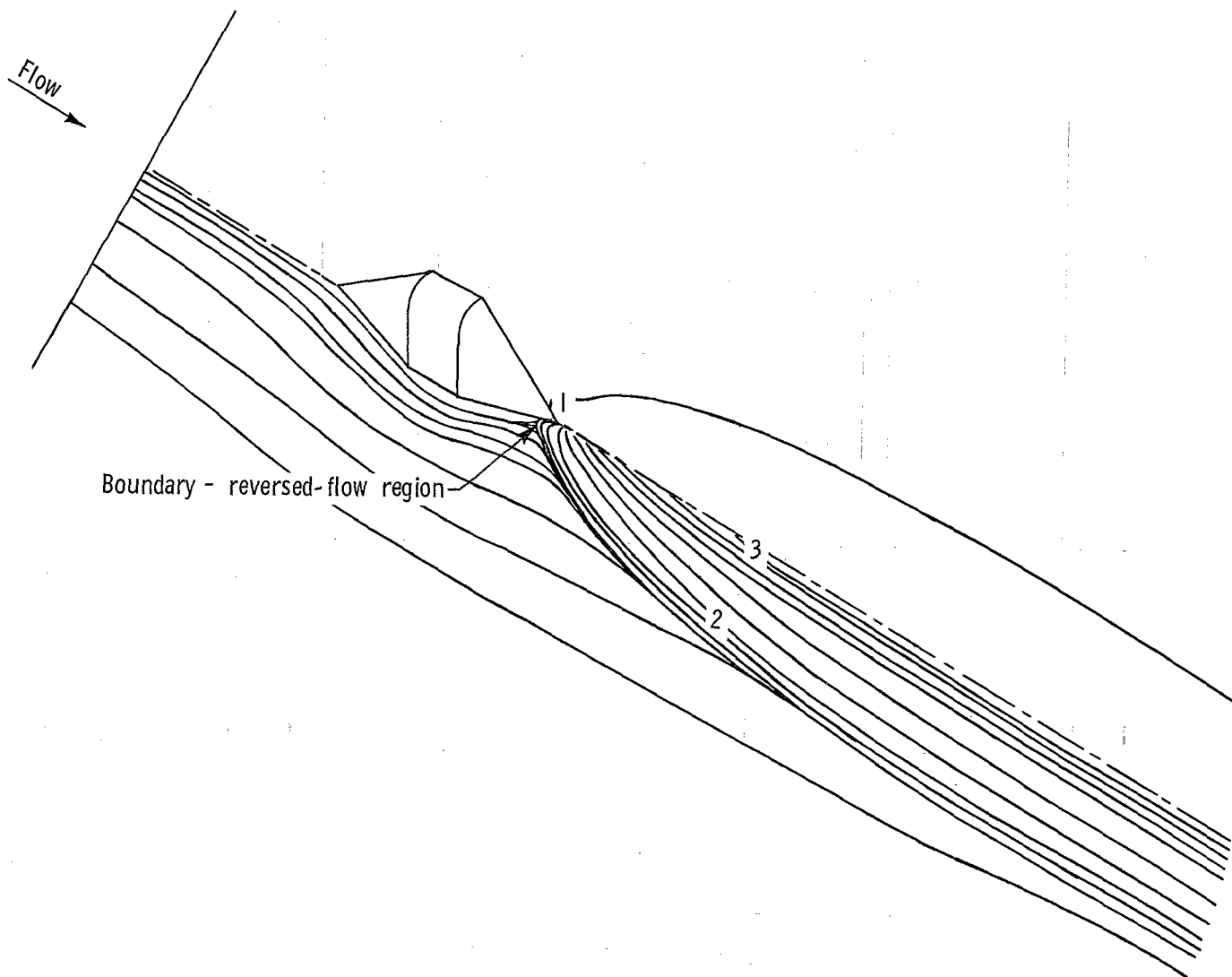
Figure 21.- Concluded.



(a) Oil-flow photograph. $M = 2.49$.

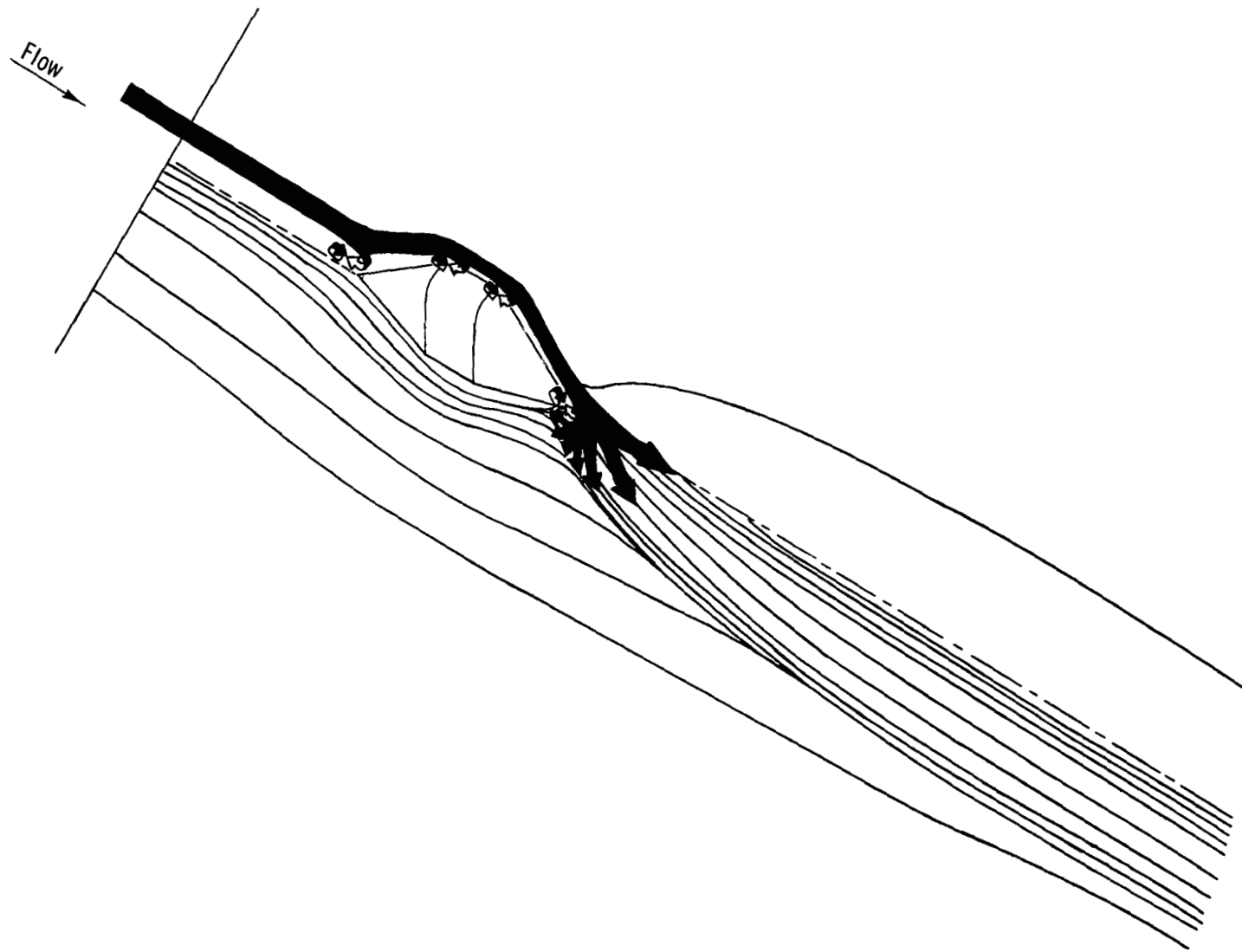
L-69-1357

Figure 22.- Flow model of flat plate with attached fairing.



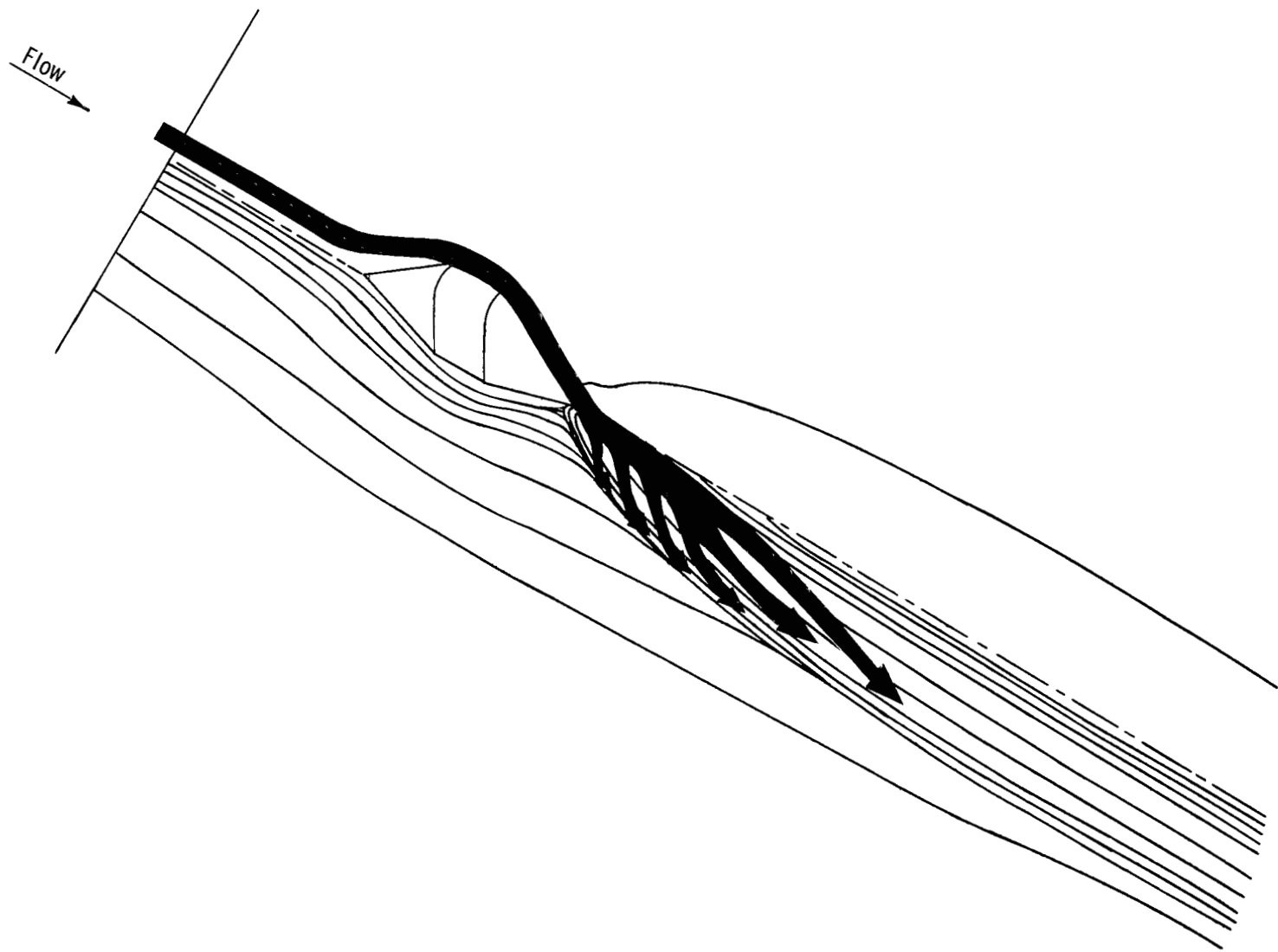
(b) Flow on plate. 1, 2, and 3 indicate distinct regions of the wake.

Figure 22.- Continued.



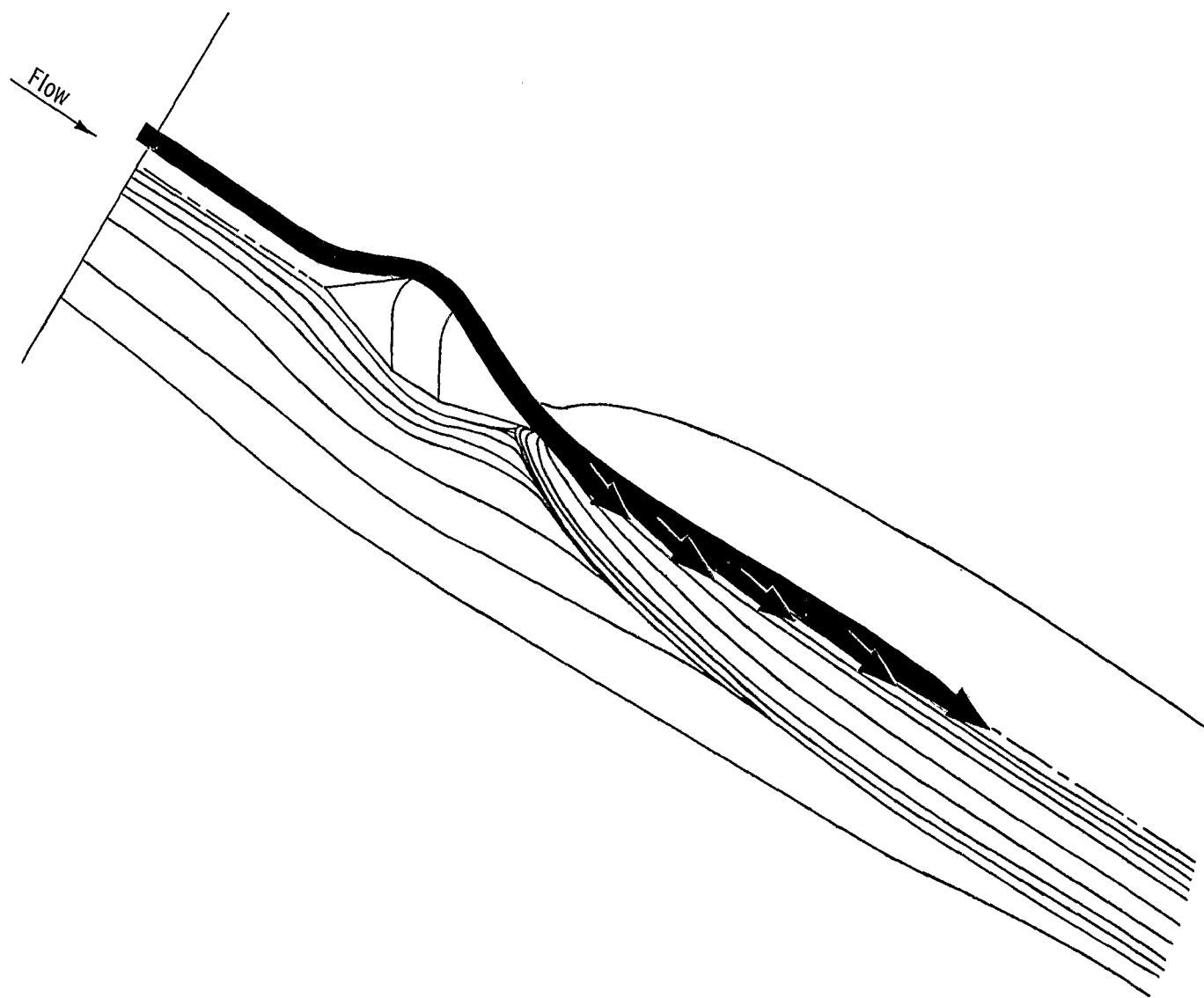
(c) Localized separation regions.

Figure 22.- Continued.



(d) Flow-impingement region.

Figure 22.- Continued.



(e) Wake-core region.

Figure 22.- Concluded.

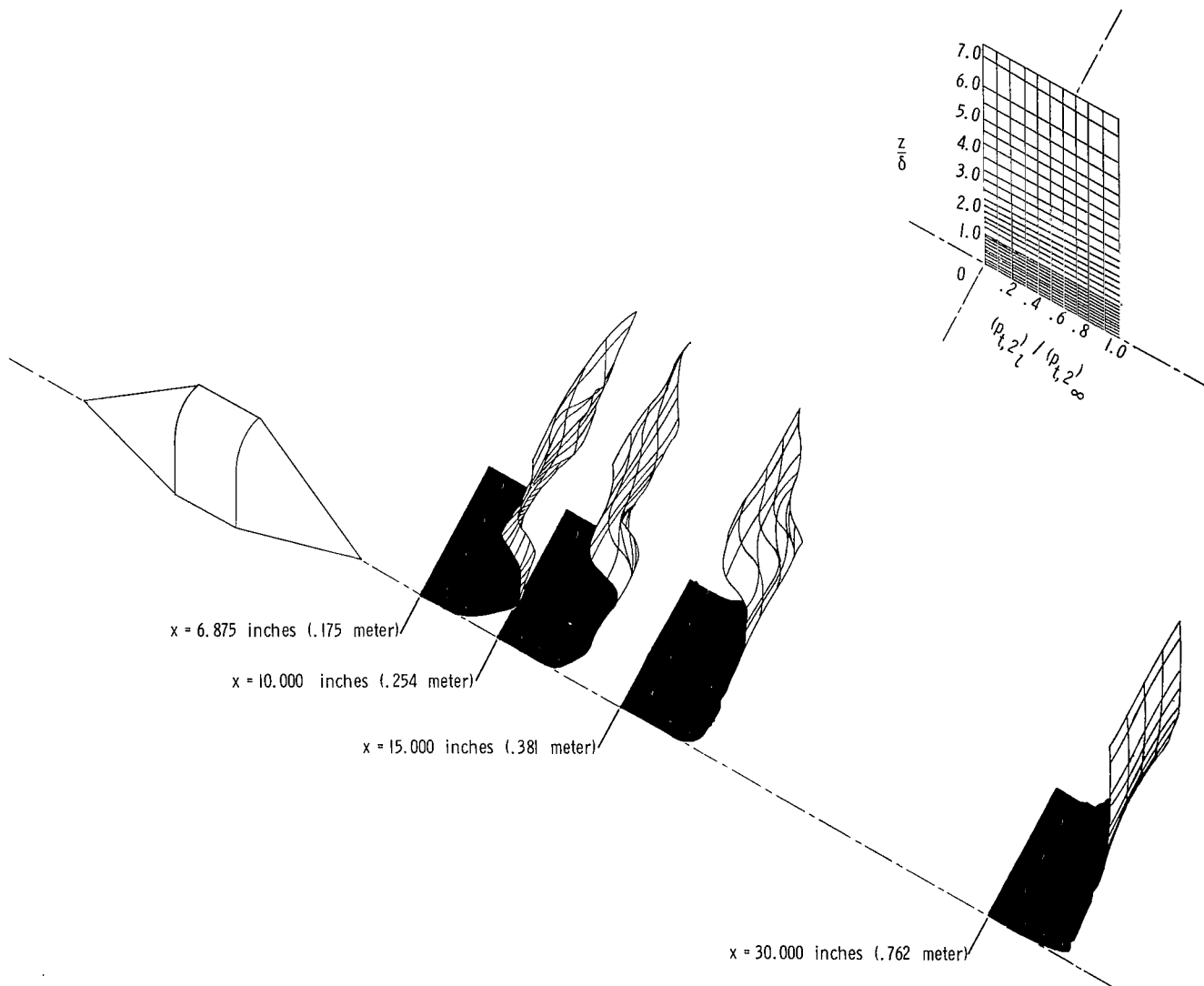
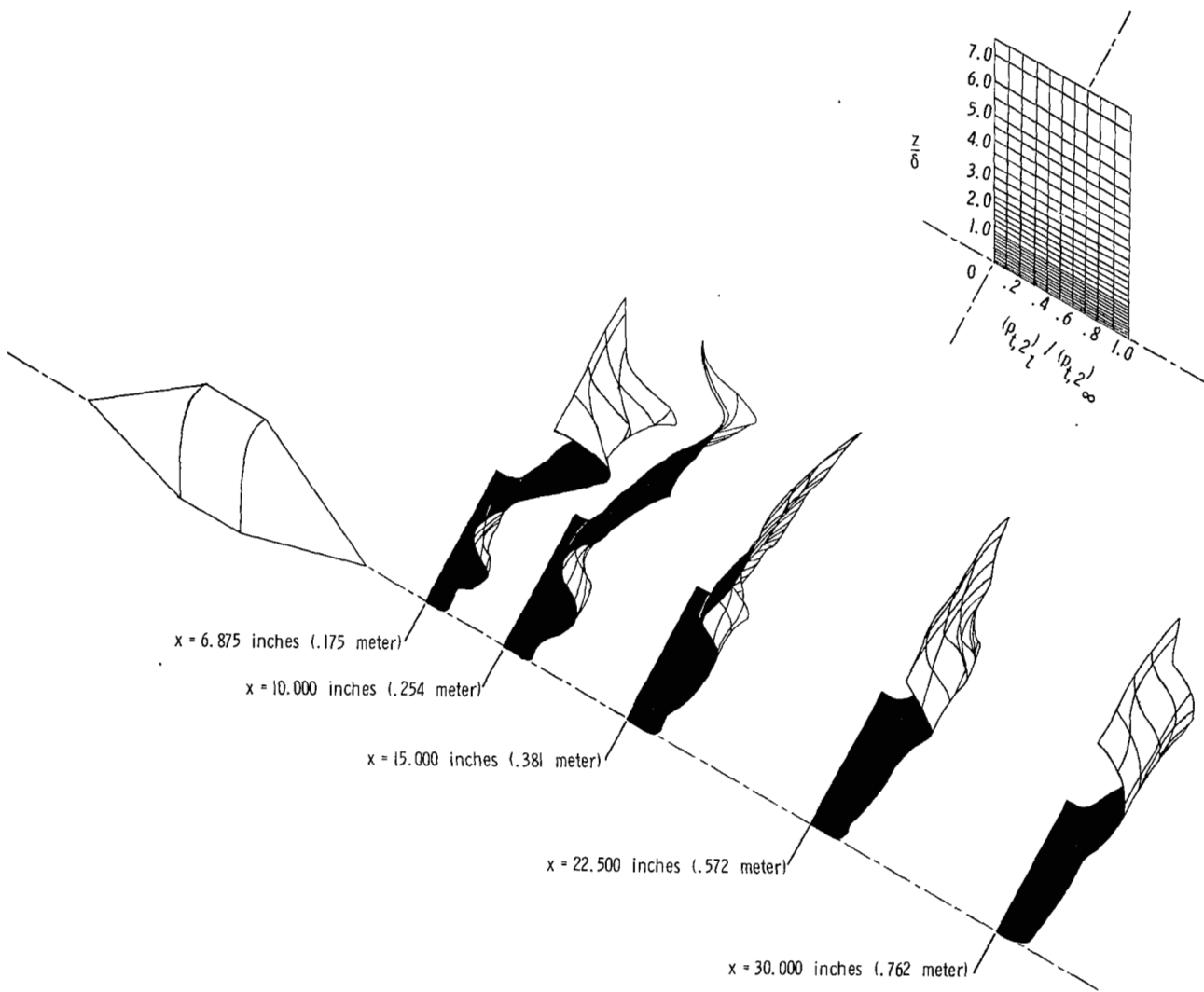
(a) $M = 2.49$.

Figure 23.- Isometric pitot-pressure distributions downstream of attached fairing.



(b) $M = 4.44$.

Figure 23.- Concluded.

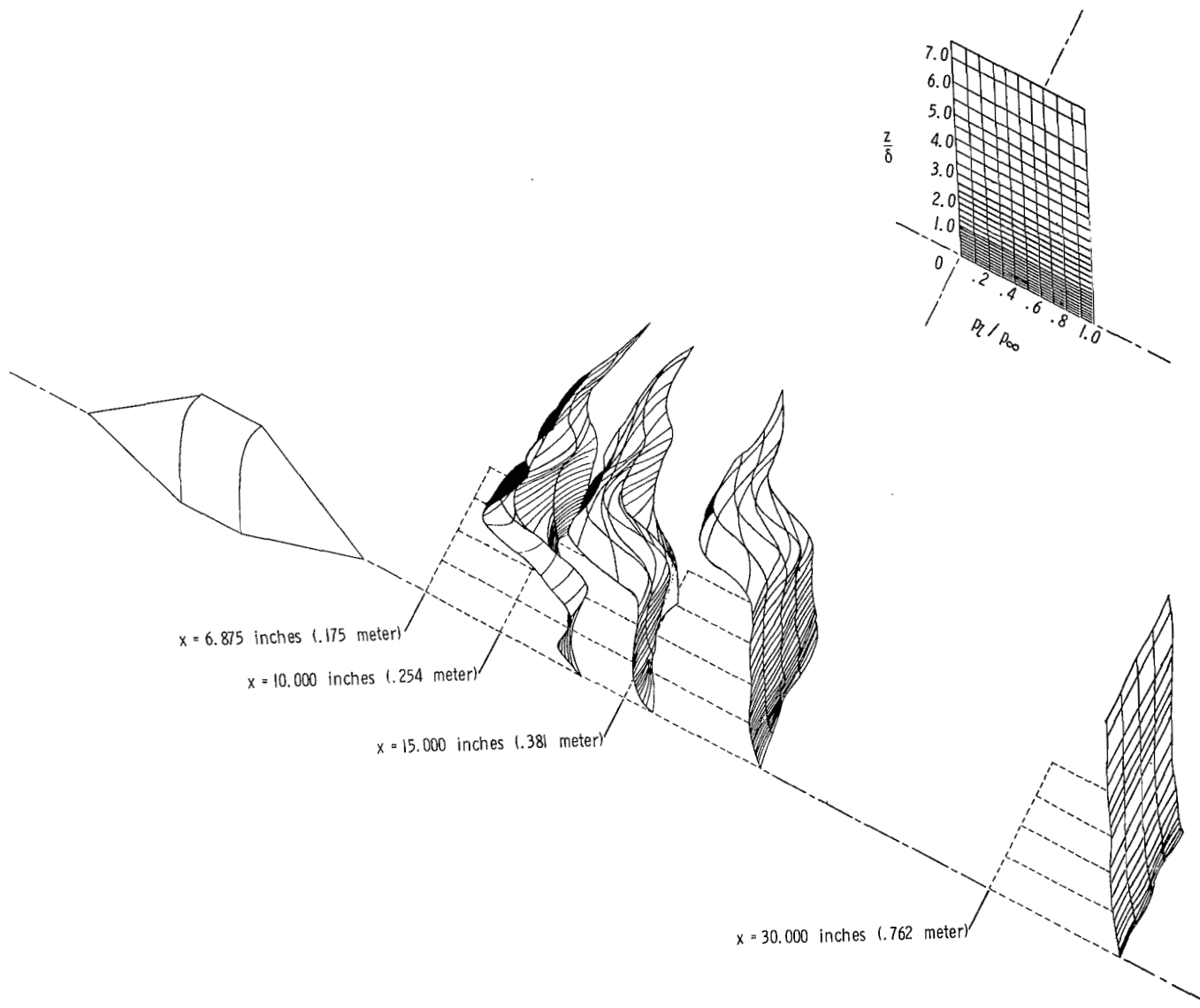
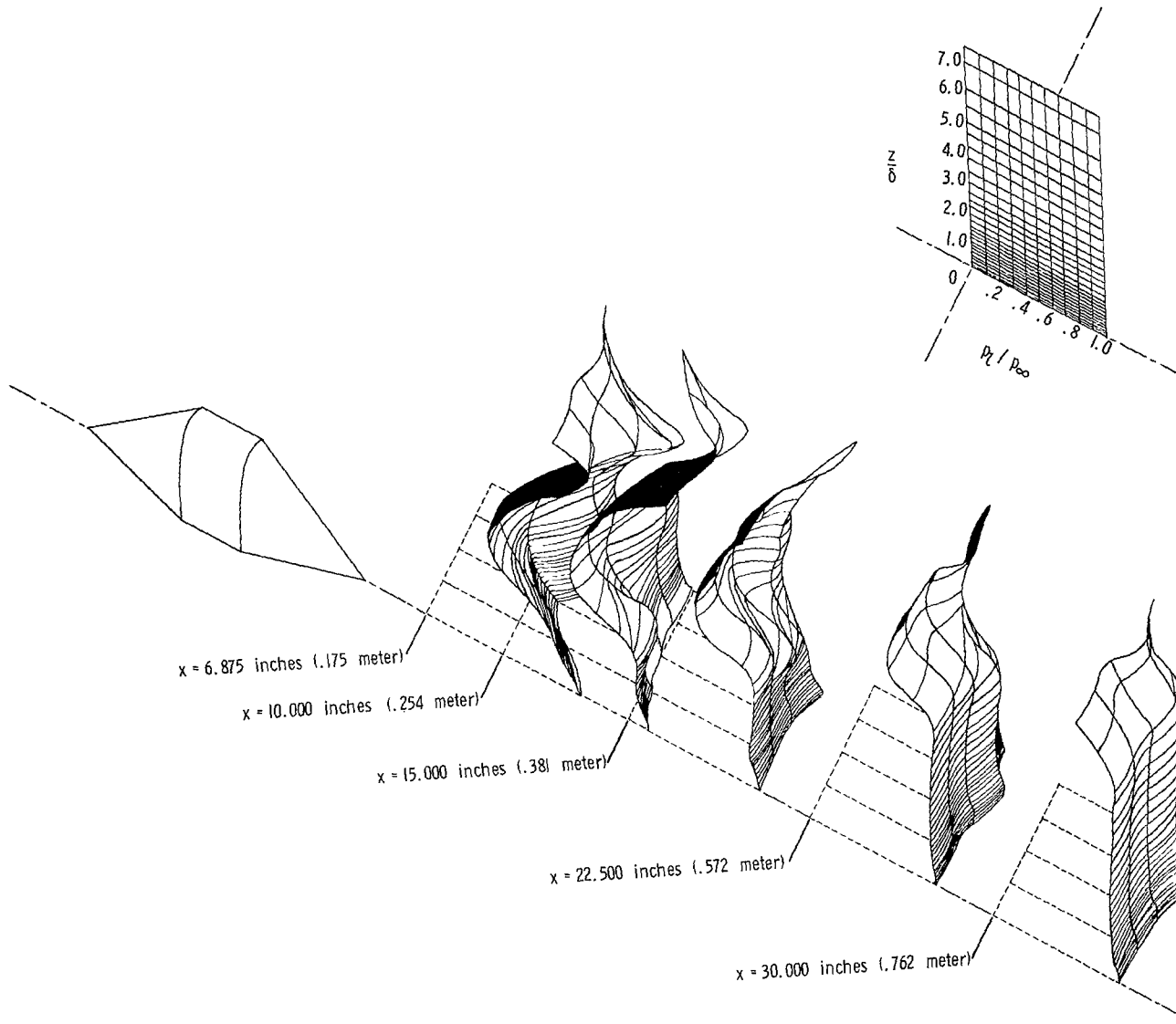
(a) $M = 2.49$.

Figure 24.- Isometric static-pressure distributions downstream of attached fairing.



(b) $M = 4.44$.

Figure 24.- Concluded.

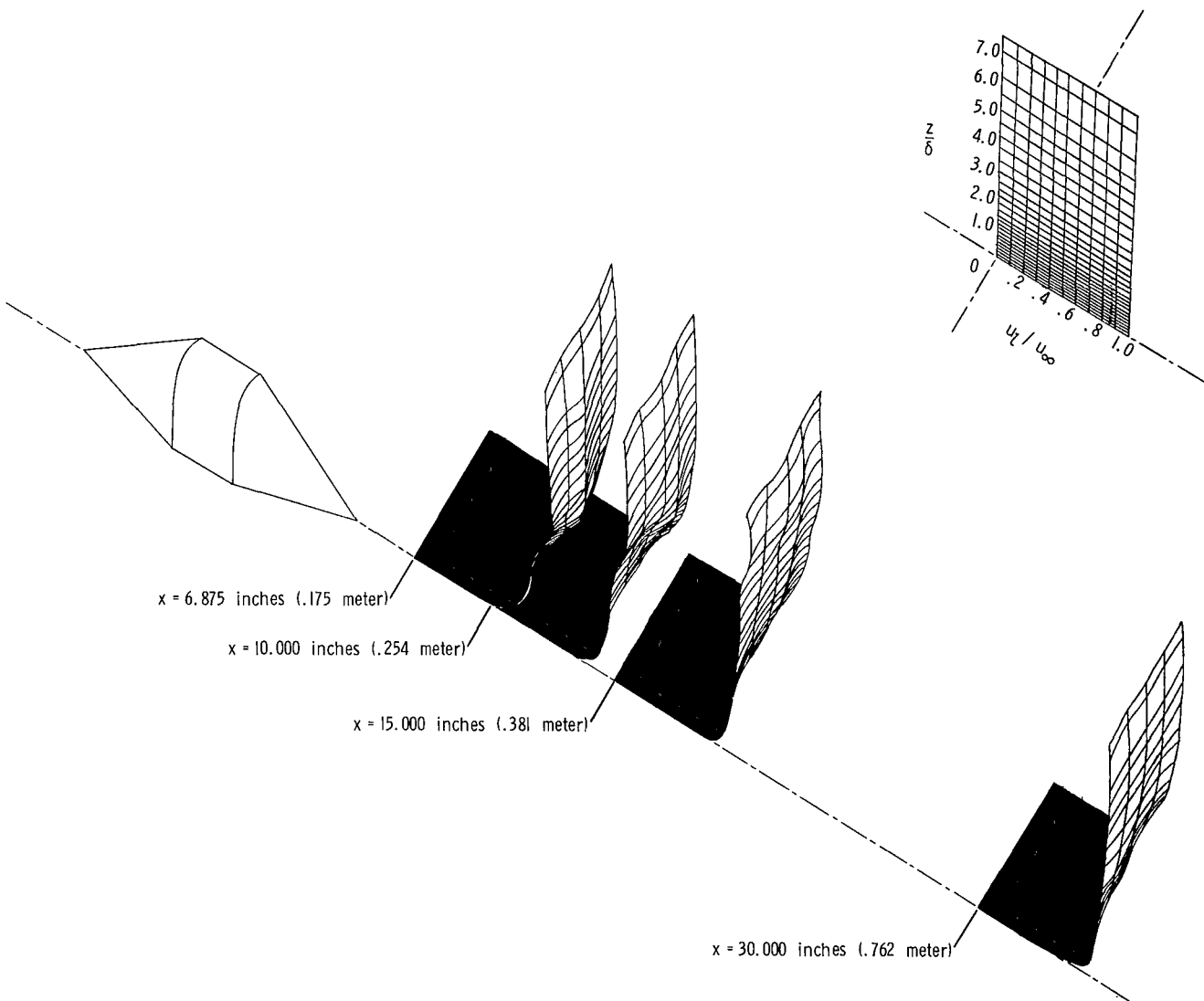
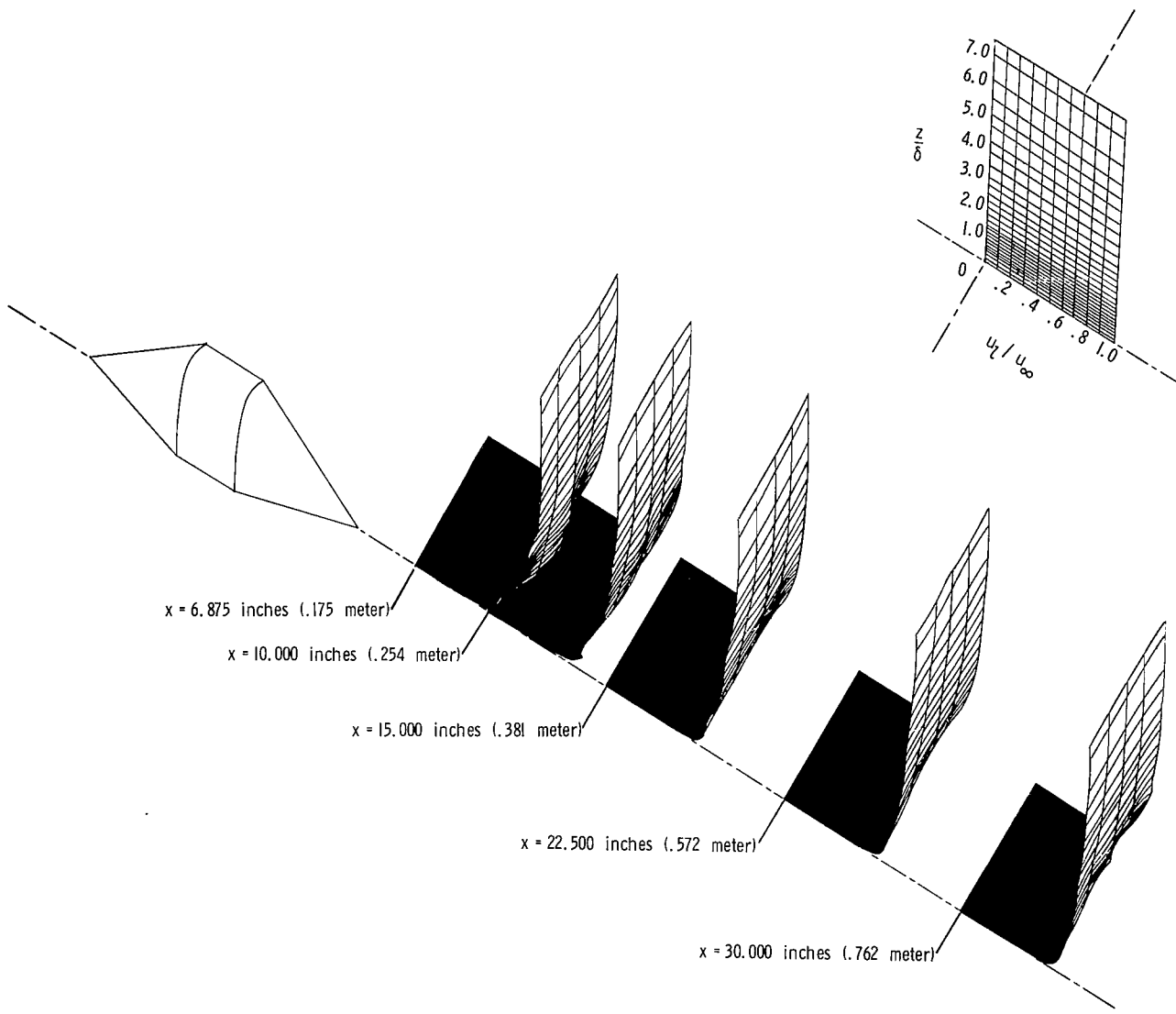
(a) $M = 2.49$.

Figure 25.- Isometric velocity distributions downstream of attached fairing.



(b) $M = 4.44$.

Figure 25.- Concluded.

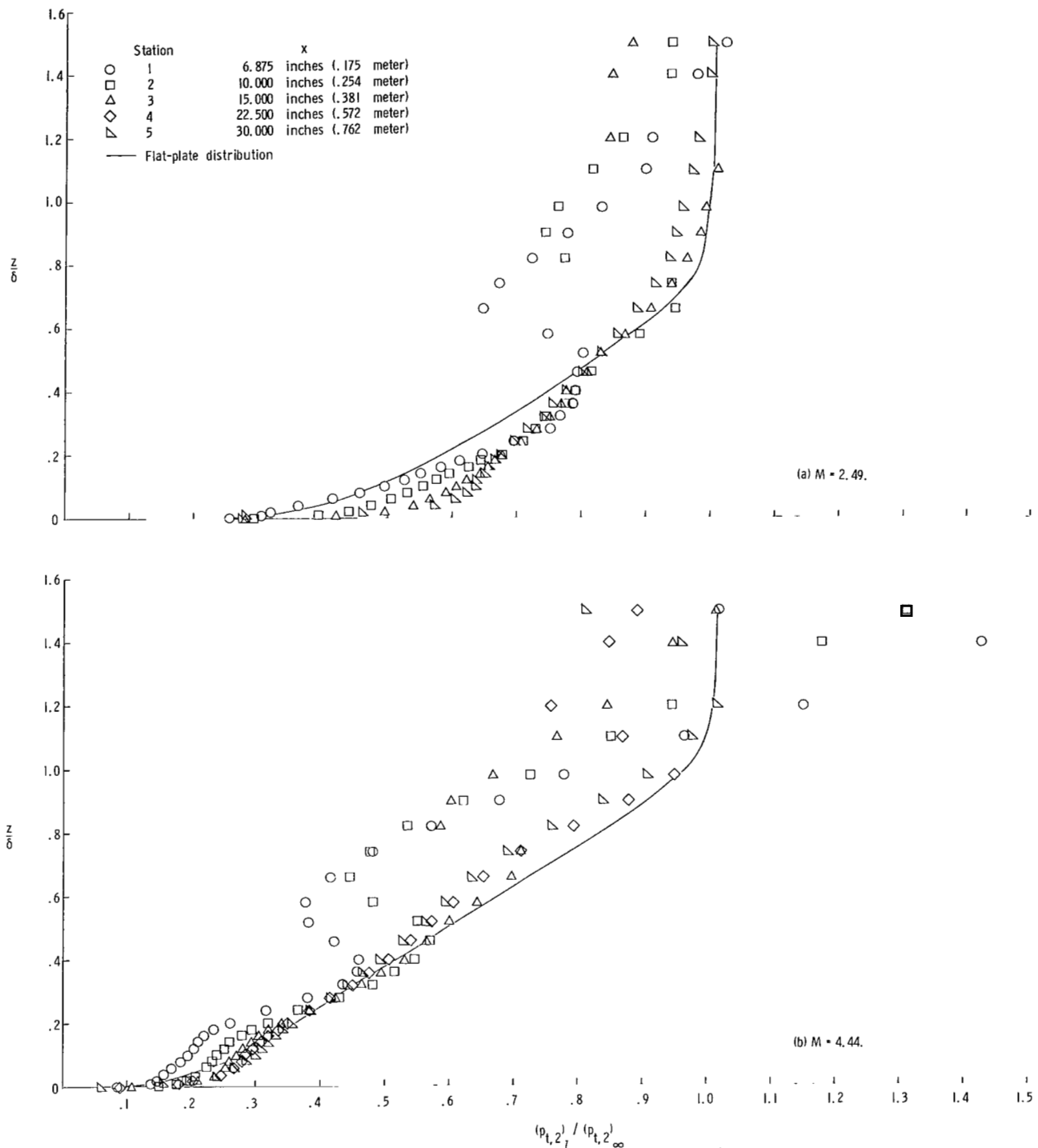


Figure 26.- Pitot-pressure distributions downstream of fairing at longitudinal stations. $y = 0$ inch.

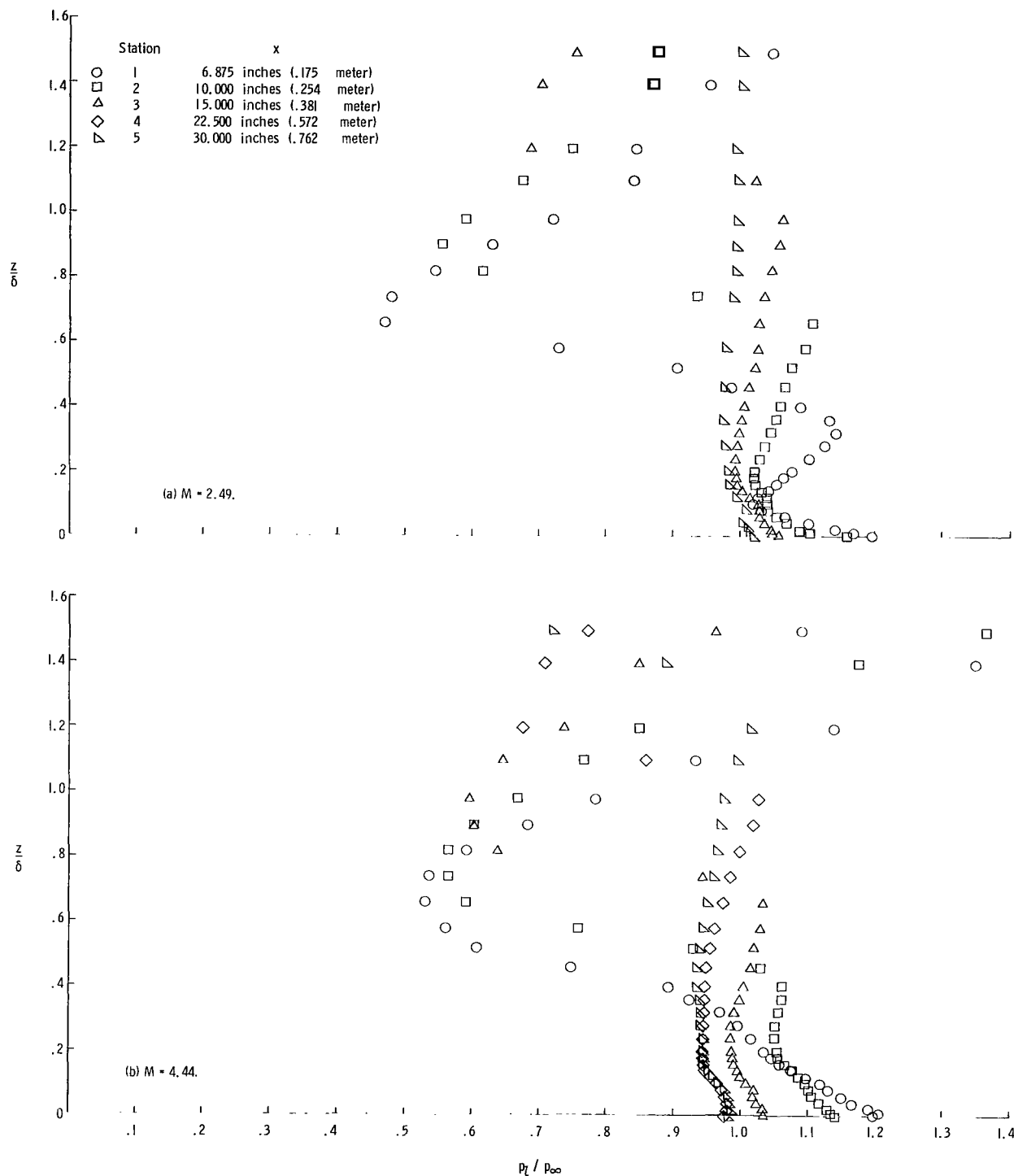


Figure 27.- Static-pressure distributions downstream of fairing at longitudinal stations. $y = 0$ inch.

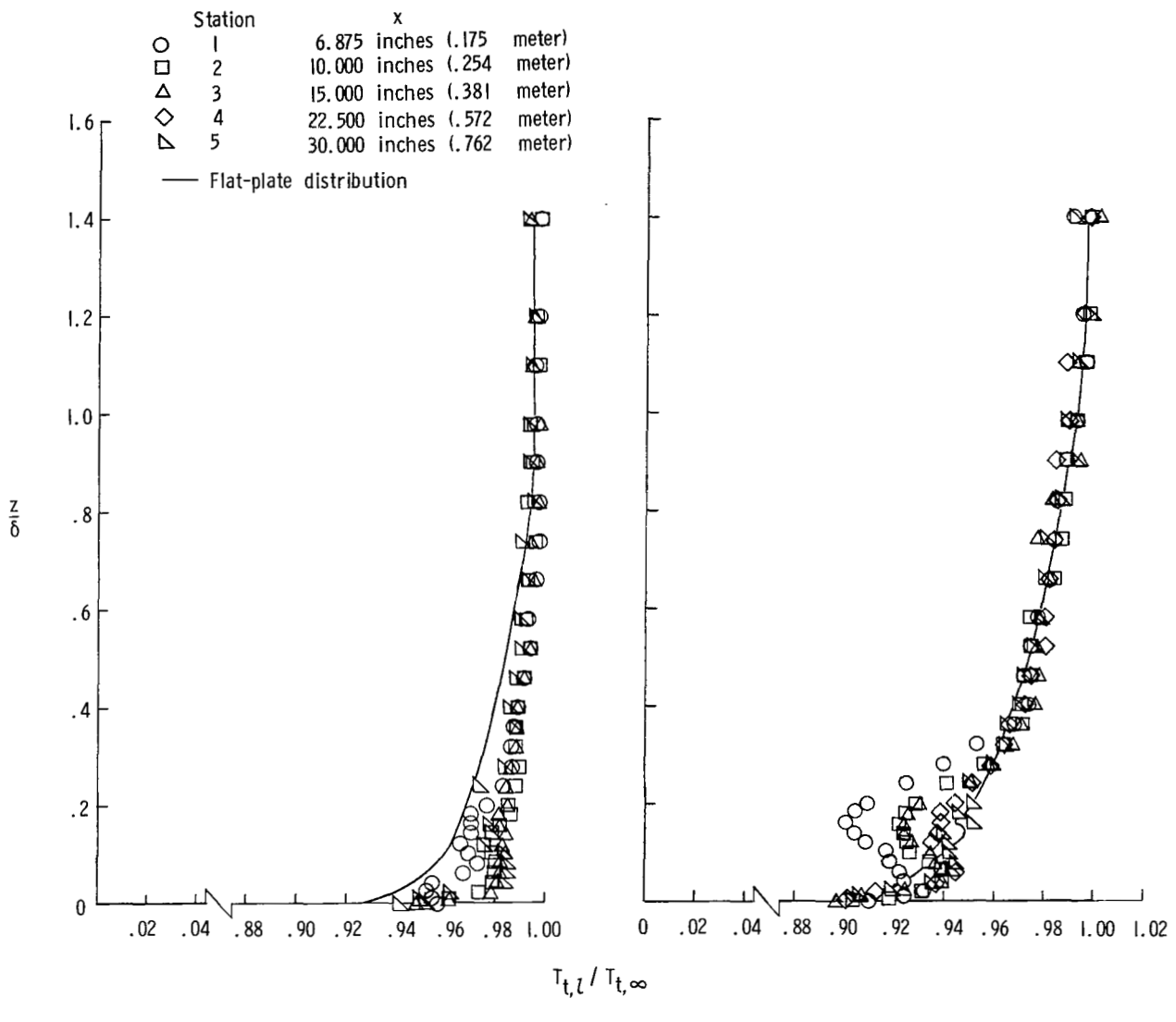


Figure 28.- Total-temperature distributions downstream of fairing at longitudinal stations. $y = 0$ inch.

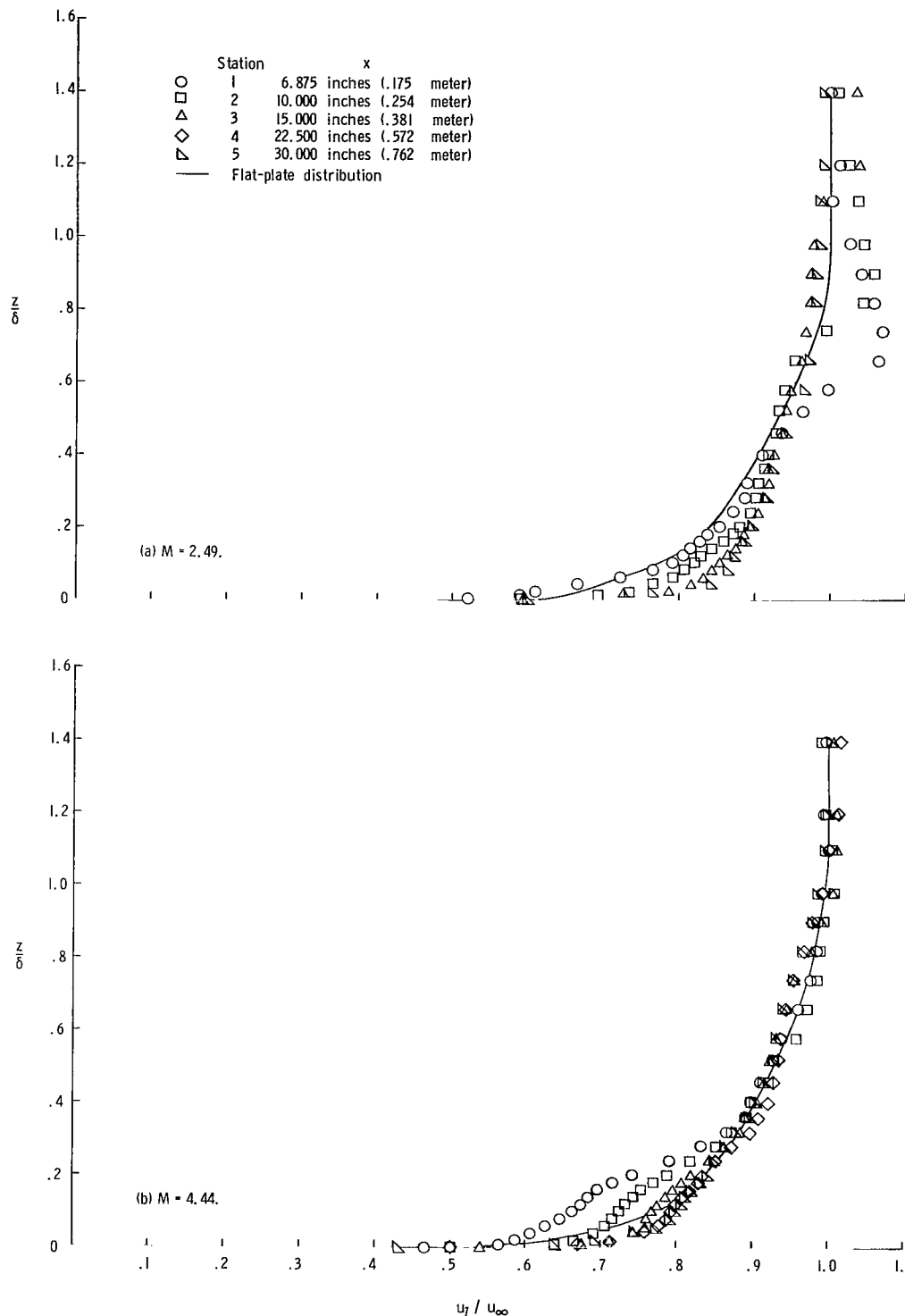
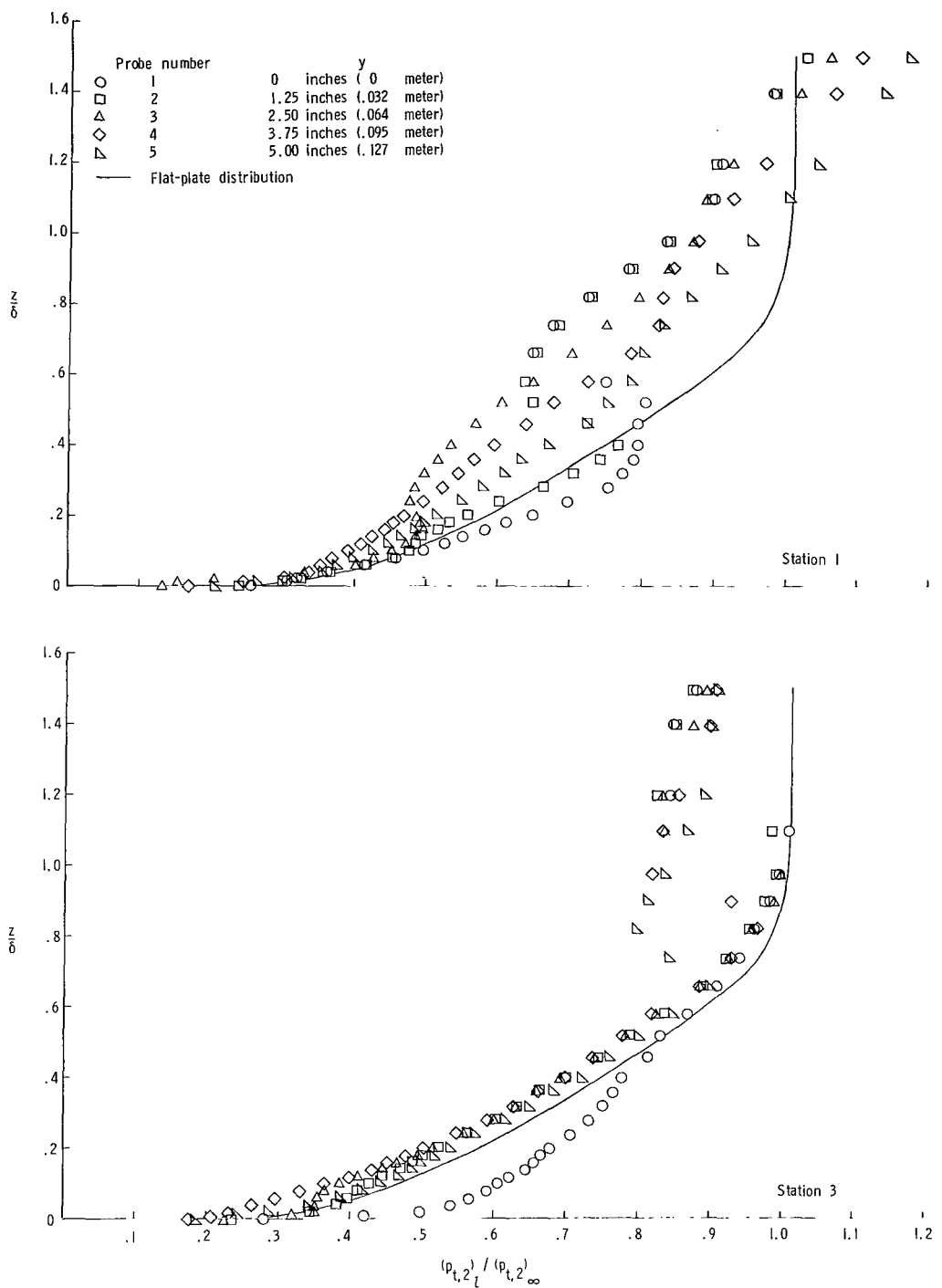


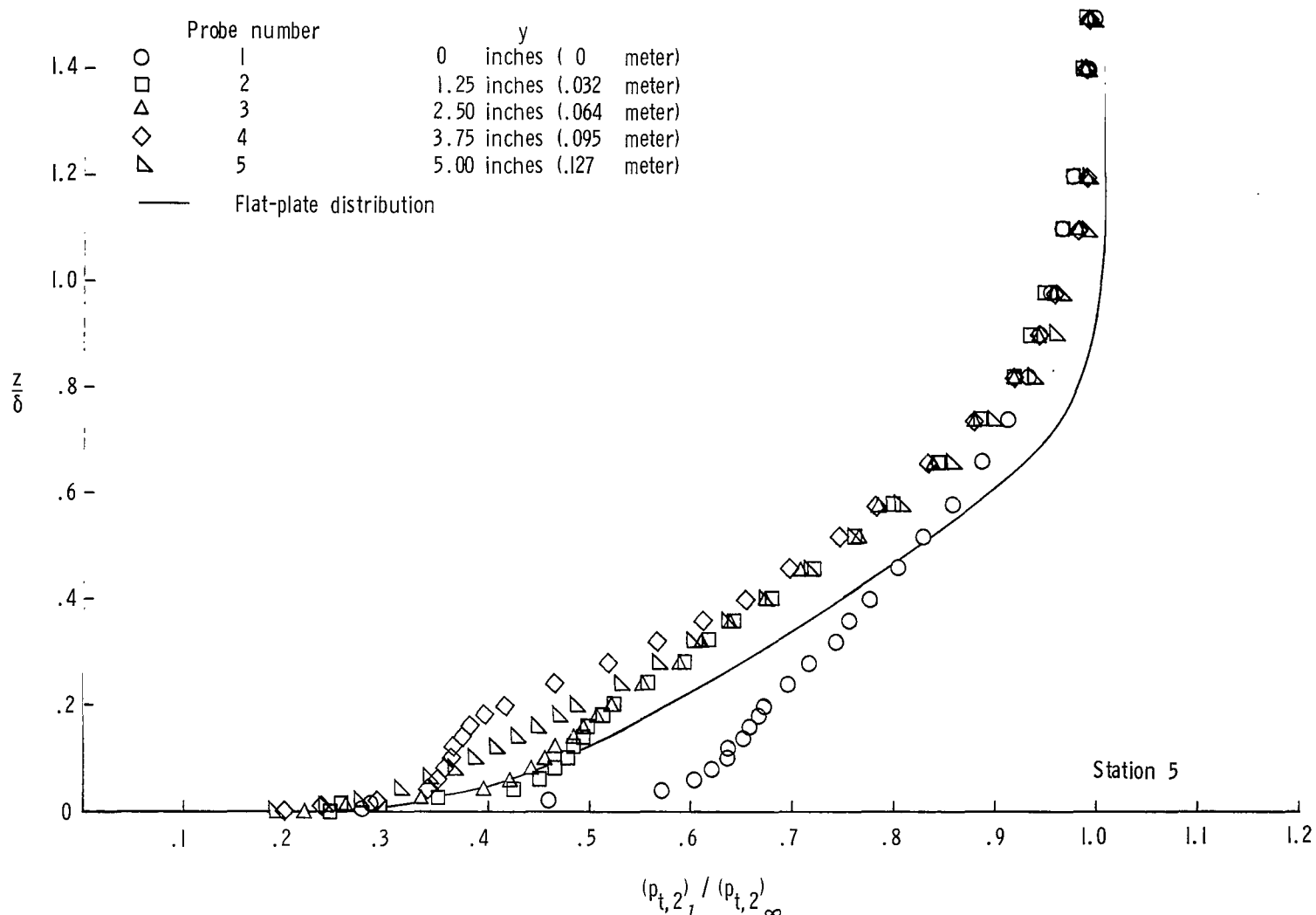
Figure 29.- Velocity distributions downstream of fairing at longitudinal stations. $y = 0$ inch.



(a) $M = 2.49$.

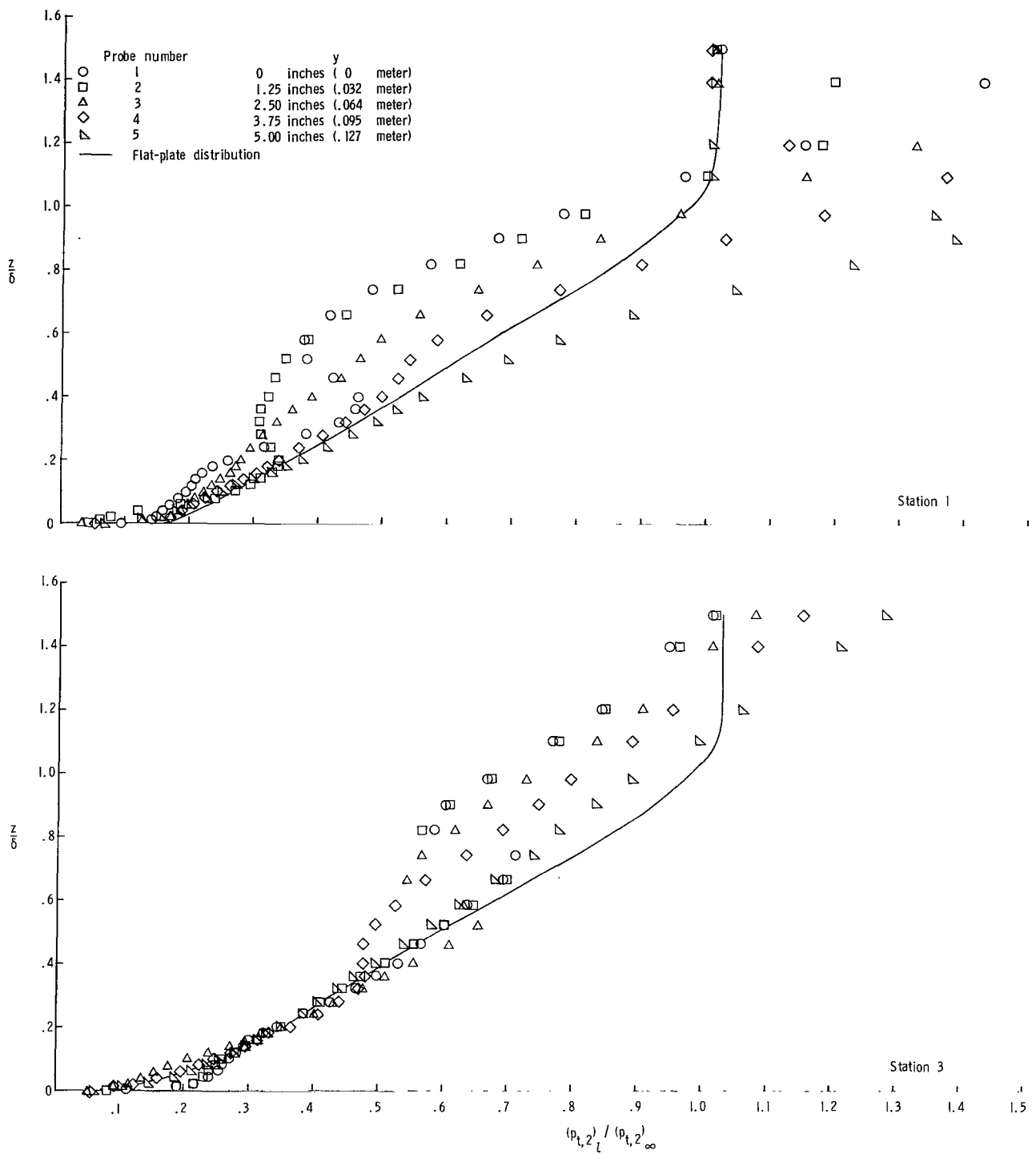
Figure 30.- Pitot-pressure distributions downstream of fairing at spanwise stations at three longitudinal stations.

1.6 -



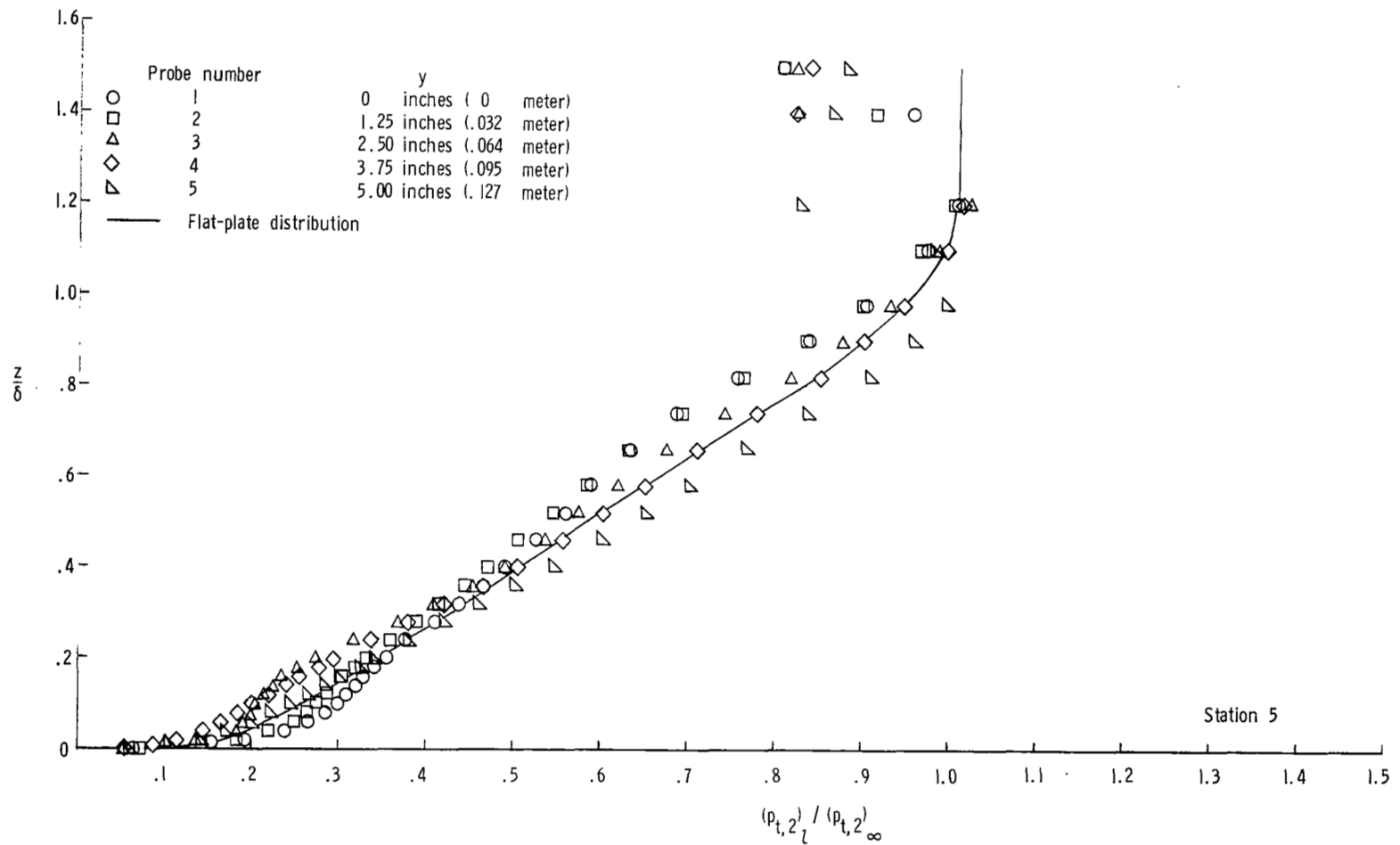
(a) Concluded.

Figure 30.- Continued.



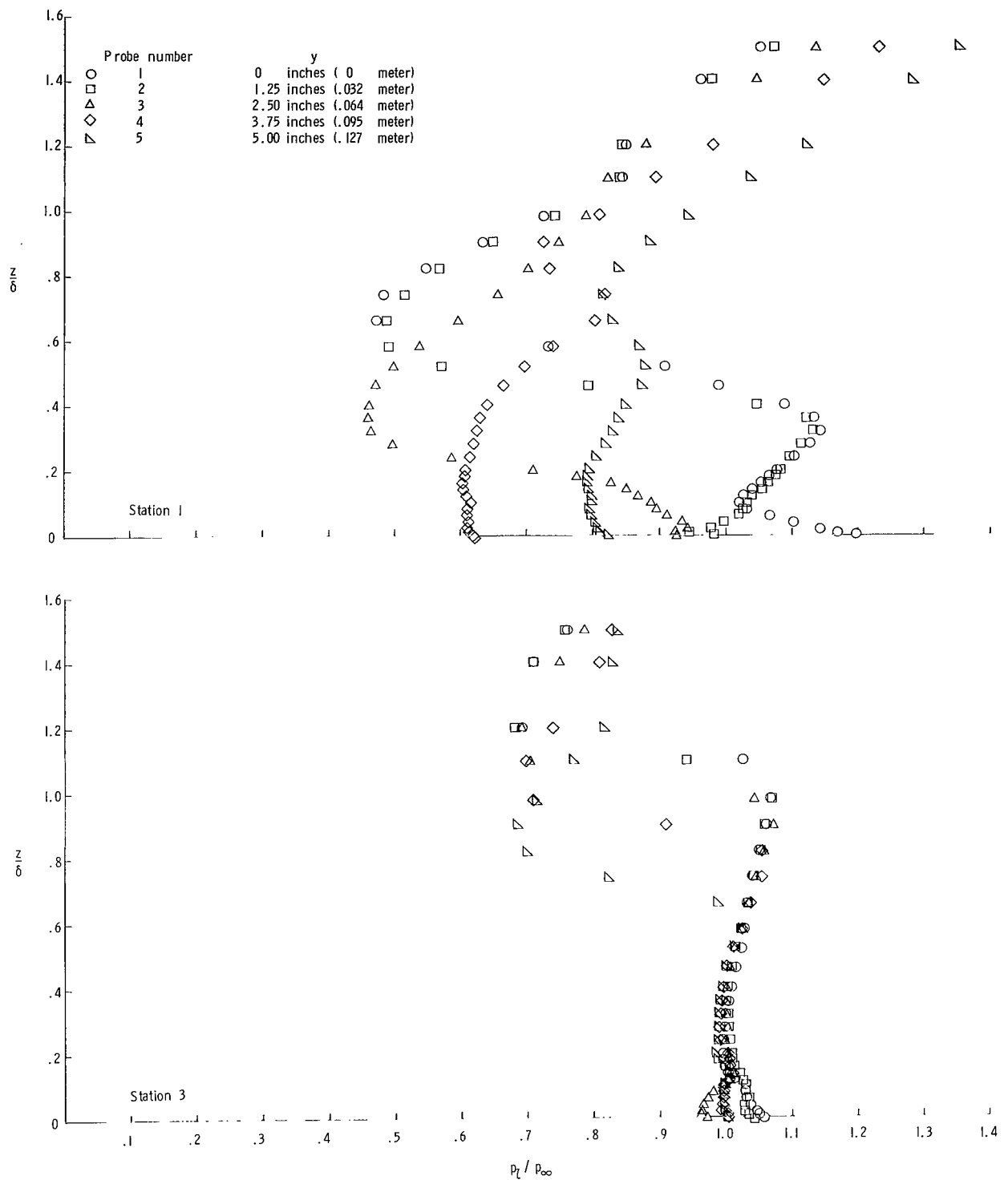
(b) $M = 4.44$.

Figure 30.- Continued.



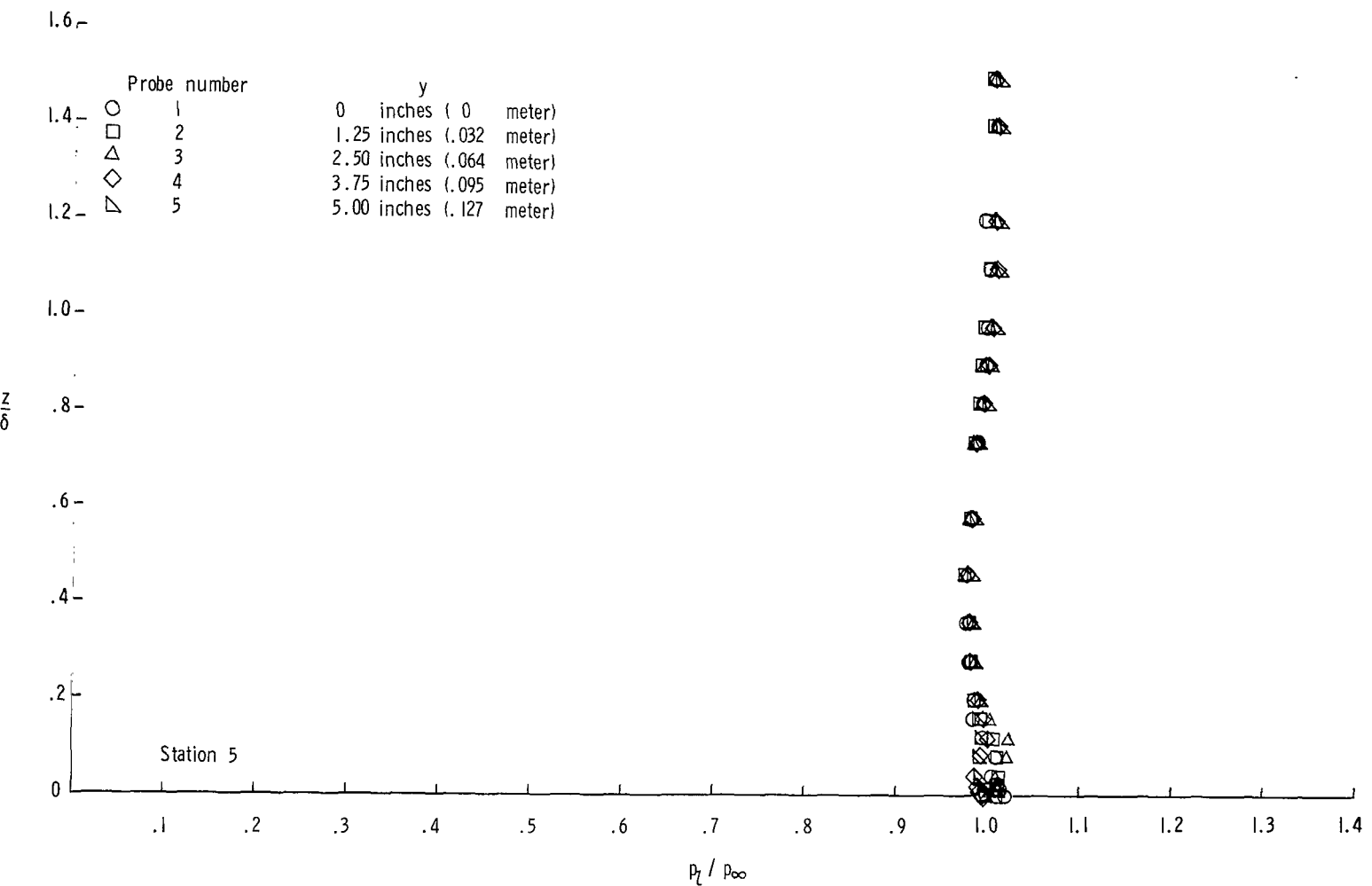
(b) Concluded.

Figure 30.- Concluded.



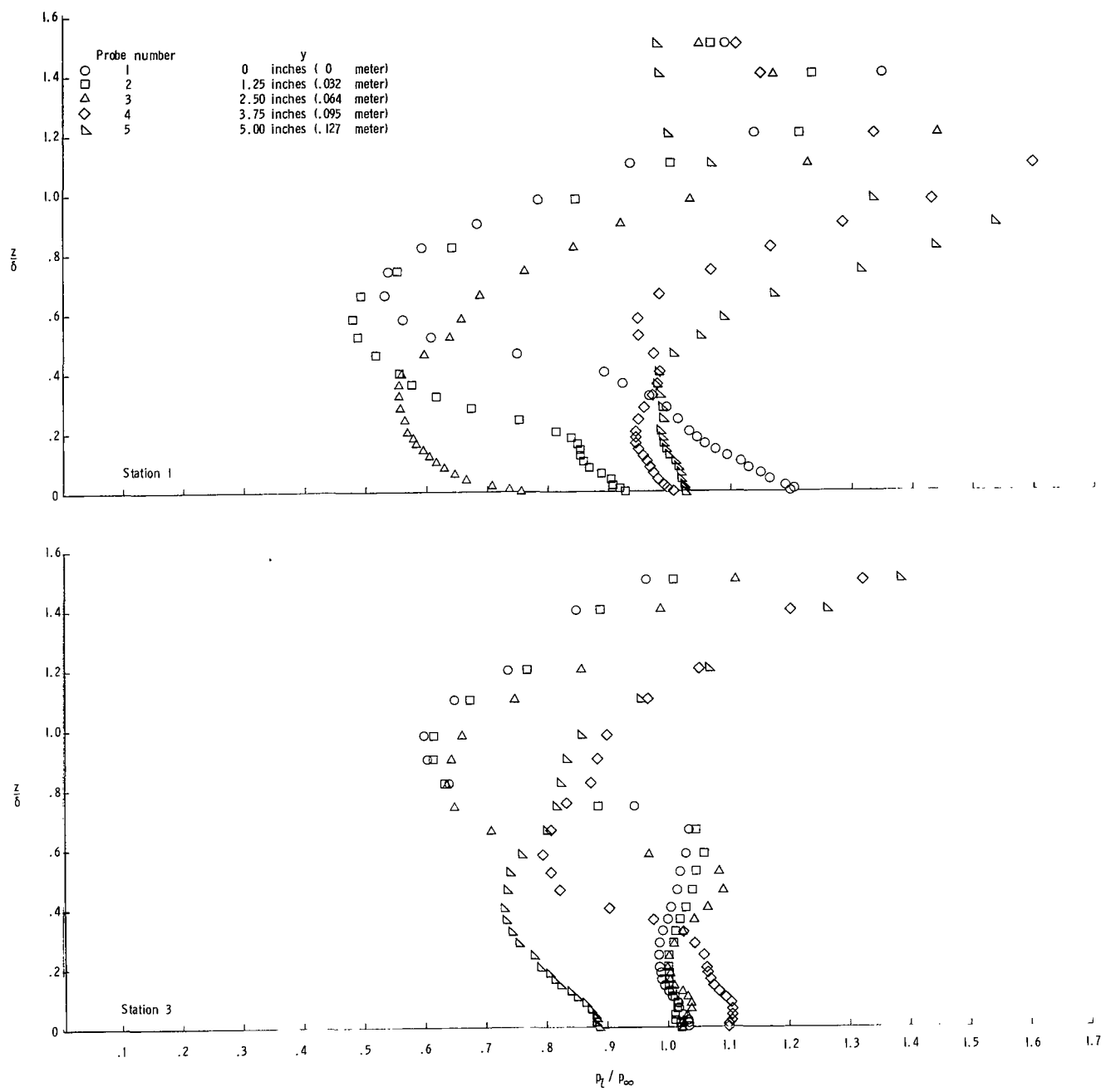
(a) $M = 2.49$.

Figure 31.- Static-pressure distributions downstream of fairing at spanwise stations at three longitudinal stations.



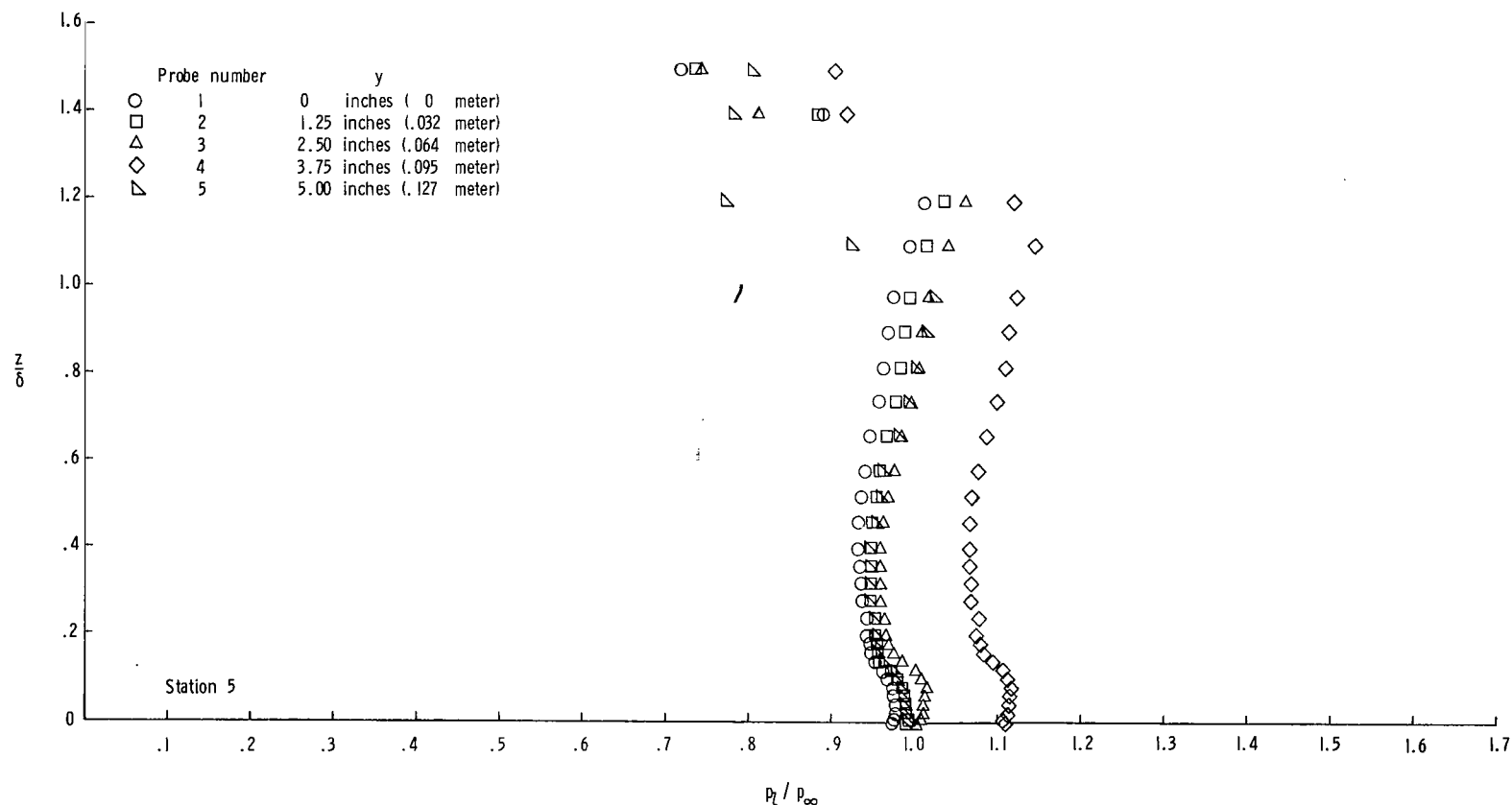
(a) Concluded.

Figure 31.- Continued.



(b) $M = 4.44$.

Figure 31.- Continued.



(b) Concluded.

Figure 31.- Concluded.

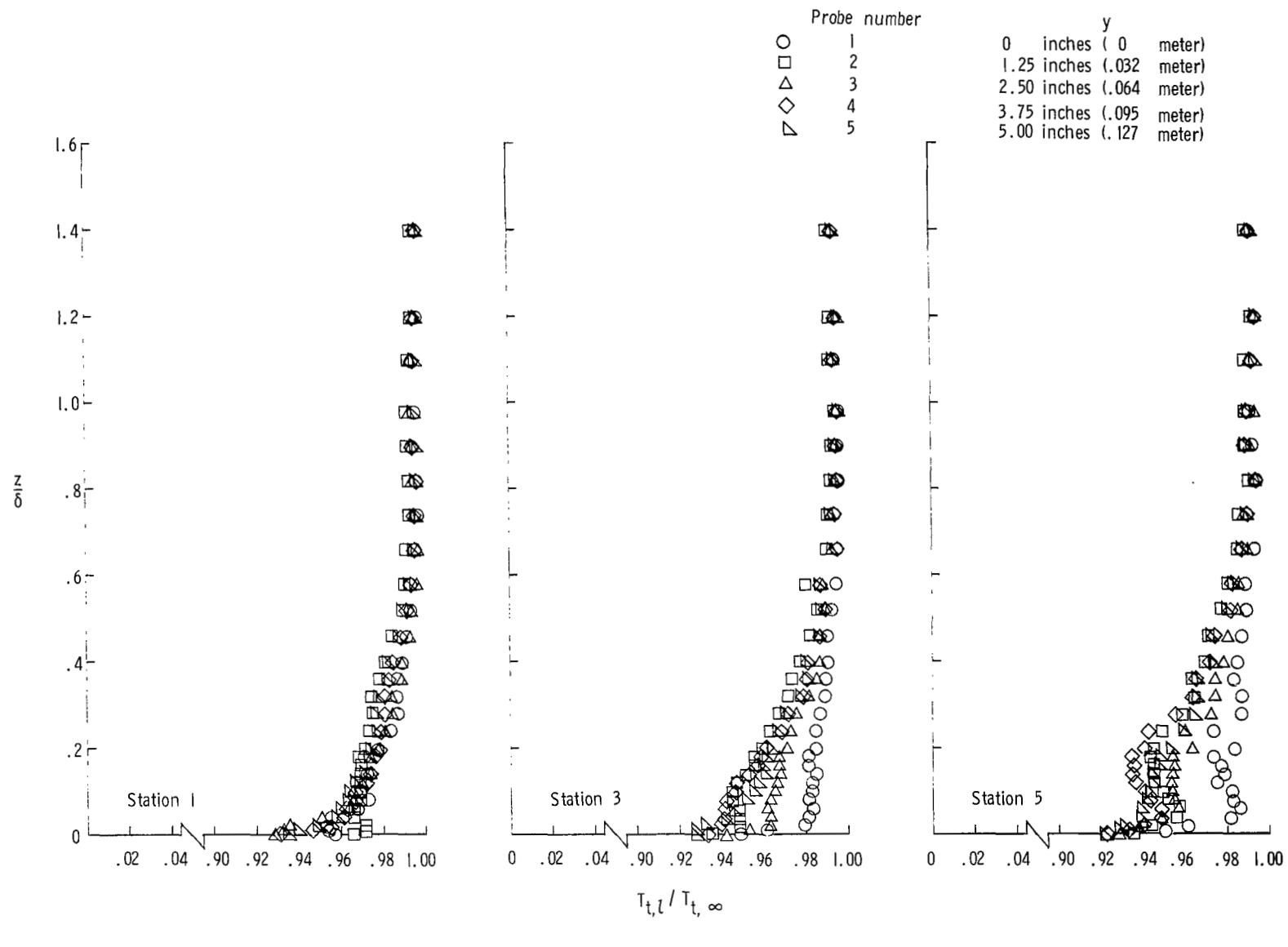
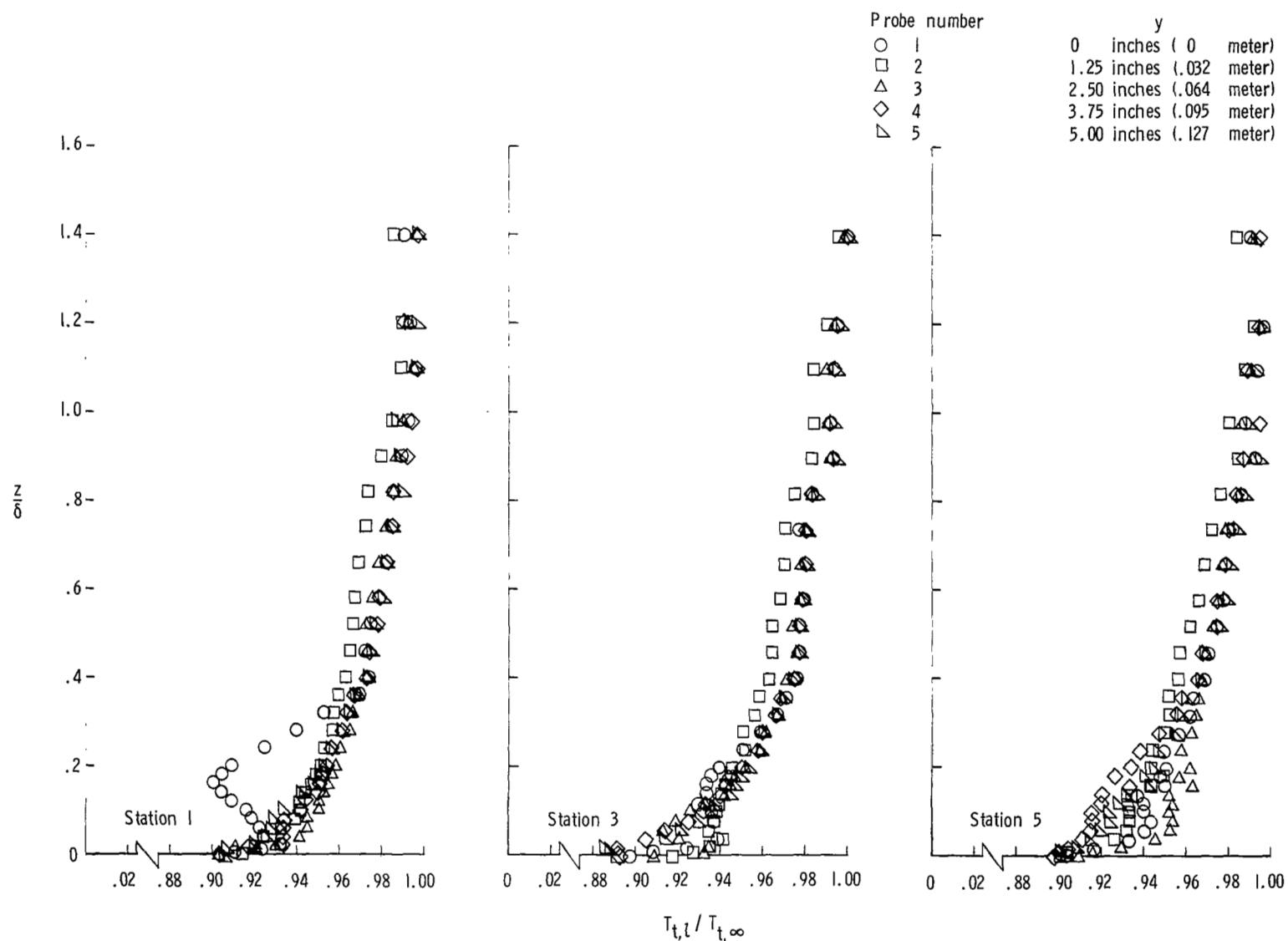
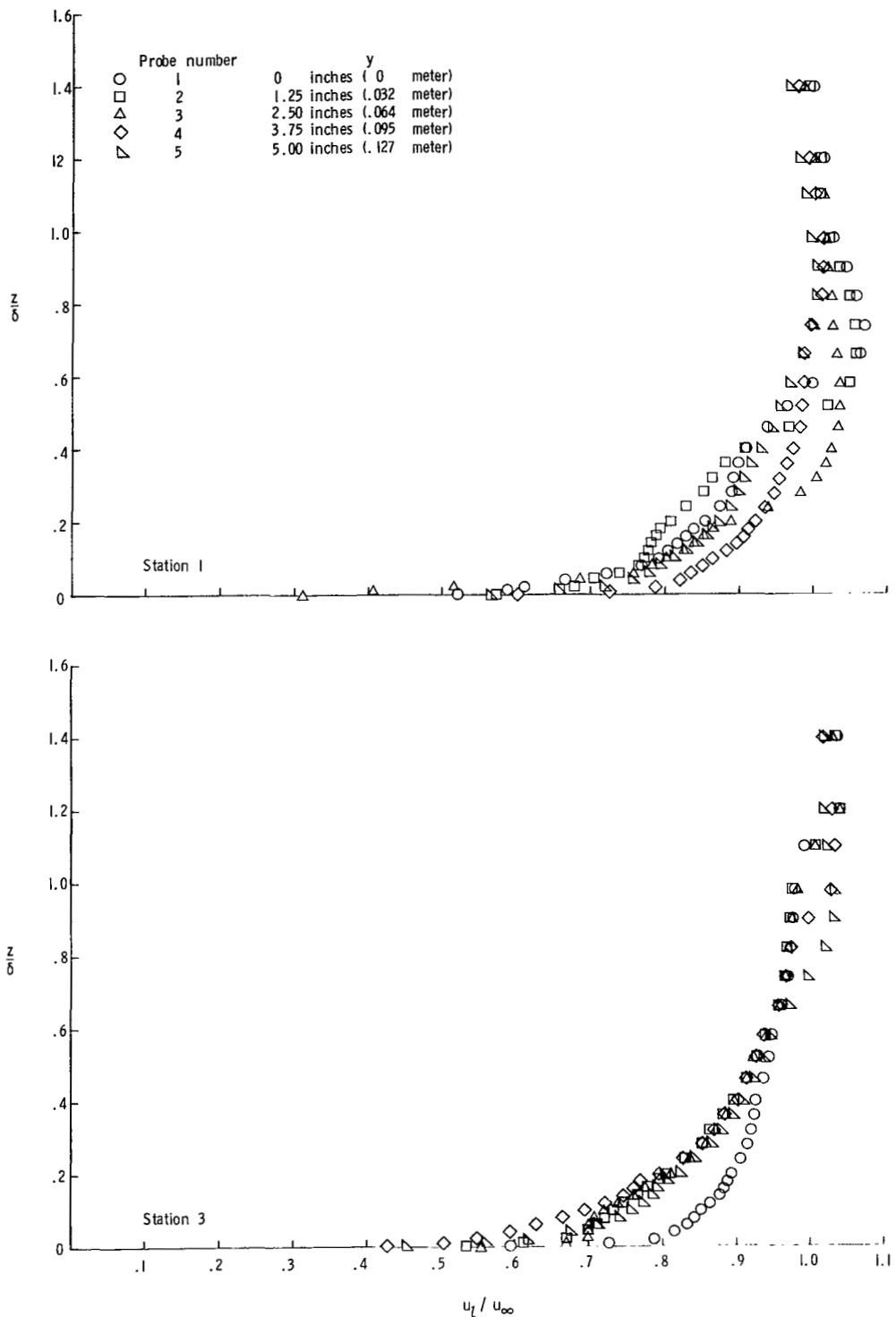


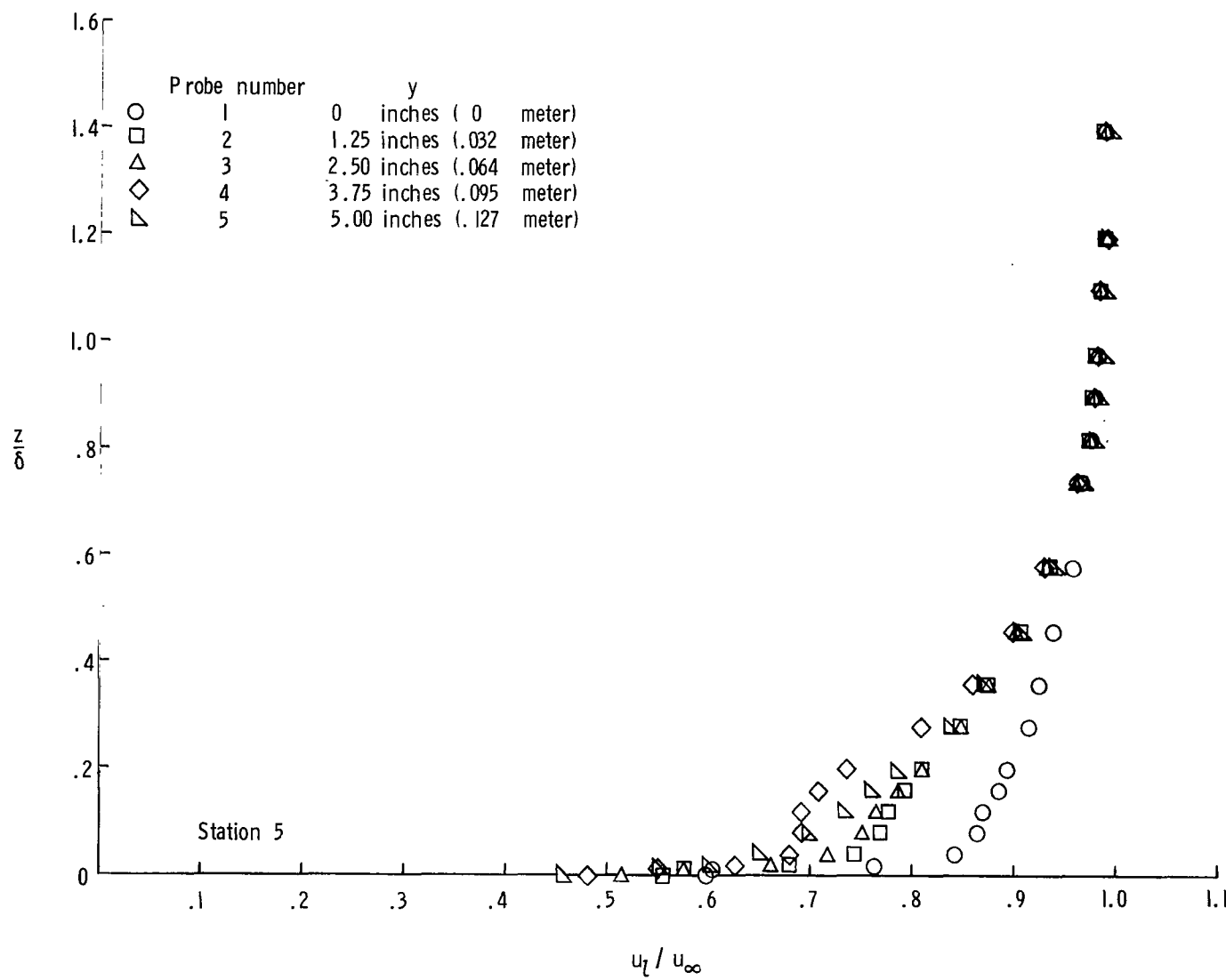
Figure 32.- Total-temperature distributions downstream of fairing at spanwise stations at three longitudinal stations.



(b) $M = 4.44$.

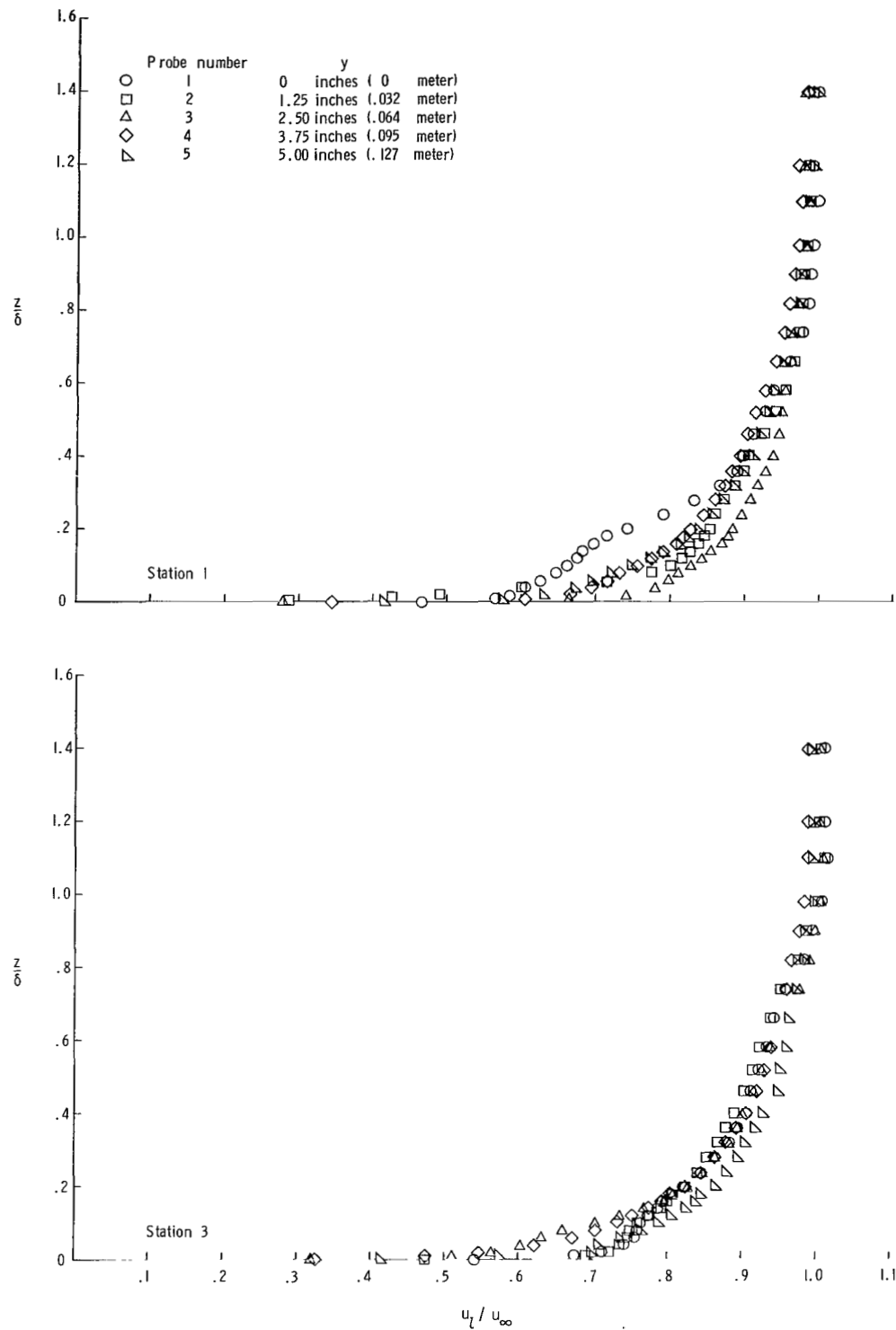
Figure 32.- Concluded.





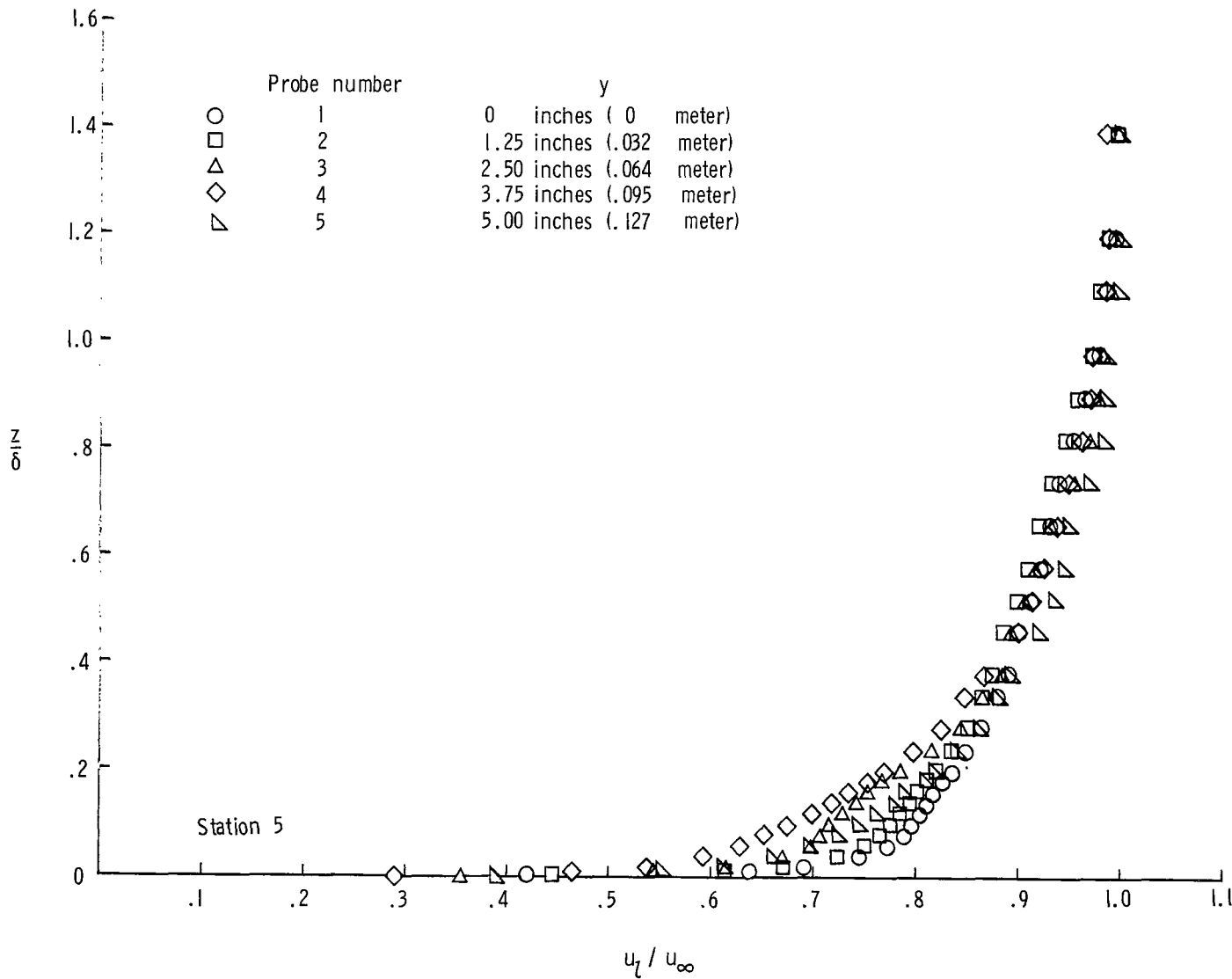
(a) Concluded.

Figure 33.- Continued.



(b) $M = 4.44$.

Figure 33.- Continued.



(b) Concluded.

Figure 33.- Concluded.

NATIONAL AERONAUTICS AND SPACE ADMINISTRATION

WASHINGTON, D.C. 20546

OFFICIAL BUSINESS

FIRST CLASS MAIL



POSTAGE AND FEES PAID
NATIONAL AERONAUTICS AND
SPACE ADMINISTRATION

65-10137-01-303 69163-69904
AIR MAIL REGISTRATION RATES/AFK
MATERIALS AIR MAIL CLASS 1, 2, 3 & 4 7117

ALL USE OF THIS MAILING UNIT IS FOR OFFICIAL PURPOSES

POSTMASTER: If Undeliverable (Section 158
Postal Manual) Do Not Return

"The aeronautical and space activities of the United States shall be conducted so as to contribute . . . to the expansion of human knowledge of phenomena in the atmosphere and space. The Administration shall provide for the widest practicable and appropriate dissemination of information concerning its activities and the results thereof."

— NATIONAL AERONAUTICS AND SPACE ACT OF 1958

NASA SCIENTIFIC AND TECHNICAL PUBLICATIONS

TECHNICAL REPORTS: Scientific and technical information considered important, complete, and a lasting contribution to existing knowledge.

TECHNICAL NOTES: Information less broad in scope but nevertheless of importance as a contribution to existing knowledge.

TECHNICAL MEMORANDUMS: Information receiving limited distribution because of preliminary data, security classification, or other reasons.

CONTRACTOR REPORTS: Scientific and technical information generated under a NASA contract or grant and considered an important contribution to existing knowledge.

TECHNICAL TRANSLATIONS: Information published in a foreign language considered to merit NASA distribution in English.

SPECIAL PUBLICATIONS: Information derived from or of value to NASA activities. Publications include conference proceedings, monographs, data compilations, handbooks, sourcebooks, and special bibliographies.

TECHNOLOGY UTILIZATION PUBLICATIONS: Information on technology used by NASA that may be of particular interest in commercial and other non-aerospace applications. Publications include Tech Briefs, Technology Utilization Reports and Notes, and Technology Surveys.

Details on the availability of these publications may be obtained from:

SCIENTIFIC AND TECHNICAL INFORMATION DIVISION

NATIONAL AERONAUTICS AND SPACE ADMINISTRATION

Washington, D.C. 20546